UNIVERSIDADE ESTADUAL PAULISTA
"JÚLIO DE MESQUITA FILHO"
Câmpus de Ilha Solteira - SP

JOHN EUGENIO PEÑALOZA MORÁN

A NOVEL PARTICLE SWARM OPTIMIZATION FORMULATION FOR TOPOLOGICAL OPTIMIZATION PROBLEMS IN DISTRIBUTION SYSTEMS

Ilha Solteira
2026

UNIVERSIDADE ESTADUAL PAULISTA
"JÚLIO DE MESQUITA FILHO"
Câmpus de Ilha Solteira - SP

JOHN EUGENIO PEÑALOZA MORÁN

A NOVEL PARTICLE SWARM OPTIMIZATION FORMULATION FOR TOPOLOGICAL OPTIMIZATION PROBLEMS IN DISTRIBUTION SYSTEMS

Thesis submitted to the School of Engineering, São Paulo State University (UNESP), Ilha Solteira, in partial fulfillment of the requirements for the degree of Doctor of Philosophy in Electrical Engineering.
Concentration area: Automation

Advisor:
Prof. Dr. Leonardo Henrique Faria Macedo Possagnolo

Ilha Solteira
2026

FICHA CATALOGRÁFICA
Desenvolvida pela Diretoria Técnica de Biblioteca e Documentação

P397n

Peñaloza Morán, John Eugenio.
A novel particle swarm optimization formulation for topological optimization problems in distribution systems / John Eugenio Peñaloza Morán. -- Ilha Solteira: [s.n.], 2026
119 f. : il.

Tese (doutorado) - Universidade Estadual Paulista. Faculdade de Engenharia de Ilha Solteira. Área de conhecimento: Automação, 2026

Orientador: Leonardo Henrique Faria Macedo Possagnolo
Inclui bibliografia

1. Combinatorial optimization. 2. Distribution systems. 3. Particle swarm optimization. 4. Reconfiguration. 5. Service restoration.

Elaborada por Raiane da Silva Santos - CRB-8/9999

IMPACTO POTENCIAL DESTA PESQUISA

Esta tese propõe um mecanismo de ponderação baseado em intervalos com potencial para lidar eficientemente com problemas de otimização combinatória de grande porte nos quais a viabilidade das soluções depende da topologia. O mecanismo transforma as informações das soluções atual, melhor individual e melhor global em prioridades para a construção de novas soluções, dispensando atualizações convencionais de velocidade e posição, funções de transferência e procedimentos de reparação da radialidade. Sua integração com um procedimento construtivo permite gerar diretamente topologias estruturalmente viáveis por meio de uma implementação simples e modular. Os resultados obtidos em sistemas de distribuição de diferentes dimensões demonstram a capacidade das abordagens propostas de encontrar soluções de alta qualidade com desempenho computacional competitivo. Além das aplicações em reconfiguração e restauração, a abordagem fornece uma base promissora para o desenvolvimento de ferramentas de otimização e de apoio à tomada de decisão em outros problemas combinatórios com representações e procedimentos construtivos compatíveis.

POTENTIAL IMPACT OF THIS RESEARCH

This thesis proposes an interval-based weighting mechanism that can efficiently address large-scale combinatorial optimization problems in which solution feasibility depends on the topology. The mechanism transforms information from the current, personal-best, and global-best solutions into priorities for constructing new solutions, avoiding conventional velocity and position updates, transfer functions, and radiality-repair procedures. Its integration with a constructive procedure enables the direct generation of structurally feasible topologies via a simple, modular implementation. The results obtained for distribution systems of different sizes demonstrate the ability of the proposed approaches to find high-quality solutions with competitive computational performance. Beyond reconfiguration and service restoration, the approach provides a promising basis for developing optimization and decision-support tools for other combinatorial problems with compatible representations and constructive procedures.

UNIVERSIDADE ESTADUAL PAULISTA

Câmpus de Ilha Solteira

CERTIFICADO DE APROVAÇÃO

TÍTULO DA TESE: A Novel Particle Swarm Optimization Formulation for Topological Optimization Problems in Distribution Systems

AUTOR: JOHN EUGENIO PEÑALOZA MORAN
ORIENTADOR: LEONARDO HENRIQUE FARIA MACEDO POSSAGNOLO

Aprovado como parte das exigências para obtenção do Título de Doutor em Engenharia Elétrica, área: Automação pela Comissão Examinadora:

Prof. Dr. LEONARDO HENRIQUE FARIA MACEDO POSSAGNOLO (Participaçao Virtual)
Departamento de Engenharia / UNESP / Câmpus de Rosana - FEC

Dr. MARIO ANDRES MEJIA ALZATE (Participaçao Virtual)
Departamento de Engenharia Elétrica / Faculdade de Engenharia de Ilha Solteira - UNESP

Prof. Dr. LUCAS TELES DE FARIA (Participaçao Virtual)
Departamento de Engenharia / UNESP / Câmpus de Rosana - FEC

Prof. Dr. ELENILSON DE VARGAS FORTES (Participaçao Virtual)
Departamento de Áreas Acadêmicas / Instituto Federal de Educação, Ciência e Tecnologia de Goiás - IFG

Prof. Dr. JOÃO ANDRÉ PINTO SOARES (Participaçao Virtual)
Departamento de Engenharia Electrotécnica / Instituto Superior de Engenharia do Porto - Portugal

Ilha Solteira, 12 de setembro de 2026.

Dedico este trabalho aos meus pais, Marlene e Jhon, por me tornarem quem sou — como pessoa e como profissional.

ACKNOWLEDGEMENTS

I am deeply grateful to my parents, Marlene and Jhon, and to my sisters, Salomé and Gabriela, for their love, unconditional support, and patience throughout this journey. I would like to express my sincere gratitude to my advisors, Professors Leonardo Macedo and Rubén Romero, for their rigorous yet generous guidance, insightful discussions, constructive criticism, and confidence in this work. I also thank Professors Tiago Pinto and Tiago Soares for their availability, valuable suggestions, and collaboration, which greatly enriched this research. My sincere thanks go to my friends and colleagues at the Power Systems Planning Laboratory (LaPSEE), School of Engineering, São Paulo State University (UNESP), Ilha Solteira, and at the Centre for Power and Energy Systems (CPES), INESC TEC, for their companionship, enriching discussions, and day-to-day support. I am also grateful to all the individuals and institutions that opened doors and provided opportunities for research, learning, and collaboration throughout this period. These opportunities were fundamental to my development, both as a researcher and as a person. I gratefully acknowledge the National Council for Scientific and Technological Development (CNPq) for the financial support that made this research possible.

This study was financed in part by the Coordenação de Aperfeiçoamento de Pessoal de Nível Superior – Brasil (CAPES) – Finance Code 001, in part by the National Council for Scientific and Technological Development (CNPq), Grant 409062/2023-5, and in part by the São Paulo Research Foundation (FAPESP), Brazil, process number #2025/16766-0.

RESUMO

Esta tese desenvolve e avalia duas abordagens de otimização discreta inspiradas na otimização por enxame de partículas (PSO) para problemas topológicos em sistemas de distribuição de energia elétrica: a *weighted tier particle swarm optimization* (WTPSO) e sua extensão baseada na otimização evolutiva por enxame de partículas (EPSO), denominada *weighted tier evolutionary particle swarm optimization* (WTEPSO). Na WTPSO, as atualizações convencionais de velocidade e posição são substituídas por um mecanismo de ponderação por intervalos que combina as características topológicas da solução atual, da melhor solução individual e da melhor solução global. As prioridades de ramo resultantes orientam o algoritmo de Prim na construção direta de topologias radiais, sem o uso de funções de transferência ou de procedimentos de reparo de radialidade. Essa estratégia busca equilibrar a exploração do espaço de busca e a intensificação em regiões promissoras, enquanto a viabilidade elétrica e operacional das soluções candidatas é verificada por meio do fluxo de potência. Na WTEPSO, o mesmo mecanismo é integrado aos processos de replicação, mutação e seleção da EPSO, permitindo que os parâmetros estratégicos evoluam durante a busca. As abordagens são aplicadas à reconfiguração e à restauração de sistemas de distribuição. Na reconfiguração, o objetivo é minimizar as perdas de potência ativa; na restauração, busca-se minimizar a demanda ponderada não restaurada e os custos das operações de chaveamento, respeitando restrições de radialidade, conectividade, tensão, corrente e capacidade das subestações. Os parâmetros das meta-heurísticas são calibrados por otimização bayesiana. Na reconfiguração, o desempenho da WTPSO e da WTEPSO é comparado com o da EPSO, o da otimização binária por enxame de partículas (BPSO) e o do método probabilístico de entropia cruzada (CE), utilizando um modelo de programação linear inteira mista (MILP) como referência. A avaliação considera sistemas de 33, 84, 136 e 415 barras e 50 execuções independentes de cada método para cada sistema, sob um orçamento comum de avaliações de fluxo de potência. Os resultados mostram que as abordagens propostas produziram soluções consistentes e de alta qualidade, com valores finais iguais ou próximos aos fornecidos pelo modelo matemático de referência. A WTPSO apresentou, de modo geral, convergência mais rápida para regiões de baixas perdas e um equilíbrio favorável entre qualidade das soluções e esforço computacional. A WTEPSO obteve distribuições finais próximas às da WTPSO e manteve desempenho competitivo, embora sua eficiência computacional relativa tenha variado com o tamanho do sistema. Na restauração, a WTPSO e a WTEPSO são comparadas com a EPSO, tendo como referência um modelo de programação cônica de segunda ordem inteira mista (MISOCP). Uma representação ampliada da rede pós-falta, baseada em uma subestação artificial, permite modelar conjuntamente as seções restauradas e não restauradas e construir planos radiais para sistemas de 53 e 417 barras sob quatro cenários de falta. Em 50 execuções independentes

por cenário, a WTPSO alcançou o valor de referência do MISOCP em suas melhores execuções nos quatro cenários avaliados, enquanto a WTEPSO o alcançou em três cenários e permaneceu próxima no quarto. Para o sistema de 417 barras, a WTPSO apresentou os menores valores médios e medianos, a menor variabilidade e o menor esforço computacional nos cenários mais exigentes. A WTEPSO também superou a EPSO em qualidade de solução e esforço computacional nesse sistema, embora tenha apresentado maior variabilidade entre as execuções. Em conjunto, os resultados indicam que o mecanismo de ponderação por intervalos constitui uma alternativa consistente para preservar as informações do enxame e orientar a construção de soluções radiais. Entre as duas abordagens propostas, a WTPSO apresentou o desempenho mais consistente, enquanto a WTEPSO demonstrou que o mecanismo construtivo pode ser integrado a uma estrutura evolutiva e autoadaptativa, oferecendo características complementares quanto à qualidade das soluções, à robustez e à eficiência computacional.

Palavras-chave: otimização combinatória; otimização por enxame de partículas; reconfiguração; restauração do serviço; sistemas de distribuição.

ABSTRACT

This thesis develops and evaluates two discrete optimization approaches inspired by particle swarm optimization (PSO) for topological problems in electric power distribution systems: weighted tier particle swarm optimization (WTPSO) and its evolutionary particle swarm optimization (EPSO)- based extension, termed weighted tier evolutionary particle swarm optimization (WTEPSO). In WTPSO, the conventional velocity and position updates are replaced by an interval-based weighting mechanism that combines the topological characteristics of the current solution, the individual-best solution, and the global-best solution. The resulting branch priorities guide Prim's algorithm in directly constructing radial topologies without using transfer functions or radiality-repair procedures. This strategy seeks to balance exploration of the search space and intensification in promising regions, while the electrical and operational feasibility of candidate solutions is verified through power-flow calculations. In WTEPSO, the same mechanism is integrated into the replication, mutation, and selection processes of EPSO, allowing the strategic parameters to evolve during the search. The approaches are applied to distribution system reconfiguration and service restoration. In reconfiguration, the objective is to minimize active-power losses; in restoration, the objective is to minimize the weighted nonrestored demand and switching-operation costs while satisfying radiality, connectivity, voltage, current, and substation-capacity constraints. The metaheuristic parameters are calibrated using bayesian optimization. For reconfiguration, the performance of WTPSO and WTEPSO is compared with that of EPSO, binary particle swarm optimization (BPSO), and the cross-entropy (CE) method, using a mixed-integer linear programming (MILP) model as a reference. The evaluation considers 33-, 84-, 136-, and 415-node systems and 50 independent runs of each method for each system under a common power-flow-evaluation budget. The results show that the proposed approaches produced consistent, high-quality solutions, with final values equal to or close to those of the reference mathematical model. Overall, WTPSO converged more rapidly toward low-loss regions and provided a favorable balance between solution quality and computational effort. WTEPSO produced final distributions close to those of WTPSO and remained competitive, although its relative computational efficiency varied with system size. For service restoration, WTPSO and WTEPSO are compared with EPSO using a mixed-integer second-order cone programming (MISOCP) model as a reference. An augmented post-fault network representation based on an artificial substation enables the joint modeling of restored and nonrestored sections and the construction of radial restoration plans for 53- and 417-node systems under four fault scenarios. Over 50 independent runs per scenario, WTPSO attained the MISOCP reference value in its best runs for all four evaluated scenarios, whereas WTEPSO attained it in three scenarios and remained close in the fourth. For the 417-node system, WTPSO

presented the lowest means and medians, the lowest variability, and the lowest computational effort in the most demanding scenarios. WTEPSO also outperformed EPSO in terms of solution quality and computational effort for this system, although it exhibited greater variability across runs. Overall, the results indicate that the interval-based weighting mechanism provides a consistent alternative for preserving swarm information and guiding the construction of radial solutions. Between the two proposed approaches, WTPSO delivered the most consistent performance, whereas WTEPSO demonstrated that the constructive mechanism can be integrated into an evolutionary and self-adaptive framework, offering complementary characteristics in terms of solution quality, robustness, and computational efficiency.

Keywords: combinatorial optimization; distribution systems; particle swarm optimization; reconfiguration; service restoration.

LIST OF FIGURES

Figure 1 Representation of a solution proposal. 48

Figure 2 Intervals used to assign branch weights based on the topological agreement of the current solution proposals s_i^k, p_i^{best}, and g^{best}. 49

Figure 3 (a) Intervals when the inertia weight is zero ($w = 0$) and (b) intervals when the inertia weight is one ($w = 1$). 51

Figure 4 Interval $[e_2, f_2]$ under the influence of c_1 and c_2 when a branch is closed in two current solution proposals (s_i^k and g^{best}) (a) when the social coefficient is greater than the cognitive coefficient ($c_2 > c_1$) and (b) when the cognitive coefficient is greater than the social coefficient ($c_1 > c_2$). . . . 51

Figure 5 Median best-so-far active-power losses as a function of the number of power-flow calculations for the WTPSO, EPSO, BPSO, CE, and WTEPSO approaches over 50 independent runs. The shaded regions represent the interquartile ranges. Results are shown for the (a) 33-node, (b) 84-node, (c) 136-node, and (d) 415-node test systems. 71

Figure 6 Box plots of the final active-power losses obtained by the WTPSO, EPSO, BPSO, CE, and WTEPSO approaches over 50 independent runs under the same power-flow-evaluation budget. Results are shown for the (a) 33-node, (b) 84-node, (c) 136-node, and (d) 415-node test systems. . 72

Figure 7 Median best-so-far active-power losses as a function of cumulative wall-clock time for the WTPSO, EPSO, BPSO, CE, and WTEPSO approaches over 50 independent runs. The shaded regions represent the interquartile ranges. Each profile is displayed up to the maximum observed runtime of the corresponding method. Results are shown for the (a) 33-node, (b) 84-node, (c) 136-node, and (d) 415-node test systems. . 76

Figure 8 Box plots of the total wall-clock times required by the WTPSO, EPSO, BPSO, CE, and WTEPSO approaches to complete the same prescribed power-flow-evaluation budget over 50 independent runs. Results are shown for the (a) 33-node, (b) 84-node, (c) 136-node, and (d) 415-node test systems. 77

Figure 9 Illustrative test system and binary encoding of the restoration process: (a) post-fault isolated system and correspondence between the affected sections and the artificial lines; and (b) restored solution proposal. . . . 85

Figure 10 Box plots of the objective function values obtained from 50 independent runs of the WTPSO, EPSO, and WTEPSO algorithms for the service restoration problem under the following fault scenarios: (a) 53-node system, section 14; (b) 53-node system, sections 11, 14, and 21; (c) 417-node system, section 92; and (d) 417-node system, section 208. . . 91

Figure 11 Average convergence profiles of the WTPSO, EPSO, and WTEPSO algorithms over 50 independent runs for the service restoration problem under the following fault scenarios: (a) 53-node system, section 14; (b) 53-node system, sections 11, 14, and 21; (c) 417-node system, section 92; and (d) 417-node system, section 208. 92

Figure 12 Box plots of the number of power flow calculations performed over 50 independent runs of the WTPSO, EPSO, and WTEPSO algorithms for the service restoration problem under the following fault scenarios: (a) 53-node, section 14; (b) 53-node system, sections 11, 14, and 21; (c) 417-node system, section 92; and (d) 417-node system, section 208. . . 93

Figure 13 Box plots of the computation times obtained over 50 independent runs of the WTPSO, EPSO, and WTEPSO algorithms for the service restoration problem under the following fault scenarios: (a) 53-node system, section 14; (b) 53-node system, sections 11, 14, and 21; (c) 417-node system, section 92; and (d) 417-node system, section 208. 94

LIST OF TABLES

Table 1 Main methodological characteristics of distribution system reconfiguration and service restoration. 37

Table 2 Comparative synthesis of the main approaches reviewed for discrete and topological optimization. 38

Table 3 Parameter search intervals adopted for the bayesian optimization (BO) calibration of the metaheuristics applied to distribution system reconfiguration. 68

Table 4 Parameters for the WTPSO, WTEPSO, EPSO, BPSO, and CE approaches for the 33-, 84-, 136-, and 415-node test systems. 69

Table 5 Benchmark results obtained with the MILP approximation for the 33-, 84-, 136-, and 415-node test systems. 70

Table 6 Descriptive statistics of the final active-power losses obtained by the WTPSO, EPSO, BPSO, CE, and WTEPSO algorithms over 50 independent runs. Means and standard deviations are reported together with the medians and the first and third quartiles. 73

Table 7 Two-sided Mann–Whitney test results ($\alpha = 0.05$) for final active-power losses, with WTPSO as the control algorithm. The p-values were adjusted using Holm's correction over the three comparisons within each test system. Cliff's δ is reported with its 95% bootstrap confidence interval. Negative effect sizes favor the WTPSO. 74

Table 8 Two-sided Mann–Whitney test results ($\alpha = 0.05$) for final active-power losses, with WTEPSO as the control algorithm. The p-values were adjusted using Holm's correction over the three comparisons within each test system. Cliff's δ is reported with its 95% bootstrap confidence interval. Negative effect sizes favor the WTEPSO. 75

Table 9 Two-sided Mann–Whitney test results ($\alpha = 0.05$) for total wall-clock times, with WTPSO as the control algorithm. The p-values were adjusted using Holm's correction over the three comparisons within each test system. Cliff's δ is reported with its 95% bootstrap confidence interval. Negative effect sizes favor WTPSO. 77

Table 10 Two-sided Mann–Whitney test results ($\alpha = 0.05$) for total wall-clock times, with WTEPSO as the control algorithm. The p-values were adjusted using Holm's correction over the three comparisons within each test system. Cliff's δ is reported with its 95% bootstrap confidence interval. Negative effect sizes favor WTEPSO. 78
Table 11 Parameter settings of the WTPSO, WTEPSO, and EPSO for the service restoration scenarios. 88
Table 12 Benchmark restoration performance obtained with the MISOCP mathematical model. 89
Table 13 Benchmark switching plans obtained with the MISOCP mathematical model. 89
Table 14 Descriptive statistics of the objective-function values obtained by the WTPSO, WTEPSO, and EPSO algorithms for the service restoration problem under different fault scenarios over 50 independent runs. 90
Table 15 Performance of the best service restoration solution obtained by the WTPSO, WTEPSO, and EPSO algorithms over 50 independent runs under different fault scenarios. 95
Table 16 Switching plans corresponding to the best service restoration solutions obtained by the WTPSO, WTEPSO, and EPSO algorithms over 50 independent runs for each fault scenario. 96
Table 17 Performance of the worst service restoration solution obtained by the WTPSO, WTEPSO, and EPSO algorithms over 50 independent runs under different fault scenarios. 97
Table 18 Switching plans corresponding to the worst service restoration solutions obtained by the WTPSO, WTEPSO, and EPSO algorithms over 50 independent runs for each fault scenario. 98

LIST OF ABBREVIATIONS AND ACRONYMS

PSO	particle swarm optimization
BPSO	binary particle swarm optimization
EPSO	evolutionary particle swarm optimization
WTEPSO	weighted tier evolutionary particle swarm optimization
WTPSO	weighted tier particle swarm optimization
CE	cross-entropy
BO	bayesian optimization
MILP	mixed-integer linear programming
MINLP	mixed-integer nonlinear programming
MISOCP	mixed-integer second-order cone programming
DG	distributed generation
DER	distributed energy resource

LIST OF SYMBOLS

Symbol	Description
SETS	
Distribution-network and reconfiguration sets	
Ω_b	Set of branches.
Ω_n	Set of nodes.
Service-restoration sets	
$\mathscr{N}$	Set of all nodes, including demand nodes, real substations, and the artificial substation.
$\mathscr{N}^D$	Set of demand nodes.
$\mathscr{N}^R$	Set of real network nodes, excluding the artificial substation.
$\mathscr{N}^S$	Set of real substation nodes.
$\mathscr{S}^F$	Set of sections affected by the fault.
$\mathscr{L}$	Set of real distribution lines.
$\mathscr{L}^C$	Set of normally closed lines.
$\mathscr{L}^O$	Set of normally open lines.
$\mathscr{L}^H$	Set of artificial lines.
$\mathscr{L}^U$	Augmented set of real and artificial lines, $\mathscr{L}^U = \mathscr{L} \cup \mathscr{L}^H$.
INDICES	
a	Application identifier, $a \in \{\text{rec}, \text{rest}\}$.
h, i, j	Indices of network nodes; in the metaheuristic formulations, i also denotes a particle and j a branch position.
s	Index of a voltage-discretization variable in the reconfiguration MILP approximation or of a real substation in the service-restoration formulation, according to context.
w	Index of a piecewise-linear power block in the reconfiguration MILP approximation.
k	Metaheuristic iteration index.
ν	Calibration-run index.
PARAMETERS	
Electrical-network parameters	
P_i^D, Q_i^D	Active and reactive power demands at node i, respectively.
R_{ij}, X_{ij}	Resistance and reactance of line ij, respectively.

Symbol	Description
Z_{ij}	Impedance magnitude of line ij.
$\overline{I}_{ij}$	Maximum current magnitude of line ij.
$\underline{V}, \overline{V}$	Lower and upper voltage-magnitude limits, respectively.
$\overline{S}_i^{\mathrm{SE}}$	Maximum apparent-power capacity of real substation i.
Reconfiguration-model parameters	
n_{SE}	Substation node in the network-reconfiguration formulation.
n_b, n_r	Numbers of nodes and branches, respectively, with $n_b = \lvert\Omega_n\rvert$ and $n_r = \lvert\Omega_b\rvert$.
N_v	Number of binary variables used in the squared-voltage discretization.
W	Number of blocks used in the piecewise-linear approximation of the squared power flows.
Δ^V	Step size of the squared-voltage discretization.
Δ_{ij}^S	Width of each piecewise-linear power-flow block for branch ij.
$m_{ij,w}^S$	Slope associated with block w of the piecewise-linear approximation for branch ij.
Service-restoration parameters	
S_i	Distribution-system section i.
σ_i	Load curtailment cost.
τ_{ij}	Cost for closing normally open switch at line ij.
η_{ij}	Cost for opening normally closed switch line ij.
$\lvert\mathscr{N}\rvert$	Number of nodes in set $\mathscr{N}$.
$\lvert\mathscr{N}^D\rvert$	Number of demand nodes in set $\mathscr{N}^D$.
Metaheuristic parameters	
$G^a = (\Omega_n^a, \Omega_b^a)$	Connected graph associated with application a.
$\mathscr{D}^a$	Network and optimization data associated with application a.
r^a	Root node adopted by Prim's algorithm for application a.
c_1, c_2	Cognitive and social coefficients, respectively.
cp	Communication probability.
$k_{\max}$	Maximum number of iterations.
k_{stg}	Maximum number of consecutive iterations without improvement.
k_w	Number of iterations required for the inertia weight w^k to reach $w_{\min}$.
N^{pop}	Population size.
$N_{\mathrm{PF}}^{\max}$	Maximum number of power-flow evaluations adopted as the stopping budget.

Symbol	Description
R_{cal}	Number of calibration runs used to evaluate each candidate parameter configuration.
θ	Candidate control-parameter configuration evaluated by Bayesian optimization.
ξ	Pseudorandom seed associated with an algorithm execution.
r_1, r_2	Independent random numbers uniformly distributed in $[0,1]$.
rr	Replication rate.
τ	Mutation rate.
$V_{\min}, V_{\max}$	Minimum and maximum particle-velocity limits, respectively.
w^k	Inertia weight at iteration k.
$w_{\min}, w_{\max}$	Minimum and maximum inertia weights, respectively.
c_{1i}, c_{1f}	Initial and final values of the time-varying acceleration coefficient in the BPSO, respectively.
L	Number of samples generated at each iteration of the cross-entropy method.
ε	Elite-sample proportion used in the cross-entropy method.
N_{elite}	Number of elite samples selected at each cross-entropy iteration, $N_{\text{elite}} = \text{round}(\varepsilon L)$.
σ	Smoothing coefficient used to update the mean of the cross-entropy sampling distribution.
β	Smoothing coefficient used to update the standard deviation of the cross-entropy sampling distribution.
VARIABLES	
Electrical-network variables	
I_{ij}^{sqr}	Squared current magnitude on line ij.
P_{ij}, Q_{ij}	Active and reactive power flows on line ij, respectively.
P_i^G, Q_i^G	Active and reactive power generation at node i, respectively.
$P_i^{\text{SE}}, Q_i^{\text{SE}}$	Active and reactive power supplied by real substation i, respectively.
V_i^{sqr}	Squared voltage magnitude at node i.
ζ_{ij}	Auxiliary variable used to decouple the voltage-drop equation when line ij is open.
Variables of the reconfiguration model and its linearization	
P_{ij}^+, P_{ij}^-	Nonnegative directional components of the active-power flow.
Q_{ij}^+, Q_{ij}^-	Nonnegative positive and negative components of the reactive-power flow.

Symbol	Description
$x_{j,s}$	Binary variable associated with squared-voltage discretization level s at node j.
$P^{c}_{ij,s}$	Auxiliary continuous variable used to linearize the correction term associated with the voltage–current product for discretization level s.
$\Delta^{P}_{ij,w}$, $\Delta^{Q}_{ij,w}$	Nonnegative variables associated with block w of the piecewise-linear approximations of the squared active- and reactive-power flows, respectively.
Topology and restoration-state variables	
y^{+}_{ij}, y^{-}_{ij}	Binary variables indicating that branch ij is energized in the i-to-j and j-to-i directions, respectively.
w_{ij}	Binary operating-state variable for real or artificial line ij.
y_i	Binary restoration-state variable for node i.
Artificial-network variables for nonrestored sections	
f^{f}_{ij}	Artificial flow through line ij.
g^{f}_{i}	Artificial injection at node i in the artificial network.
Artificial-network variables for substation assignment	
$f^{c}_{ij,s}$	Artificial flow through real line ij in the artificial network associated with real substation s.
$g^{c}_{i,s}$	Artificial injection at node i in the artificial network associated with real substation s.
$w^{c}_{ij,s}$	Binary variable equal to one when in-service real line ij is assigned to the artificial network of substation s.
$y^{c}_{i,s}$	Binary variable equal to one when energized node i is assigned to real substation s.
Metaheuristic state and evaluation quantities	
s^{k}_{i}	Binary topology represented by particle i at iteration k.
p^{best}_{i}	Individual-best topology stored by particle i.
g^{best}	Global-best topology found by the population.
ϕ^{k}_{ij}	Priority assigned to branch j of particle i at iteration k.
N_{PF}	Cumulative number of power-flow evaluations.
$\mathscr{C}^{a}(s)$	Power-flow convergence indicator for topology s in application a.
$\text{feasible}^{a}(s)$	Electrical-feasibility indicator for topology s in application a.
$J^{a}(s)$	Application-specific objective value of topology s.
$F^{a}(s)$	Fitness assigned to topology s in application a.

TABLE OF CONTENTS

1 INTRODUCTION 22
1.1 BACKGROUND AND MOTIVATION 22
1.2 RESEARCH GAP, RESEARCH QUESTIONS, AND HYPOTHESIS 23
1.3 OBJECTIVES 24
1.3.1 General objective 24
1.3.2 Specific objectives 24
1.4 SCOPE AND METHODOLOGICAL OVERVIEW 25
1.5 MAIN CONTRIBUTIONS 26
1.6 THESIS ORGANIZATION 27

2 LITERATURE REVIEW 29
2.1 INTRODUCTION 29
2.2 PARTICLE SWARM OPTIMIZATION FOR DISCRETE AND COMBINATORIAL OPTIMIZATION 30
2.2.1 Binary PSO and Transfer-Function-Based Approaches 30
2.2.2 Hybrid and self-adaptive PSO variants 30
2.2.3 Alternative discrete representations and search paradigms 31
2.3 FEASIBILITY HANDLING IN DISCRETE AND TOPOLOGICAL OPTIMIZATION 32
2.3.1 Penalization and feasibility-based selection 32
2.3.2 Repair and decoding procedures 33
2.3.3 Feasibility-preserving representations and constructive methods 33
2.4 METAHEURISTICS FOR TOPOLOGICAL OPTIMIZATION IN DISTRIBUTION SYSTEMS 34
2.4.1 Distribution system reconfiguration 34
2.4.2 Distribution system service restoration 35
2.4.3 Common requirements and methodological differences 37
2.5 COMPARATIVE SYNTHESIS OF THE REVIEWED APPROACHES 38
2.6 RESEARCH GAP AND CHAPTER CONCLUSIONS 39

3 PARTICLE SWARM OPTIMIZATION FOR TOPOLOGICAL PROBLEMS IN DISTRIBUTION SYSTEMS 41

3.1 CRITICAL ANALYSIS OF PARTICLE SWARM OPTIMIZATION APPLIED TO TOPOLOGICAL OPTIMIZATION PROBLEMS 41
3.2 PROBLEM-DEPENDENT COMPONENTS OF TOPOLOGICAL METAHEURISTICS 43
3.2.1 Solution representation and initial population 43
3.2.2 Candidate generation and information preservation 44
3.2.3 Structural and operational feasibility 44
3.3 IMPLICATIONS FOR RECONFIGURATION AND SERVICE RESTORATION 45
3.4 METHODOLOGICAL REQUIREMENTS FOR DISTRIBUTION SYSTEM TOPOLOGY OPTIMIZATION 45

4 WEIGHTED TIER PARTICLE SWARM OPTIMIZATION 47
4.1 INTRODUCTION 47
4.2 GENERATION OF RADIAL TOPOLOGIES 48
4.3 COMPUTATION OF INTERVAL BOUNDS 50
4.4 FITNESS EVALUATION AND CONSTRAINT HANDLING 53
4.5 GENERATION OF INITIAL RADIAL TOPOLOGIES 55
4.5.1 Initialization for distribution system reconfiguration 55
4.5.2 Initialization for distribution system restoration 58
4.6 COMPLETE WTPSO OPTIMIZATION PROCEDURE 59
4.7 MODULARITY OF THE WTPSO AND EXTENSION TO THE WTEPSO 59
4.8 PARAMETER CALIBRATION VIA BAYESIAN OPTIMIZATION 61

5 APPLICATION TO DISTRIBUTION SYSTEM RECONFIGURATION 63
5.1 INTRODUCTION 63
5.2 MATHEMATICAL FORMULATION OF THE RECONFIGURATION PROBLEM 63
5.3 APPLICATION OF THE METAHEURISTICS TO THE RECONFIGURATION PROBLEM 66
5.4 RESULTS 67
5.4.1 Parameter calibration and experimental settings 67
5.4.2 Benchmark results from the MILP formulation 69
5.4.3 Comparative analysis of the metaheuristics 70

6 APPLICATION TO DISTRIBUTION SYSTEM SERVICE RESTORATION 79
6.1 INTRODUCTION 79

6.2 MATHEMATICAL FORMULATION OF THE RADIAL SERVICE RESTORATION PROBLEM 80
6.3 APPLICATION OF THE METAHEURISTICS TO THE SERVICE RESTORATION PROBLEM 84
6.4 RESULTS 86
6.4.1 Benchmark results from the MISOCP formulation 87
6.4.2 Solution quality and robustness 90
6.4.3 Convergence behavior 91
6.4.4 Computational effort 92
6.4.5 Best- and worst-case restoration solutions 93

7 CONCLUSIONS AND FUTURE WORKS 100
7.1 CONCLUSIONS 100
7.2 FUTURE WORKS 101

REFERENCES 102

APPENDIX A - Formulation of the Weighted Tier Evolutionary Particle Swarm Optimization (WTEPSO) 108
A.1 MOTIVATION 108
A.2 OVERVIEW OF EPSO 108
A.3 MAIN EQUATIONS OF EPSO 109
A.4 WEIGHTED TIER EVOLUTIONARY PARTICLE SWARM OPTIMIZATION (WTEPSO) 111
A.5 COMPUTATION OF INTERVAL BOUNDS 113
A.6 COMPLETE WTEPSO OPTIMIZATION PROCEDURE 116
A.7 FINAL REMARKS 116

APPENDIX B - SCIENTIFIC PRODUCTION 119

1 INTRODUCTION

1.1 BACKGROUND AND MOTIVATION

Electric power distribution systems are operated through a combination of continuous and discrete decisions that must simultaneously satisfy electrical, topological, and operational requirements. Among these decisions, the operating status of switching devices plays a central role because it determines the network topology and directly affects active power losses, voltage magnitudes, equipment loading, and continuity of supply. Distribution system reconfiguration and service restoration are representative problems involving this type of decision (Behbahani *et al.*, 2024a; Campoverde *et al.*, 2024).

Solving these problems is challenging because the number of possible network configurations grows combinatorially with the system size. In addition, each candidate configuration must satisfy requirements such as radiality, connectivity, power balance, voltage limits, branch current limits, and substation capacity limits. Mathematical programming formulations can provide reference solutions and bounds on solution quality. When solved to a prescribed optimality gap, they certify the quality of the incumbent solution relative to the best bound obtained by the solver. However, their computational burden may increase as the number of switching decisions, electrical constraints, and network components increases (Kerckhove; D'hulst; Hertem, 2024; Souza; Romero; Franco, 2018). This limitation motivates the investigation of alternative methods that can obtain high-quality solutions with lower computational effort.

Among population-based metaheuristics, the particle swarm optimization (PSO) is distinguished by its simple structure and by the coordinated use of individual experience and information shared by the swarm (Kennedy; Eberhart, 1995). Nevertheless, its original formulation was developed for continuous search spaces, in which velocity and position have well-defined geometric interpretations. Consequently, alternative representations and update mechanisms are required when PSO is applied to discrete and combinatorial search spaces (Zyl; Engelbrecht, 2023). In distribution system reconfiguration and service restoration, the main decisions are discrete and topology-dependent: the state assigned to each switching device contributes to a network configuration that must remain electrically and structurally feasible. Adapting the search principles of PSO to this decision space while preserving topological feasibility during solution construction is therefore the central motivation of this thesis.

1.2 RESEARCH GAP, RESEARCH QUESTIONS, AND HYPOTHESIS

Several adaptations have enabled PSO to operate in discrete search spaces. These approaches employ transfer functions, probabilistic state-transition rules, rounding procedures, set-based representations, or binary operators to represent and update discrete particle states (Zyl; Engelbrecht, 2023). Although such mechanisms allow discrete decisions to be generated, they do not necessarily account for the structural relationships among the decision variables. This limitation is relevant in topology-dependent problems, in which individually valid binary states may collectively produce disconnected, meshed, or otherwise infeasible network configurations.

Repair procedures can be applied to recover feasibility (Lagaros *et al.*, 2023), but they may modify the configuration originally generated by the particle update mechanism. Consequently, the evaluated solution may differ substantially from the position determined by the swarm dynamics. Constructive procedures offer an alternative by enforcing structural feasibility during solution generation. However, their integration with PSO requires a mechanism to translate the information contained in the current, personal-best, and global-best solutions into priorities that effectively guide the constructive process.

The methodological gap addressed in this thesis, therefore, lies in the need for a discrete mechanism that reinterprets the inertia, cognitive, and social components of PSO while directly guiding a feasibility-preserving constructive procedure. To address this gap, this thesis develops the weighted tier particle swarm optimization (WTPSO) and adapts its interval-based weighting mechanism to the evolutionary framework of the evolutionary particle swarm optimization (EPSO) (Miranda; Fonseca, 2002a), resulting in the weighted tier evolutionary particle swarm optimization (WTEPSO).

Based on this research gap, the work is guided by the following research questions:

RQ1: How can the inertia, cognitive, and social components of PSO be reinterpreted in a discrete search space so that they directly guide the construction of new solution proposals without relying on conventional velocity and position updates or transfer functions?

RQ2: How can the proposed interval-based weighting mechanism be incorporated into the evolutionary framework of the EPSO so that its strategic parameters evolve through mutation and selection while structurally feasible candidate solutions continue to be generated directly?

RQ3: How do the WTPSO and WTEPSO compare with mathematical-programming benchmarks and established metaheuristics in terms of solution quality, robustness, convergence behavior, number of power flow calculations, and computational time when applied to distribution system reconfiguration and service restoration?

The central hypothesis of this thesis is that the information traditionally represented by the inertia, cognitive, and social components of PSO can be reformulated through an interval-based weighting mechanism. When combined with an appropriate constructive algorithm, this mechanism is expected to preserve the swarm's fundamental information-sharing principles while directly generating topologically feasible candidate solutions. It is further hypothesized that incorporating this mechanism into the evolutionary framework of the EPSO enables the relative influence of the search components to evolve through mutation and selection, providing an adaptive and competitive search process for the two distribution system applications considered in this thesis.

1.3 OBJECTIVES

1.3.1 General objective

To develop and evaluate discrete optimization approaches based on PSO and interval-based weighting for the direct construction of topologically feasible candidate solutions, considering distribution system reconfiguration and service restoration as application problems.

1.3.2 Specific objectives

To accomplish the overall objective, the following specific objectives are established:

1. To analyze the limitations of conventional velocity- and position-based PSO formulations when applied to discrete and topology-dependent optimization problems.
2. To formulate an interval-based weighting mechanism that represents the information conveyed by the current, personal-best, and global-best solutions and translates this information into priorities for the construction of new solution proposals.
3. To develop the WTPSO by combining the proposed weighting mechanism with a constructive topology-generation procedure, including a strategy for generating an initial population of diverse radial configurations.
4. To adapt the proposed weighting mechanism to the evolutionary framework of the EPSO, resulting in the WTEPSO, in which the strategic parameters evolve through mutation and selection.
5. To adapt the WTPSO and WTEPSO to the specific representations, objective functions, and operational constraints of distribution system reconfiguration and service restoration.
6. To establish a consistent computational framework for parameter calibration, solution evaluation, stopping criteria, and comparison with established metaheuristics.

7. To evaluate the proposed approaches through a consistent statistical and computational protocol based on mathematical programming benchmarks and multiple independent runs.

1.4 SCOPE AND METHODOLOGICAL OVERVIEW

The methodological scope of this thesis is centered on discrete topology optimization in radial electric power distribution systems. The proposed interval-based weighting mechanism assigns priorities to the decision variables according to the states observed in the current, personal-best, and global-best solutions. These priorities are subsequently processed by a constructive procedure based on Prim's algorithm (Prim, 1957). As a result, radial candidate topologies are generated directly, without requiring transfer functions to convert continuous velocities into binary states or repair procedures to recover radiality. Electrical and operational feasibility is subsequently assessed through power flow analysis.

Two algorithmic approaches are developed from this mechanism. The first is the WTPSO, which replaces the conventional velocity and position update equations with the proposed interval-based weighting and topology-construction procedure. The second is the WTEPSO, which adapts the same weighting mechanism to the EPSO evolutionary framework. In the WTEPSO, copies of the particles are generated, their strategic parameters are mutated, candidate solutions are constructed, and competition determines which particles and associated parameters are retained in the population.

The first application concerns distribution system reconfiguration under normal operating conditions. In this problem, the branch states are optimized to obtain a radial operating topology that minimizes active power losses while satisfying voltage, current, connectivity, and equipment-capacity constraints (Behbahani *et al.*, 2024a). Solutions obtained from an MILP formulation are used as benchmarks for evaluating the metaheuristics.

The second application concerns the restoration of distribution system service following the isolation of a permanent fault (Campoverde *et al.*, 2024). In this problem, the algorithms determine additional switching actions that prioritize restoring the affected demand while limiting the number of operations and satisfying applicable topological and electrical requirements. The representation is based on an augmented post-fault network that associates each affected section with an artificial substation connection (Souza; Romero; Franco, 2018; Vargas *et al.*, 2021). Benchmark solutions are obtained from an MISOCP formulation.

The computational evaluation considers distribution systems of different sizes and multiple operating or fault scenarios. The parameters of the metaheuristics are determined through a common parameter-calibration method based on BO (Bischl *et al.*, 2023). Each algorithm is then evaluated over multiple independent runs. The assessment includes descriptive statistics, hypothesis tests, convergence characteristics, power-flow calculations, and computational time.

This framework is intended to distinguish occasional high-quality solutions from performance that is consistently reproduced across independent executions.

The conclusions of this thesis are restricted to the deterministic test systems, operating conditions, fault scenarios, objective functions, and stopping criteria considered in the computational experiments. The proposed interval-based weighting principle may be extended to other combinatorial optimization problems, provided that a compatible constructive procedure is available. However, the empirical evidence presented in this thesis is limited to distribution system reconfiguration and service restoration, and no claim of general performance across all classes of discrete optimization problems is made.

1.5 MAIN CONTRIBUTIONS

The main contributions of this thesis are summarized as follows:

1. **Interval-based representation of swarm information:** A new weighting mechanism is formulated to represent the information contained in the current, personal-best, and global-best solutions directly in a discrete search space. The mechanism maps agreement and disagreement among these reference solutions to weighting intervals for the decision variables.

2. **Development of the WTPSO:** A new PSO-based approach is developed in which the conventional velocity and position update equations are replaced by interval-based weighting and constructive solution generation. This formulation operates without transfer functions and preserves the principal information sources of the original PSO.

3. **Development of the WTEPSO:** The proposed weighting mechanism is adapted to the evolutionary framework of the EPSO. This extension combines constructive discrete solution generation with the mutation and selection of strategic parameters, allowing their influence to evolve during the optimization process.

4. **Integration with feasibility-preserving topology construction:** The proposed weighting mechanism is integrated with Prim's algorithm to generate radial candidate topologies directly. The contribution lies in how swarm information is converted into branch priorities for the constructive procedure, rather than in Prim's algorithm itself.

5. **Adaptation to two distribution system optimization problems:** A common algorithmic principle is adapted to distribution system reconfiguration and service restoration, which have different objective functions and operating conditions but share a discrete and topology-dependent decision structure.

6. **Diversity- and quality-guided initialization for distribution system reconfiguration:** A dedicated initialization procedure is developed to generate a diverse set of feasible, high-quality radial topologies for the initial population of the reconfiguration problem. This procedure avoids purely random initialization and provides the proposed algorithms with a more informative starting population.

1.6 THESIS ORGANIZATION

The remainder of this thesis is organized as follows.

Chapter 2 reviews particle swarm optimization for discrete and combinatorial problems, including binary formulations, transfer-function-based approaches, hybrid and self-adaptive variants, and alternative discrete search paradigms. It also examines constraint- and feasibility-handling strategies, with particular emphasis on feasibility-preserving representations and constructive methods. The chapter then reviews metaheuristic approaches to distribution system reconfiguration and service restoration, and concludes with a comparative synthesis and the research gap this thesis addresses.

Chapter 3 presents a critical analysis of PSO-based methods for topology-dependent optimization in distribution systems. It discusses their problem-dependent components, including solution representation and initialization, candidate generation and information preservation, and structural and operational feasibility. Based on the common requirements and differences between reconfiguration and service restoration, the chapter establishes the methodological requirements for the proposed approaches.

Chapter 4 introduces the proposed WTPSO. It describes the representation and constructive generation of radial topologies, the tier-weighted branch-priority mechanism, the fitness-evaluation and constraint-handling procedure, the application-specific initialization procedures for reconfiguration and service restoration, and the complete WTPSO optimization procedure. The chapter also discusses the modularity of the proposed mechanism, introduces its extension to the evolutionary framework of the EPSO, and presents the BO procedure used for parameter calibration. The complete mathematical formulation and algorithmic procedure of the resulting WTEPSO are provided in Appendix A.

Chapter 5 applies the WTPSO and WTEPSO to distribution system reconfiguration. It presents the underlying nonlinear mathematical formulation, the MILP approximation used to obtain the benchmark solutions, the problem-specific representation and evaluation of candidate topologies, and the adaptations required by the evaluated metaheuristics. The computational study compares the metaheuristic results with the MILP benchmark values and evaluates solution quality, robustness, convergence behavior, computational effort, and the statistical significance and effect sizes of the observed differences.

Chapter 6 applies the proposed approaches to distribution system service restoration. It presents the mathematical formulation, the augmented post-fault network representation, and the problem-specific construction and evaluation of restoration plans. The results are compared with benchmarks from an MISOCP formulation and analyzed for solution quality, robustness, convergence behavior, and computational effort. The chapter also examines the operational performance and switching plans of the best- and worst-performing solutions observed across the independent runs.

Chapter 7 summarizes the principal methodological and computational findings, assesses the fulfillment of the thesis objectives, and presents directions for future research.

Appendix A provides the complete mathematical formulation and pseudocodes of the WTEPSO, including strategic-parameter mutation, tier-weighted topology construction, candidate evaluation, and selection within the evolutionary framework of the EPSO.

Appendix B lists the scientific production associated with the development of this thesis.

2 LITERATURE REVIEW

2.1 INTRODUCTION

The PSO was originally developed for continuous optimization, in which particle positions and velocities are represented by real-valued vectors and updated through algebraic operations (Kennedy; Eberhart, 1995). Its simple structure and use of individual and collective search information have motivated several extensions to discrete and combinatorial problems. These extensions include binary representations, transfer functions, probabilistic state transitions, set-based operators, and problem-specific update mechanisms (Kennedy; Eberhart, 1997; Macedo *et al.*, 2021; Zyl; Engelbrecht, 2023). Although they broaden the applicability of PSO, they also modify the original interpretations of position, velocity, and movement and may require additional mechanisms to generate admissible solutions.

This issue is particularly relevant in topology-dependent optimization, where individually valid decisions may collectively produce a disconnected, meshed, or otherwise inadmissible network. Distribution system reconfiguration and service restoration are representative examples. Both select branch states to define radial network topologies, but they differ in operating conditions, objective function, and treatment of unavailable or nonrestored components (Behbahani *et al.*, 2024a; Campoverde *et al.*, 2024; Wang *et al.*, 2020). Solution representation, candidate generation, and feasibility handling are therefore central to applying metaheuristics to these problems.

This chapter reviews the methodological elements directly related to this thesis's contributions. First, the main extensions of PSO to discrete and combinatorial optimization are examined. The principal strategies for handling structural and operational constraints are then discussed. Subsequently, metaheuristic applications to distribution system reconfiguration and service restoration are reviewed with emphasis on solution encoding, radiality preservation, and candidate evaluation. The chapter concludes with a comparative synthesis that identifies the research gap in preserving swarm information while directly constructing structurally feasible solutions. This synthesis supports the critical analysis developed in Chapter 3.

2.2 PARTICLE SWARM OPTIMIZATION FOR DISCRETE AND COMBINATORIAL OPTIMIZATION

Discrete extensions of PSO differ mainly in the particle representation, the transition mechanism used to generate new solutions, and the way in which the current, personal-best, and global-best solutions influence the search. The following subsections organize these methods into three groups: binary and transfer-function-based approaches, hybrid and self-adaptive variants, and alternative discrete representations.

2.2.1 Binary PSO and Transfer-Function-Based Approaches

The binary particle swarm optimization proposed by Kennedy e Eberhart (1997) represents particle positions as binary vectors. Velocity no longer denotes a physical displacement; instead, a transfer function maps it into a probability used to assign or change each binary state. The original formulation employs a sigmoid function, while later variants use S-, V-, Z-, U-, and X-shaped functions or adaptive and time-varying mappings (Beheshti, 2020; Guo; Wang; Guo, 2020; Mirjalili *et al.*, 2020; Beheshti, 2021b; Beheshti, 2021a).

These formulations retain the information sources of conventional PSO, because velocity is still calculated using the current, personal-best, and global-best positions. However, the transfer function and its binary update rule determine how that information is translated into a discrete candidate. S-shaped functions commonly define the probability of assigning one to a variable, whereas V-shaped functions usually define the probability of changing its current state. Adaptive variants alter the transition behavior during the search to initially favor broader exploration and later favor more localized changes.

Transfer functions provide a general interface between continuous swarm dynamics and binary decisions, but they normally update variables independently. Dependencies among branch states and properties such as connectivity, radiality, or sequencing are not represented explicitly. Consequently, binary encoding alone does not ensure structural feasibility; the required relationships must be introduced through the representation, a repair or decoding procedure, or a feasibility-preserving constructor (Macedo *et al.*, 2021).

2.2.2 Hybrid and self-adaptive PSO variants

Hybrid discrete PSO variants incorporate mechanisms such as crossover, mutation, local search, population reinitialization, clustering, or search-space reduction. These additions seek to preserve diversity, escape suboptimal regions, or refine promising solutions. Examples include the combination of BPSO with the sine–cosine algorithm and adaptive population structures that regulate exploration and exploitation according to the state of the swarm (Kumar; Bharti,

2021; Jin *et al.*, 2024). Such mechanisms can improve performance but also introduce additional operators and parameters whose effects should be distinguished from those of the underlying PSO.

The evolutionary particle swarm optimization (EPSO) combines PSO information sharing with evolutionary principles (Miranda; Fonseca, 2002a; Miranda; Fonseca, 2002b). Particles generate offspring, their strategic weights are mutated, and competing candidates are subjected to selection. The relative influence of the current state, personal experience, and collective information can therefore evolve during the optimization process rather than remaining fixed.

Hybridization and self-adaptation modify the search dynamics but do not independently define a valid representation for a discrete, structurally constrained problem. Their effectiveness depends on the transition or construction mechanism with which they are combined. Parameter adaptation may improve exploration, for example, but cannot by itself guarantee that the generated branch states form an admissible topology.

2.2.3 Alternative discrete representations and search paradigms

Other discrete approaches redefine the particle representation or the notion of movement instead of applying a transfer function to continuous velocity. Binary quantum-behaved formulations use probabilistic attractors and discrete state transitions, and recent variants incorporate adaptive parameters, diversity-preservation mechanisms, local search, and repair procedures (Sun *et al.*, 2007; Li; Fang; Zhu, 2023; Li *et al.*, 2024). Search-space reduction and multi-swarm structures have also been used to concentrate the search on promising combinations while preserving population diversity (Li; Xue; Zhang, 2021; Babukarthik *et al.*, 2021).

Set-based PSO provides a more direct reinterpretation of the conventional algorithm. Particle positions and movements are defined through operations on sets rather than arithmetic operations on real-valued vectors. This representation is appropriate when a solution is naturally expressed as a subset of components, such as selected edges, facilities, features, or switching actions (Zyl; Engelbrecht, 2023).

These paradigms demonstrate that discrete PSO need not depend on the bitwise transformation of a continuous velocity. A problem-compatible representation can produce more meaningful transitions and facilitate the inclusion of structural information. Nevertheless, operation in a discrete space does not automatically ensure feasibility; relationships among selected components must still be considered during candidate generation.

2.3 FEASIBILITY HANDLING IN DISCRETE AND TOPOLOGICAL OPTIMIZATION

In constrained combinatorial problems, admissible solutions may constitute only a small fraction of the search space. Variable-domain constraints define the values allowed for individual decisions, structural constraints establish relationships such as connectivity and radiality, and operational constraints impose limits on the resulting system state. In distribution systems, branch statuses are discrete; connectivity and radiality are structural properties; and voltage, current, and equipment capacity limits generally require power-flow analysis. An incomplete radiality condition may accept disconnected or meshed configurations as feasible (Wang *et al.*, 2020; Mahdavi *et al.*, 2023; Sun *et al.*, 2023).

Constraint-handling methods can be distinguished by the stage at which they address feasibility. Penalty and feasibility-based rules act during evaluation or selection; repair and decoding intervene between candidate generation and evaluation; and feasibility-preserving representations incorporate selected constraints directly into the construction process (Kulkarni *et al.*, 2021; Lagaros *et al.*, 2023; Rahimi *et al.*, 2023).

2.3.1 Penalization and feasibility-based selection

Penalty methods reduce the attractiveness of infeasible candidates according to the magnitude or number of their violations. They preserve the original search mechanism and can permit useful exploration near the feasibility boundary. Their behavior, however, depends on the balance between the objective function and the penalty terms. Weak penalties may favor infeasible solutions, whereas excessive penalties may discard useful near-feasible information. The difficulty increases when heterogeneous violations, such as disconnection, undervoltage, and equipment overload, must be combined in a common scale (Lagaros *et al.*, 2023).

Feasibility-based rules separate objective quality from constraint violation. Feasible candidates are preferred to infeasible ones; feasible candidates are compared through their objective values; and infeasible candidates are ranked according to their violation. This reduces dependence on penalty coefficients and can retain information from solutions approaching the feasible region (Çimen; Garip; Boz, 2021; Lagaros *et al.*, 2023; Rahimi *et al.*, 2023).

Neither approach prevents invalid candidates from being generated. When structural violations can be identified from the graph, rejecting them before power-flow analysis avoids expensive evaluations of topologies that cannot represent admissible operating states.

2.3.2 Repair and decoding procedures

Repair procedures modify an infeasible candidate until selected requirements are satisfied. In network optimization, this may involve reconnecting isolated components or removing edges that create loops. Repair allows generic search operators to be retained and can exploit problem knowledge, but extensive corrections may weaken the correspondence between the candidate generated by the metaheuristic and the solution ultimately evaluated (Salcedo-Sanz, 2009; Kulkarni *et al.*, 2021; Rahimi *et al.*, 2023). Repair can also introduce bias, because different infeasible candidates may be mapped to the same solution or a deterministic correction may repeatedly favor particular structures (Kramer, 2010; Lagaros *et al.*, 2023).

Decoder-based methods operate on an auxiliary representation, such as component priorities, continuous weights, or random keys, and map it to the combinatorial solution under evaluation. A suitably designed decoder can generate only feasible solutions while allowing the metaheuristic to use its original search operators. Random-key methods are a well-established example and have been combined with specialized decoders for radial distribution system reconfiguration (Gonçalves; Resende, 2011; Vargas; Romero; Franco, 2018).

The encoded-to-decoded mapping is not necessarily one-to-one. Different auxiliary vectors may generate the same topology, while a small change in one key may produce a substantial structural modification; therefore, the observed search behavior results from the interaction between the metaheuristic and the decoder. The current, personal-best, and global-best solutions must also remain compatible with the representation updated by the algorithm and the solutions actually evaluated (Kramer, 2010; Gonçalves; Resende, 2011).

Repair and decoding thus serve distinct roles. Repair corrects a candidate that has already violated the constraints, whereas decoding interprets an auxiliary representation to construct the final solution. A decoder can preserve feasibility by design, but its mapping and possible search bias must still be examined.

2.3.3 Feasibility-preserving representations and constructive methods

Feasibility-preserving approaches incorporate selected constraints into the representation or construction procedure. They reduce the effective search space by avoiding structurally invalid candidates rather than penalizing or correcting them after generation (Kramer, 2010; Kulkarni *et al.*, 2021; Rahimi *et al.*, 2023).

Graph-based representations are particularly suitable for topological optimization. A connected radial network can be represented as a spanning tree of the graph containing the available nodes and branches. Prim's algorithm constructs a minimum-weight spanning tree by successively adding admissible edges that connect new nodes to the growing tree (Prim, 1957). When

a metaheuristic generates or modifies the edge weights, the graph algorithm acts as a solution constructor rather than as an independent optimizer. Spanning-tree operators and Prim-based construction have been used in distribution system reconfiguration and restoration to generate radial candidates directly (Gautam *et al.*, 2020; Luo *et al.*, 2020; Sudhakar; Prasad, 2023).

Constructive feasibility reduces radiality repairs and reserves power-flow evaluations for structurally admissible topologies. It does not, however, guarantee compliance with voltage, current, power-balance, or substation-capacity limits, which depend on the operating point and must still be verified electrically. Structural construction is therefore commonly combined with operational evaluation and, when required, penalization or feasibility-based selection.

The constructor may itself introduce bias through branch ordering, edge weights, and tie-breaking rules. Its design must ensure that changes generated by the metaheuristic are meaningfully reflected in the resulting topology. For distribution system applications, a suitable division is to enforce connectivity and radiality during construction and verify operating constraints through power-flow analysis.

2.4 METAHEURISTICS FOR TOPOLOGICAL OPTIMIZATION IN DISTRIBUTION SYSTEMS

Distribution system reconfiguration and service restoration are discrete topological problems with nonlinear operating constraints. In both cases, performance depends not only on the general search mechanism but also on the network representation, the treatment of radiality and connectivity, and the cost of evaluating candidate solutions. Reconfiguration normally improves a network under normal or planned operation while supplying all in-service loads. Restoration acts after fault isolation and may leave healthy sections de-energized when complete restoration is infeasible. These differences affect the topology representation, objective function, and feasibility criteria.

2.4.1 Distribution system reconfiguration

Distribution system reconfiguration determines the states of sectionalizing and tie switches to obtain an improved operating topology. The classical objective is active power loss reduction, although the voltage profile, load balance, reliability, switching costs, renewable energy accommodation, and voltage stability have also been considered (Civanlar *et al.*, 1988; Baran; Wu, 1989; Mahdavi *et al.*, 2021; Behbahani *et al.*, 2024b). All in-service sections are normally required to remain energized in a connected radial configuration.

The problem has been addressed through branch exchange, mathematical programming, evolutionary algorithms, swarm-based methods, machine learning, and hybrid approaches.

Metaheuristics are particularly attractive when nonlinear power-flow calculations, multiple objectives, distributed resources, or large combinatorial spaces are considered (Mahdavi *et al.*, 2021; El-Fergany, 2024; Behbahani *et al.*, 2024b). Binary encodings provide a direct representation of branch states, but independent changes can create meshed or disconnected networks. Modifying the transition function of BPSO may improve search behavior without guaranteeing topological feasibility (Hizarci; Demirel; Turkay, 2022).

Problem-dependent mechanisms have therefore been introduced. Branch exchange preserves radiality by closing a branch and opening another in the resulting loop. Specialized evolutionary operators restrict offspring to radial configurations (Landeros; Koziel; Abdel-Fattah, 2019). Random-key decoders and spanning-tree-based algorithms construct connected radial candidates from auxiliary search variables (Vargas; Romero; Franco, 2018; Gautam *et al.*, 2020). Prim-based procedures similarly convert metaheuristic branch priorities into spanning trees (Luo *et al.*, 2020). Other methods restrict the search to predefined loops, corridors, or switch groups, reducing computational effort while potentially excluding configurations outside those structures (Gerez *et al.*, 2019; Geri *et al.*, 2023).

Candidate topologies are usually evaluated using a distribution power-flow analysis that provides losses, bus voltages, branch currents, and substation injections. The cumulative number of power-flow evaluations is therefore a meaningful measure of computational effort, particularly when algorithms generate different numbers of candidates per iteration. Fair comparisons also require a common electrical model, feasibility criteria, and stopping condition.

Mathematical programming provides optimality information or strong reference solutions when the formulation remains tractable, while metaheuristics offer flexibility for nonlinear evaluation and large combinatorial instances (Silveira *et al.*, 2021; Kerckhove; D'hulst; Hertem, 2024). Current research extends reconfiguration to active and dynamic networks with time-varying demand, renewable generation, remotely controlled switches, storage, and distributed generation (DG). Despite this broader scope, scalability, consistent evaluation, and radiality preservation remain fundamental requirements (Behbahani *et al.*, 2024b; El-Fergany, 2024).

2.4.2 Distribution system service restoration

Service restoration is initiated after a permanent fault has been isolated. The isolation actions may disconnect healthy downstream sections, and additional switching is used to restore as much interrupted demand as possible. Load restoration is generally the primary objective, while load priority, switching effort, operating losses, restoration time, and equipment availability may also be considered.

Restoration has been addressed through heuristic switching rules, graph traversal, branch exchange, mathematical programming, evolutionary algorithms, PSO, tabu search, ant colony

optimization, and other metaheuristics. Problem-dependent search remains important when multiple faults, large networks, or operational restrictions are considered. Tabu search has been applied to real networks with radiality and switching constraints, and Prim-based construction has been combined with metaheuristics to generate radial restoration proposals (Bosisio *et al.*, 2023; Sudhakar; Prasad, 2023).

Unlike conventional reconfiguration, restoration may include intentionally nonrestored healthy sections because of voltage, current, or source-capacity limits. A disconnected component is therefore not necessarily structurally invalid. Augmented-network formulations address this distinction by connecting affected sections to an artificial substation through artificial branches. This permits energized components supplied by real substations and nonrestored components to be represented within a unified graph (Vargas *et al.*, 2021). The same principle can support constructive metaheuristics in which real and artificial branches jointly define each candidate.

Evaluation must first identify the sections connected to real sources, because a closed branch within a de-energized component does not imply that the supply has been restored. The amount of restored demand and the switching effort are then calculated, and power-flow analysis verifies voltage, current, and source-capacity limits. Objective prioritization or appropriately scaled coefficients are commonly used to ensure that restoring demand takes precedence over reducing switching operations. Critical loads and different switch types may receive specific weights or operating costs.

Restoration can determine either a final post-fault topology or an ordered sequence of switching actions. Sequential formulations verify intermediate states and provide more detailed operational guidance, but they increase the number of variables and the number of electrical evaluations. The selected temporal representation must therefore be stated when methods are compared.

The integration of distributed energy resource (DER), storage, and grid-forming resources has extended restoration toward microgrid formation and islanded operation. Graph methods, clustering, mathematical programming, and heuristic algorithms have been used to form self-supplied islands (Igder; Liang; Mitolo, 2022). Reinforcement-learning approaches have also been proposed for dynamic microgrid formation and topology-aware outage management (Igder; Liang, 2023; Jacob *et al.*, 2024). Although they can provide rapid online decisions, they introduce requirements related to training scenarios, generalization, and verification under unseen conditions. Mathematical formulations remain essential benchmarks, but their computational effort may increase substantially with network size, fault multiplicity, and sequential decisions (Vargas *et al.*, 2021).

Table 1 - Main methodological characteristics of distribution system reconfiguration and service restoration.

Characteristic	Reconfiguration	Service restoration
Operating condition	Normal or planned operation	Post-fault emergency operation
Primary objective	Reduction of losses or improvement of operating performance	Maximization of restored demand, followed by reduction of switching operations
Load status	All in-service sections are normally energized	Healthy sections may remain nonrestored
Unavailable branches	Defined by the initial network and maintenance conditions	Faulted branches are unavailable, and isolation branches have imposed states
Topological structure	Radial topology connecting in-service sections to real substations	Radial energized components and an explicit representation of nonrestored sections
Temporal representation	Frequently, a static final topology	May be single-stage or include an ordered switching sequence
Operational evaluation	Losses, voltages, currents, and equipment limits	Energized load, voltages, currents, source capacities, and switching effort

Source: The author.

2.4.3 Common requirements and methodological differences

Reconfiguration and restoration share a graph-based branch-selection structure, but their solutions have different operational interpretations. Table 1 summarizes the principal distinctions.

Both applications require a meaningful correspondence between the search variables and network topology, preservation of the appropriate radiality and connectivity conditions, electrical evaluation of operating limits, and computational scalability. Their main difference lies in connectivity: reconfiguration normally supplies every in-service section, whereas restoration distinguishes energized, faulted, and temporarily nonrestored sections. A feasibility test designed exclusively for reconfiguration may therefore reject a valid restoration plan.

Their objectives also create different search landscapes. Reconfiguration candidates typically meet the same demand and are differentiated primarily by losses and other power-flow quantities. Restoration candidates may first differ in energized demand and switching requirements. Nevertheless, a common metaheuristic can address both problems when the representation, topology constructor, objective function, and feasibility assessment are adapted consistently. Comparisons among algorithms should retain these problem-dependent components and evaluation conditions so that observed differences can be attributed primarily to their search mechanisms.

Table 2 - Comparative synthesis of the main approaches reviewed for discrete and topological optimization.

Approach	Search mechanism	Feasibility treatment	Main trade-off
Transfer-function BPSO	Continuous velocity mapped into binary decisions	Usually penalty, rejection, or repair	General formulation, but mainly bitwise transitions
Hybrid and self-adaptive	Evolutionary, local-search, or parameter-adaptation mechanisms	Depends on the accompanying representation	Greater flexibility, with additional operators and parameters
Alternative discrete representations	Sets, probabilistic attractors, clusters, or specialized operators	Often embedded in the representation	Better structural correspondence, but lower generality
Penalty and feasibility rules	Original search mechanism is retained	Violations affect objective values or ranking	Simple integration, but invalid candidates are still generated
Repair	Candidates are corrected before evaluation or replacement	Problem-dependent modification	Recovers proposals, but may distort the generated information
Decoder	Auxiliary vectors are mapped into combinatorial solutions	May guarantee feasibility by construction	Separates search and construction, but mapping may be biased or many-to-one
Constructive graph method	Topologies are generated through graph-compatible rules	Structural feasibility is preserved	Avoids invalid topologies, but depends on the constructor and edge priorities

Source: The author.

2.5 COMPARATIVE SYNTHESIS OF THE REVIEWED APPROACHES

The reviewed methods combine solution representation, search dynamics, and feasibility handling in different ways. Objective values reported in separate studies are not directly comparable when test systems, operating limits, power-flow models, stopping conditions, and computational platforms differ. The methodological comparison in Table 2, therefore, focuses on how each family generates solutions and incorporates constraints.

For distribution systems, generic binary encodings remain attractive because branch states are naturally binary. Their independent updates, however, do not represent the dependencies imposed by radiality and connectivity. Branch exchange, specialized operators, random-key decoding, restricted search spaces, and spanning-tree construction incorporate these dependencies

in different ways (Landeros; Koziel; Abdel-Fattah, 2019; Vargas; Romero; Franco, 2018; Gautam *et al.*, 2020; Geri *et al.*, 2023). Restoration requires the additional distinction among energized, faulted, and nonrestored sections, for which an augmented graph provides a systematic representation (Vargas *et al.*, 2021).

Structural and operational constraints should be addressed at appropriate stages. Connectivity and radiality can often be enforced before evaluation, whereas voltage, current, power balance, and equipment-capacity limits require the electrical operating point. This separation prevents power-flow calculations from being spent on structurally inadmissible candidates. Mathematical formulations and metaheuristics then serve complementary purposes: the former provide optimality information and benchmarks when tractable, while the latter offer flexibility for specialized representations and large combinatorial instances (Silveira *et al.*, 2021; Kerckhove; D'hulst; Hertem, 2024).

Because metaheuristics are stochastic, their assessment should be based on multiple independent runs and descriptive statistics. Accordingly, performance is examined from complementary perspectives: solution quality and robustness are assessed by the statistical distribution of the objective values obtained; convergence behavior is analyzed across iterations; and computational effort is evaluated by the number of power-flow calculations and execution time. The minimum objective values are also compared with the available benchmark solutions. Together, these measures provide a broader assessment of solution quality, consistency, convergence, and computational efficiency.

2.6 RESEARCH GAP AND CHAPTER CONCLUSIONS

The literature provides numerous discrete PSO variants, hybrid mechanisms, graph constructors, and constraint-handling strategies. The research gap addressed in this thesis is therefore not the absence of methods capable of producing discrete solutions, but the integration of swarm search information with a representation that directly reflects the structure of a topological problem, and, more importantly, guaranteeing that information is transferred from one swarm to another.

Transfer-function methods retain the conventional velocity equation, but the combined influence of the current, personal-best, and global-best solutions becomes indirect after stochastic bitwise conversion. Repair may then be required when the resulting vector violates structural constraints. Decoders and constructive methods address feasibility more directly, but auxiliary priorities do not always preserve an explicit and interpretable correspondence with the information sources of PSO; moreover, the constructor may dominate the observed search behavior. Hybrid and self-adaptive mechanisms improve diversity and parameter control without independently resolving this representation issue.

The review consequently identifies the need for a search framework that:

1. represents discrete branch-selection decisions directly;
2. retains explicit contributions from the current, personal-best, and global-best solutions during candidate generation;
3. controls the relative influence of these sources without depending exclusively on continuous velocity and bitwise transfer functions;
4. generates structurally feasible topologies directly, reducing rejection and repair; and
5. supports reconfiguration and restoration through problem-dependent graph representations and a common search principle.

The last two requirements reflect the fact that radiality and connectivity are properties of the complete branch set rather than of individual decisions. Reconfiguration and restoration share this branch-selection structure, although restoration must additionally represent faulted and nonrestored sections. These differences should therefore be incorporated through the network representation and evaluation procedure rather than requiring an unrelated search mechanism for each application.

This chapter established the literature basis for integrating swarm information with feasibility-preserving topology construction. Chapter 3 examines the limitations of conventional particle updates in this context and derives the design principles subsequently used in the formulation of the WTPSO.

3 PARTICLE SWARM OPTIMIZATION FOR TOPOLOGICAL PROBLEMS IN DISTRIBUTION SYSTEMS

This chapter connects the literature review presented in Chapter 2 with the methodological development introduced in the following chapter. It examines the assumptions underlying the conventional particle-update mechanism and their implications for generating network topologies. Distribution system reconfiguration and service restoration are considered as representative applications because both require combinations of branch states that define admissible radial configurations.

The discussion first examines the conventional particle-update mechanism and its interpretation in a topological search space. It then identifies the problem-dependent requirements associated with solution representation, population initialization, candidate generation, and feasibility assessment. Finally, these observations are translated into design requirements for a particle-based method that preserves swarm information while directly constructing radial topologies.

3.1 CRITICAL ANALYSIS OF PARTICLE SWARM OPTIMIZATION APPLIED TO TOPOLOGICAL OPTIMIZATION PROBLEMS

The behavior of the swarm in conventional PSO is governed by the previous movement of each particle, its individual experience, and the information shared by the population. For particle i at iteration k, these elements are quantified through the velocity and position updates (Kennedy; Eberhart, 1995; Houssein *et al.*, 2021)

$$v_i^{k+1} = w v_i^k + c_1 r_1 \left[p_i^{\text{best}} - s_i^k \right] + c_2 r_2 \left[g^{\text{best}} - s_i^k \right], \tag{1}$$

$$s_i^{k+1} = s_i^k + v_i^{k+1}, \tag{2}$$

where s_i^k and v_i^k denote the position and velocity of the particle, p_i^{best} is its personal-best position, and g^{best} is the global-best position. The inertia weight w regulates the retention of the previous movement, while c_1 and c_2 control the influence of individual and collective experience. The random values r_1 and r_2, sampled from $[0,1]$, introduce stochastic variation into the transition.

The update of s_i^{k+1} is obtained through algebraic operations involving vectors of the same dimension and composition. This mechanism is naturally interpreted when particle positions lie in a real-valued vector space: vector subtraction defines a direction, scalar multiplication scales its magnitude, and vector addition yields another point in the same space. For continuous problems with bounded variables, the generated point can be returned to the prescribed domain through conventional boundary-handling rules. Satisfaction of the variable bounds does not guarantee compliance with every nonlinear constraint, but the algebraic movement itself remains well-defined and consistent with the representation (Marini; Walczak, 2015; Joshi; Gyanchandani; Wadhvani, 2021).

The situation changes when some decision variables are binary or integer. These domains are not closed under the addition and scalar multiplication used in (1) and (2); therefore, a direct update generally produces values outside the permitted discrete sets. In an mixed-integer nonlinear programming (MINLP) formulation, this difficulty coexists with nonlinear equality and inequality constraints. Thus, even when s_i^k, p_i^{best}, and g^{best} are individually feasible, their algebraic combination is not necessarily feasible. Additional mappings or problem-dependent procedures are required to recover the variable domains and the constraints, as reviewed in Chapter 2.

It is also important to distinguish the mathematical formulation of the optimization problem from the particle representation used by the metaheuristic. Although reconfiguration and restoration can be formulated as MINLP problems, a metaheuristic does not necessarily manipulate every continuous and discrete variable of those formulations. A particle may encode only the branch-selection decisions, while the continuous electrical state is determined subsequently by solving the power flow. This reduces the dimension of the search vector but does not resolve the topological constraint.

When branch states represent a particle position, each element has a clear numerical and physical interpretation. Nevertheless, a radial topology is defined by the relationship among all selected branches. The numerical difference between two branch-status vectors indicates which components differ, but it does not constitute a topologically valid direction of movement. Similarly, the algebraic combination of radial solutions does not necessarily produce another radial solution because the set of spanning-tree configurations is discrete and is not closed under the operations in (1) and (2). The resulting branch combination may disconnect part of the network, create loops, or fail to represent the required number of energized components.

This limitation becomes more restrictive as the solution dimension and the number of structural relationships increase. A feasible current topology may therefore generate an infeasible successor, even when both the personal-best and global-best topologies are feasible. As discussed in Section 2.3, correction or construction procedures can restore structural feasibility, but extensive transformation can weaken the correspondence between the information combined by

the swarm and the topology ultimately evaluated.

The conventional formulation consequently relies on three conditions that should not be assumed automatically in a topological problem: the particle representation must belong to a space in which the required algebraic operations are defined; those operations must provide a meaningful notion of movement; and the updated position must retain a coherent relationship with the solution subjected to evaluation. Continuous numerical problems generally satisfy the first two conditions directly, whereas radial network optimization does not.

The central methodological challenge is therefore not the numerical representation of binary states itself. It is the definition of a transition mechanism that combines the qualitative principles of PSO—retention of current information, individual experience, and collective experience—without assuming that arithmetic displacement between branch-status vectors preserves the graph structure. This observation provides the basis for the problem-dependent requirements examined in the following section.

3.2 PROBLEM-DEPENDENT COMPONENTS OF TOPOLOGICAL METAHEURISTICS

Although metaheuristics differ in their transition mechanisms, their application to distribution system topology problems requires a common set of problem-dependent components: solution representation, initial population generation, candidate construction, objective function evaluation, feasibility treatment, and a stopping criterion. The choice of these components can influence performance as strongly as the general search mechanism.

3.2.1 Solution representation and initial population

A solution representation must identify the state of the branches relevant to the operating problem and permit unambiguous reconstruction of the associated network topology. A binary vector ordered according to the available branches provides a direct physical interpretation, but an arbitrary vector does not necessarily satisfy radiality or connectivity. An auxiliary representation based on priorities or weights can instead be translated into a radial topology through a graph constructor. In either case, the representation updated by the metaheuristic must remain consistent with the topology used to calculate the objective function.

Population initialization must provide structurally admissible candidates with sufficient diversity. Purely random branch states may produce a large proportion of invalid networks, especially as the problem size increases. A graph-based procedure can generate radial candidates directly; for example, random branch priorities can be processed by a spanning-tree algorithm such as Prim's algorithm (Prim, 1957). The purpose of initialization is not only to obtain feasible topologies but also to cover different regions of the admissible search space without imposing

excessive bias toward a narrow family of configurations.

3.2.2 Candidate generation and information preservation

The transition mechanism determines how the current population uses previously successful solutions. In PSO, the new candidate should reflect information from the current, personal-best, and global-best positions. In a topological problem, this information can be interpreted as the relative preference assigned to the branches that appear in those configurations. A construction procedure can then transform the resulting branch preferences into a complete radial topology.

This separation between preference generation and topology construction is useful only if the two stages remain coherent. If the constructor overrides most of the information produced by the search mechanism, the new topology may behave almost independently of the particle update. Conversely, if branch preferences meaningfully influence the probability of selecting each admissible edge, the resulting candidate retains a traceable relationship with the configurations from which it was generated.

The constructor must also permit adequate exploration. Always selecting the strongest inherited branches can rapidly concentrate the population, whereas excessive randomization can weaken the influence of the best solutions. A suitable mechanism must therefore regulate the relative contributions of current and historical information while preserving sufficient diversity to explore alternative radial configurations.

3.2.3 Structural and operational feasibility

Structural and operational feasibility should be treated at different stages. Connectivity and radiality can be verified or enforced using the network graph before performing an electrical calculation. A topology that violates these requirements cannot represent an admissible operating configuration and need not be subjected to power-flow analysis.

A structurally valid topology may nevertheless violate voltage-magnitude, branch-current, power-balance, or substation-capacity limits. These constraints depend on the operating state and are assessed through power-flow analysis. The objective value and the operational-feasibility information obtained from this calculation determine whether the candidate replaces the current or historical solution. This separation avoids unnecessary electrical evaluations while preserving the physical assessment required by the problem.

3.3 IMPLICATIONS FOR RECONFIGURATION AND SERVICE RESTORATION

Reconfiguration and service restoration share the same fundamental branch-selection structure, but the meaning of connectivity differs, as summarized in Section 2.4.3. In reconfiguration, the selected branches must normally form a radial topology connecting all in-service sections to real substations. Candidate configurations are mainly differentiated by electrical performance, such as active power losses, because the supplied demand is generally unchanged.

Restoration begins from an isolated post-fault network. Faulted branches are unavailable, isolation decisions may be imposed, and some healthy sections may remain nonrestored when complete supply recovery is infeasible. The representation must therefore distinguish sections energized from real sources from those assigned to the nonrestored portion of the network. An augmented graph containing artificial connections can express these states within a common constructive framework, while the objective function prioritizes restored demand and subsequently accounts for switching effort and operational restrictions.

These differences do not require unrelated search mechanisms. A common particle-based principle can generate branch preferences for both applications, provided that the graph supplied to the constructor reflects the operating condition of each problem. Reconfiguration uses the available normal-operation network, whereas restoration uses the augmented post-fault network. The objective function and electrical-feasibility assessment are likewise problem-dependent.

This distinction supports a modular method: the swarm mechanism determines how information is combined; the network representation defines which branches and sources are available; the graph constructor produces a structurally admissible topology; and the power-flow model evaluates its operating condition. Keeping these roles explicit permits the same search principle to be examined in both applications without treating them as identical optimization problems.

3.4 METHODOLOGICAL REQUIREMENTS FOR DISTRIBUTION SYSTEM TOPOLOGY OPTIMIZATION

The preceding analysis indicates that a particle-based method for distribution system topology optimization should satisfy the following requirements:

1. represent branch-selection information in a form compatible with the network graph;
2. maintain explicit contributions from the current, personal-best, and global-best solutions;
3. translate these contributions into branch preferences without relying on independent bitwise transitions;
4. generate connected radial topologies directly, thereby reducing rejection and repair;

5. preserve population diversity during initialization and candidate generation;
6. separate structural construction from power-flow-based operational evaluation; and
7. support reconfiguration and restoration through problem-dependent graph models and a common search principle.

These requirements clarify the methodological gap identified in Chapter 2. The central challenge is to combine swarm information in a manner that remains meaningful after a graph constructor converts it into a complete network topology. Feasibility preservation should not eliminate exploration, and the construction procedure should not obscure the contributions of the solutions guiding the particle.

The following chapter develops the weighted tier particle swarm optimization (WTPSO) from these requirements. The method replaces the conventional velocity–position update with a tier-weighted branch-priority mechanism that combines information from the current, individual-best, and global-best topologies. Prim's algorithm processes the resulting branch priorities to construct radial topologies directly. The complete formulation, application-specific initialization procedures, fitness evaluation and constraint handling, topology-construction rules, and parameter-calibration procedure are presented in that chapter. The modularity of the proposed mechanism and its extension to the evolutionary framework of the EPSO, resulting in the WTEPSO, are also introduced.

4 WEIGHTED TIER PARTICLE SWARM OPTIMIZATION

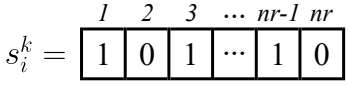
4.1 INTRODUCTION

This chapter presents the mathematical and algorithmic formulation of the proposed WTPSO, developed in response to the limitations identified in Chapter 3. Its central contribution is a structure-preserving combinatorial transition mechanism that replaces the conventional velocity–position update defined by (1) and (2). The proposed mechanism uses the information contained in the current position s_i^k, the individual-best position p_i^{best}, and the global-best position g^{best} to assign priorities to the network branches. Prim's algorithm subsequently processes these priorities to directly construct new connected radial topologies. Although the conventional arithmetic movement of the particles is replaced, the proposed formulation retains the principal information-sharing elements of PSO: a population of particles, current and individual-best positions, global guidance, iterative best-solution updates, and parameters regulating individual influence, social influence, and the exploration–exploitation balance. The resulting mechanism applies to both distribution system reconfiguration and service restoration. The graph construction, branch encoding, objective function, and application-specific feasibility conditions are defined separately in the corresponding application chapters.

Initially, this chapter describes the binary representation and constructive generation of radial topologies. The tier-weighted branch-priority mechanism is then introduced, and the expressions defining its interval bounds as functions of w, c_1, and c_2 are derived. The resulting structure-preserving topology-generation procedure is formalized through pseudocode, including its stochastic sampling and deterministic tie-breaking rules. The general fitness-evaluation and constraint-handling procedure is then defined, explicitly separating topological radiality from electrical and operational feasibility. The initialization procedures for reconfiguration and service restoration are presented next, followed by the complete WTPSO optimization procedure and its iteration-dependent inertia weight.

The modularity of the proposed mechanism and its extension to the WTEPSO are subsequently discussed, while the complete mathematical formulation and pseudocodes of the WTEPSO are provided in Appendix A. Finally, the common parameter-calibration procedure based on BO is presented, whereas the application-specific calibration settings and results are reported in the corresponding application chapters.

Figure 1 - Representation of a solution proposal.



Source: The author.

4.2 GENERATION OF RADIAL TOPOLOGIES

Let $G = (\Omega_n, \Omega_b)$ denote the connected graph associated with the application, where $n_b = |\Omega_n|$ and $n_r = |\Omega_b|$ are the numbers of nodes and branches, respectively. Each solution proposal is represented by a binary branch-status vector $s_i^k \in \{0,1\}^{n_r}$, as illustrated in Fig. 1. Its entry $s_{ij}^k = 0$ indicates that branch j is open in particle i at iteration k, whereas $s_{ij}^k = 1$ indicates that it is closed. The application under consideration defines the correspondence between the vector positions and the network branches. In reconfiguration, positions are associated with the branches whose operating statuses can be modified. In restoration, they are associated with the branches included in the post-fault topology-construction graph. The detailed encoding used in each case is defined in the corresponding application chapter. Although the entries of s_i^k are numerical, they act as discrete indicators encoding the network topology and cannot be directly manipulated through the conventional arithmetic velocity–position operations of PSO. For a radial solution, the closed branches must form a connected spanning tree. Consequently, the vector contains exactly $n_b - 1$ entries equal to one.

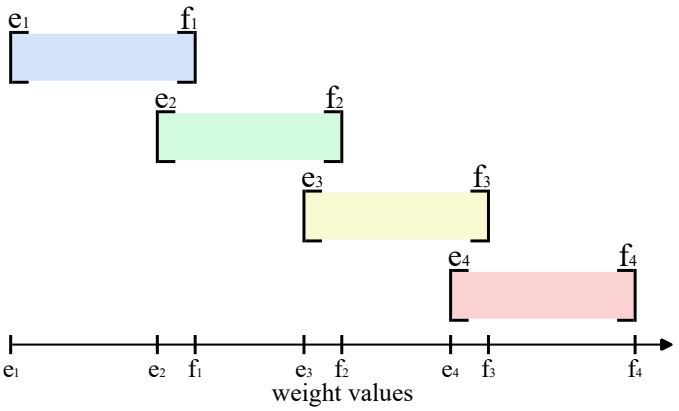
Prim's algorithm is used as the fundamental strategy for generating radial topologies. As an exact and computationally efficient method, it can be naturally integrated into metaheuristic frameworks and has previously been applied to distribution system reconfiguration (Luo *et al.*, 2020; Vargas; Romero; Franco, 2018; Sudhakar; Prasad, 2023). In this work, the same constructive principle is used for both reconfiguration and restoration, with Prim's algorithm operating on the graph defined for each application. Its low processing time is particularly relevant when compared with the computational cost of the power flow evaluations required to assess solution quality.

The WTPSO departs from the linear combination of (1)–(2) and introduces a structure-preserving combinatorial mechanism guided by three principles:

- The solution proposals s_i^k, p_i^{best}, and g^{best} must contribute to generating s_i^{k+1}.
- The quality information existing in s_i^k, p_i^{best}, and g^{best} must be transferred to s_i^{k+1}.
- The transfer of quality information and the guarantee of a radial topology in s_i^{k+1} are achieved using Prim's algorithm.

To achieve this, each branch is assigned a weight before applying Prim's algorithm. The

Figure 2 - Intervals used to assign branch weights based on the topological agreement of the current solution proposals s_i^k, p_i^{best}, and g^{best}.



Source: The author.

weight reflects the level of topological agreement among s_i^k, p_i^{best}, and g^{best} regarding the closed status of that branch. Four intervals are defined: $[e_1, f_1]$, $[e_2, f_2]$, $[e_3, f_3]$, and $[e_4, f_4]$, corresponding to decreasing topological agreement:

- If branch b_j is closed in all three solution proposals, i.e., $(s_{ij}^k, p_{ij}^{\text{best}}, g_j^{\text{best}}) = (1,1,1)$, its weight is sampled from the interval $[e_1, f_1]$.
- If branch b_j is closed in two solution proposals, i.e., exactly two entries of $(s_{ij}^k, p_{ij}^{\text{best}}, g_j^{\text{best}})$ are equal to 1, its weight is sampled from the interval $[e_2, f_2]$.
- If branch b_j is closed in only one solution proposal, i.e., exactly one entry of $(s_{ij}^k, p_{ij}^{\text{best}}, g_j^{\text{best}})$ is equal to 1, its weight is sampled from the interval $[e_3, f_3]$.
- If branch b_j is open in all three solution proposals, i.e., $(s_{ij}^k, p_{ij}^{\text{best}}, g_j^{\text{best}}) = (0,0,0)$, its weight is sampled from the interval $[e_4, f_4]$.

After sampling the branch weights, Prim's algorithm determines the new radial topology. As illustrated in Fig. 2, the intervals are ordered so that $[e_1, f_1]$ generates the smallest weights, favoring branches consistently closed across the current solution proposals. The remaining intervals correspond to progressively lower levels of topological agreement.

The stochastic sampling of weights within each interval introduces controlled diversity while preserving structural patterns. The intentional overlap between intervals increases flexibility, prevents overly deterministic behavior, and supports exploration of alternative high-quality solutions without compromising radiality.

Based on this mechanism, the next subsection defines the mathematical expressions used to determine the bounds of the intervals $[e_1, f_1]$, $[e_2, f_2]$, $[e_3, f_3]$, and $[e_4, f_4]$, expressed as functions of the parameters w, c_1, and c_2.

4.3 COMPUTATION OF INTERVAL BOUNDS

Although the parameters w, c_1, and c_2 originate from the traditional PSO formulation, their mathematical roles are reinterpreted in the WTPSO, while their conceptual purpose of regulating the exploration–exploitation balance is preserved. Instead of influencing particle velocity, as in the classical update mechanism, these parameters now govern the interval-based weighting strategy for selecting branches when constructing new solution proposals.

The bounds of each interval $[e_m, f_m]$, where $m \in \{1,2,3,4\}$, are defined as a function of the inertia weight w and the cognitive and social coefficients, c_1 and c_2, respectively. The parameter m indicates the level of topological agreement, with $m = 1$ assigned to branches that are closed in all the current solution proposals, s_i^k, p_i^{best}, and g^{best}, and $m = 4$ to branches open in all of them.

The inertia weight $w \in [0,1]$ regulates the degree of overlap between intervals and, consequently, the level of randomness in the weight assignment process. This effect is captured by the base bounds e_m^w and f_m^w, computed as:

$$[e_m^w, f_m^w] = [(m-1)(1-w), (m-1)(1-w)+1] \qquad \forall m \in \{1,2,3,4\} \tag{3}$$

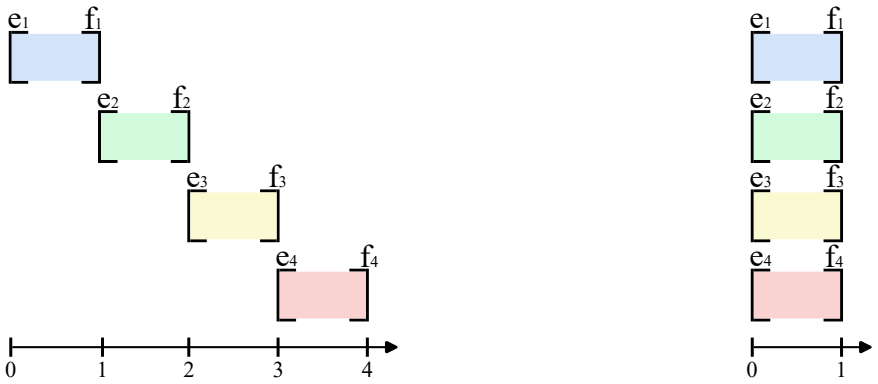
These expressions generate four intervals of equal length whose relative position depends on the value of w. For instance, when $w = 0$, the resulting intervals are $[0,1]$, $[1,2]$, $[2,3]$, and $[3,4]$ for $m = 1,2,3,4$, respectively, producing non-overlapping regions and therefore a more deterministic selection scheme, as illustrated in Fig. 3a. In contrast, when $w = 1$, all intervals are $[0,1]$, yielding complete overlap and a stochastic behavior, as shown in Fig. 3b.

Therefore, increasing w within $[0,1]$ expands the overlap between intervals and intensifies the stochasticity of the interval-based weighting strategy, whereas smaller values of w make the process more deterministic.

Subsequently, the cognitive and social coefficients, c_1 and c_2, respectively, assume values in the interval $[0,0.5]$ and influence the length of the four intervals by adjusting their boundaries according to the desired influence of p_i^{best} and g^{best} on the generation of new solution proposals. The coefficient c_1 guides each particle toward its own best local solution, while c_2 drives the particles toward the global best solution; incorporating these coefficients into the computation of the interval bounds allows the algorithm to regulate how much individual and collective learning affects the weight assignment process.

To illustrate how the cognitive and social coefficients affect the interval bounds, consider an iteration k in which branch b_j has the status entries $(s_{ij}^k, p_{ij}^{\text{best}}, g_j^{\text{best}}) = (1,0,1)$. This implies that two of the solution proposals (s_i^k and g^{best}) consider branch b_j closed, which corresponds to the

Figure 3 - (a) Intervals when the inertia weight is zero ($w = 0$) and (b) intervals when the inertia weight is one ($w = 1$).



(a) $w = 0$ (b) $w = 1$

Source: The author.

Figure 4 - Interval $[e_2, f_2]$ under the influence of c_1 and c_2 when a branch is closed in two current solution proposals (s_i^k and g^{best}) (a) when the social coefficient is greater than the cognitive coefficient ($c_2 > c_1$) and (b) when the cognitive coefficient is greater than the social coefficient ($c_1 > c_2$).



(a) $c_2 > c_1$ (b) $c_1 > c_2$

Source: The author.

second interval $[e_2, f_2]$. If the influence of g^{best} (i.e., $c_2 > c_1$) is established as more significant, the strategy should favor a smaller weight to increase the likelihood that branch b_j remains closed in the new solution proposal. This is achieved by reducing the upper bound of the interval, as shown in Fig. 4a, resulting in a shorter range shifted toward lower values. Conversely, if the influence of p_i^{best} is established as stronger ($c_1 > c_2$), then a higher weight is more likely to ensure the branch becomes open in the new solution proposal. In this case, the lower bound of the interval is increased, as illustrated in Fig. 4b, shifting the interval toward higher values. These interval modifications reflect the dynamic weighting mechanism guided by the relative contributions of the cognitive and social coefficients in the WTPSO.

This reasoning extends to the remaining cases, in which interval adjustments follow the same principle, guided by topological agreement and by the influence of c_1 and c_2.

Following this logic, the final expressions for calculating the bounds of each interval $[e_m, f_m]$, incorporating the influence of c_1, c_2, and w, are presented below. Four distinct cases are considered, each corresponding to a different level of topological agreement.

- Branch b_j closed in all the current solution proposals: $(s_{ij}^k, p_{ij}^{\text{best}}, g_j^{\text{best}}) = (1,1,1)$.

$$[e_1, f_1] = [e_1^w, f_1^w - (c_1 + c_2)] \tag{4}$$

- Branch b_j closed in two current solution proposals:

  a) s_i^k *and* p_i^{best}*:* $(s_{ij}^k, p_{ij}^{\text{best}}, g_j^{\text{best}}) = (1,1,0)$.

$$[e_{2a}, f_{2a}] = [e_2^w + c_2, f_2^w - c_1] \tag{5}$$

  b) s_i^k *and* g^{best}*:* $(s_{ij}^k, p_{ij}^{\text{best}}, g_j^{\text{best}}) = (1,0,1)$.

$$[e_{2b}, f_{2b}] = [e_2^w + c_1, f_2^w - c_2] \tag{6}$$

  c) p_i^{best} *and* g^{best}*:* $(s_{ij}^k, p_{ij}^{\text{best}}, g_j^{\text{best}}) = (0,1,1)$.

$$[e_{2c}, f_{2c}] = [e_2^w, f_2^w - (c_1 + c_2)] \tag{7}$$

- Branch b_j closed in only one current solution proposal:

  a) s_i^k*:* $(s_{ij}^k, p_{ij}^{\text{best}}, g_j^{\text{best}}) = (1,0,0)$.

$$[e_{3a}, f_{3a}] = [e_3^w + (c_1 + c_2), f_3^w] \tag{8}$$

  b) p_i^{best}*:* $(s_{ij}^k, p_{ij}^{\text{best}}, g_j^{\text{best}}) = (0,1,0)$.

$$[e_{3b}, f_{3b}] = [e_3^w + c_2, f_3^w - c_1] \tag{9}$$

  c) g^{best}*:* $(s_{ij}^k, p_{ij}^{\text{best}}, g_j^{\text{best}}) = (0,0,1)$.

$$[e_{3c}, f_{3c}] = [e_3^w + c_1, f_3^w - c_2] \tag{10}$$

- Branch b_j open in all the current solution proposals: $(s_{ij}^k, p_{ij}^{\text{best}}, g_j^{\text{best}}) = (0,0,0)$.

$$[e_4, f_4] = [e_4^w + (c_1 + c_2), f_4^w] \tag{11}$$

Where e_1^w, e_2^w, e_3^w, e_4^w and f_1^w, f_2^w, f_3^w, f_4^w denote the lower and upper bounds of each interval, computed based on the inertia weight w, according to (3). Thus, the bounds presented in (4)–(11) are calculated in advance, in a pre-processing phase, whenever the parameters w, c_1 and c_2 are kept fixed throughout the optimization process. Otherwise, the bounds must be recalculated at each iteration as these parameters vary.

Using the interval bounds defined above, Algorithm 1 summarizes the complete structure-preserving procedure for constructing s_i^{k+1}. For each test system, the substation node is adopted

Algorithm 1 - Tier-weighted construction of a radial topology

Require: Connected graph $G = (\Omega_n, \Omega_b)$ with ordered branches $\Omega_b = (b_1, \ldots, b_{n_r})$; root node $r = n_{\mathrm{SE}}$; binary vectors s_i^k, p_i^{best}, and g^{best}; parameters w, c_1, and c_2
Ensure: New binary radial topology s_i^{k+1}

for $m = 1, \ldots, 4$ **do**
  $[e_m^w, f_m^w] \leftarrow [(m-1)(1-w), (m-1)(1-w)+1]$
end for
for $j = 1, \ldots, n_r$ **do**
  $(x, p, g) \leftarrow (s_{ij}^k, p_{ij}^{\mathrm{best}}, g_j^{\mathrm{best}})$
  if $(x, p, g) = (1,1,1)$ **then**
    $\alpha \leftarrow 1, \quad [e_\alpha, f_\alpha] \leftarrow [e_1^w, f_1^w - (c_1 + c_2)]$
  else if $(x, p, g) = (1,1,0)$ **then**
    $\alpha \leftarrow 2\mathrm{a}, \quad [e_\alpha, f_\alpha] \leftarrow [e_2^w + c_2, f_2^w - c_1]$
  else if $(x, p, g) = (1,0,1)$ **then**
    $\alpha \leftarrow 2\mathrm{b}, \quad [e_\alpha, f_\alpha] \leftarrow [e_2^w + c_1, f_2^w - c_2]$
  else if $(x, p, g) = (0,1,1)$ **then**
    $\alpha \leftarrow 2\mathrm{c}, \quad [e_\alpha, f_\alpha] \leftarrow [e_2^w, f_2^w - (c_1 + c_2)]$
  else if $(x, p, g) = (1,0,0)$ **then**
    $\alpha \leftarrow 3\mathrm{a}, \quad [e_\alpha, f_\alpha] \leftarrow [e_3^w + (c_1 + c_2), f_3^w]$
  else if $(x, p, g) = (0,1,0)$ **then**
    $\alpha \leftarrow 3\mathrm{b}, \quad [e_\alpha, f_\alpha] \leftarrow [e_3^w + c_2, f_3^w - c_1]$
  else if $(x, p, g) = (0,0,1)$ **then**
    $\alpha \leftarrow 3\mathrm{c}, \quad [e_\alpha, f_\alpha] \leftarrow [e_3^w + c_1, f_3^w - c_2]$
  else
    $\alpha \leftarrow 4, \quad [e_\alpha, f_\alpha] \leftarrow [e_4^w + (c_1 + c_2), f_4^w]$
  end if
  Draw $u_{ij}^k \sim \mathscr{U}(0,1)$
  $\phi_{ij}^k \leftarrow e_\alpha + (f_\alpha - e_\alpha) u_{ij}^k$
end for
$T_i^{k+1} \leftarrow \mathrm{DeterministicPrim}\big(G, \phi_i^k, r\big)$
  Prim rule: an edge is eligible if exactly one endpoint belongs to the partial tree; among eligible edges, select the one with the lexicographically smallest pair (ϕ_{ij}^k, j).
$s_i^{k+1} \leftarrow \mathrm{BinaryEdgeVector}\big(T_i^{k+1}, \Omega_b\big)$
return s_i^{k+1}

Source: The author.

as the fixed root r of Prim's algorithm. For each branch, the appropriate interval is selected according to its status in the three guiding topologies, s_i^k, p_i^{best}, and g^{best}. A weight is then sampled from this interval, and the resulting branch weights are supplied to Prim's algorithm to generate the new radial topology.

4.4 FITNESS EVALUATION AND CONSTRAINT HANDLING

The topology-construction procedure and the application-specific feasibility assessment are treated as two distinct stages. Let $a \in \{\mathrm{rec}, \mathrm{rest}\}$ identify the reconfiguration or restoration application, respectively. In both cases, the application graph $G = (\Omega_n, \Omega_b)$ is constructed before the optimization process from the corresponding network representation.

For each particle, the tier-weighted branch-priority mechanism generates a branch-weight

vector, which is subsequently processed by Prim's algorithm. Provided that the application graph is connected, Prim's algorithm returns a spanning tree that contains all nodes of the graph and exactly $|\Omega_n| - 1$ branches. Therefore, the generated topology is connected and acyclic by construction, without requiring a radiality-repair procedure or topological penalty. This structural guarantee does not, however, imply satisfaction of the electrical and operational constraints associated with the application.

Each radial solution proposal s_i^k is subsequently evaluated using the corresponding network data $\mathscr{D}^a$. Let $\mathscr{C}^a(s_i^k)$ denote the convergence indicator of the application-specific power-flow evaluation:

$$\mathscr{C}^a(s_i^k) = \begin{cases} 1, & \text{if the power-flow evaluation converges,} \\ 0, & \text{otherwise.} \end{cases} \tag{12}$$

When $\mathscr{C}^a(s_i^k) = 1$, the resulting electrical quantities are used to verify the operating constraints defined for application a. These constraints may include voltage and current limits, branch-flow limits, power-balance conditions, load-supply requirements, and other application-specific operational conditions. Their complete definitions are provided in the corresponding application chapters.

The overall feasibility indicator is defined as

$$\text{feasible}^a(s_i^k) = \begin{cases} 1, & \mathscr{C}^a(s_i^k) = 1 \text{ and all constraints associated} \\ & \text{with application } a \text{ are satisfied,} \\ 0, & \text{otherwise.} \end{cases} \tag{13}$$

Let $J^a(s_i^k)$ denote the application-specific objective value, expressed in minimization form. The fitness assigned to a candidate topology during the iterative optimization process is

$$F^a(s_i^k) = \begin{cases} J^a(s_i^k), & \text{feasible}^a(s_i^k) = 1, \\ +\infty, & \text{feasible}^a(s_i^k) = 0. \end{cases} \tag{14}$$

For reconfiguration, J^{rec} represents the active-power-loss objective, while for restoration, J^{rest} represents the restoration objective defined in its application chapter. Thus, radiality is guaranteed by the topology-construction procedure, whereas power-flow convergence and full electrical feasibility are assessed separately.

In the algorithms presented in this chapter, these operations are summarized by

$$(\text{feasible}^a, J^a) \leftarrow \text{EvaluateSolution}\,(\mathscr{D}^a, s)\,. \tag{15}$$

The operation EvaluateSolution performs the application-specific power-flow calculation, verifies the corresponding operating constraints, and returns the objective value when the solution is feasible. Otherwise, it returns $\text{feasible}^a = 0$, and the calling algorithm assigns $F^a(s) = +\infty$ according to (14).

4.5 GENERATION OF INITIAL RADIAL TOPOLOGIES

The initialization strategy depends on the application considered. For distribution system reconfiguration, the original operating topology is included in the population, while the remaining topologies are generated through a guided stochastic procedure based on cycle identification and apparent-power ranking. For distribution system restoration, the population is generated from the post-fault network using randomly weighted spanning trees. Both procedures construct radial topologies, which are subsequently evaluated according to the application-specific objective function and electrical-feasibility criteria.

4.5.1 Initialization for distribution system reconfiguration

At the initialization stage, N^{pop} radial topologies are assembled to form the initial population. The original operating topology is assigned to the first member, s_1^0, while the remaining $N^{\text{pop}} - 1$ topologies are generated using the guided stochastic procedure described below. Although random spanning trees can be generated by assigning random branch weights and applying Prim's algorithm, this strategy may produce low-quality initial topologies, particularly for large systems. Moreover, radiality alone does not guarantee power-flow convergence or satisfaction of the electrical operating limits. The proposed initialization therefore combines a cycle-based topology-construction rule with an apparent-power-based ranking criterion.

First, an auxiliary fully meshed configuration is formed by closing all available branches. A single AC power flow is performed for this configuration, and the resulting apparent branch-power values, S_j^{power}, are stored as fixed reference values. The auxiliary configuration is used exclusively to obtain these values; it is neither included in the population nor assigned a fitness value. This reference power-flow operation is performed as a preprocessing step and is not included in the common power-flow-evaluation budget.

To generate each new topology, the procedure starts with all available branches closed. At each branch-opening step h, a cycle Γ_h is identified in the current energized topology through a depth-first search starting from the substation node $r = n_{\text{SE}}$. After a branch is opened, the cycle-identification procedure is repeated on the updated topology.

Only branches belonging to Γ_h are eligible for opening. Thus, a branch outside the currently identified cycle cannot be selected, regardless of its apparent power value. The eligible branches are ordered by increasing (S_j^{power}, j), where the branch index j provides deterministic tie-breaking when equal apparent-power values occur.

Suppose that the current cycle contains $q = |\Gamma_h|$ eligible branches, ordered as $(j_1, \ldots, j_q)$. Following the rank-based selection scheme proposed in Mendoza *et al.* (2006), the interval $[0,1]$ is divided into q equal subintervals. The probability density and its cumulative distribution function are defined as

$$\begin{aligned} f_\rho(x) &= -2(\rho-1)x + \rho, \\ \Phi_\rho(x) &= \int_0^x f_\rho(t)\,dt = \rho x - (\rho-1)x^2, \qquad 0 \le x \le 1, \end{aligned} \tag{16}$$

where $\rho \in [1,2]$ controls the preference for branches occupying the first positions in the ranking. The probability assigned to branch j_ℓ is

$$\pi_\ell = \Phi_\rho\left(\frac{\ell}{q}\right) - \Phi_\rho\left(\frac{\ell-1}{q}\right), \qquad \ell = 1, \ldots, q. \tag{17}$$

In this work, $\rho = 1.5$ is adopted, resulting in $f_\rho(x) = 1.5 - x$. Consequently, branches carrying lower apparent power in the auxiliary configuration have a higher probability of being opened, while branches occupying the remaining ranking positions retain a nonzero selection probability. This preserves stochastic diversity among the generated topologies.

The probabilities satisfy $\sum_{\ell=1}^{q} \pi_\ell = 1$. A random number $u \sim \mathscr{U}(0,1)$ is generated, and the first ranking position whose cumulative probability reaches or exceeds u is selected. The corresponding branch is then opened.

Because the selected branch is part of a cycle, it is a non-bridge edge. Opening it breaks the current cycle without disconnecting the network. The cycle is updated after each opening, whereas the reference values S_j^{power} remain fixed. Therefore, no additional reference power flow is required during the topology-construction process.

For a connected network containing n_r available branches and n_b nodes, the required number of branch openings is

$$n_{\text{lig}} = n_r - n_b + 1. \tag{18}$$

After n_{lig} branch openings, connectivity has been preserved and the resulting topology contains exactly $n_b - 1$ closed branches. Therefore, the resulting topology is a radial spanning tree. The cycle-based eligibility rule guarantees connectivity and radiality, whereas the apparent-

Algorithm 2 - Guided stochastic generation of the initial population for distribution system reconfiguration

Require: Network data $\mathscr{D}^{\text{rec}}$; connected graph $G = (\Omega_n, \Omega_b)$, with $n_b = |\Omega_n|$ nodes and $n_r = |\Omega_b|$ branches; root node $r = n_{\text{SE}}$; population size N^{pop}
Ensure: Initial population S^0; fitness vector F^0; number of power-flow evaluations N_{PF}

$S^0 \leftarrow \emptyset$, $F^0 \leftarrow \emptyset$, $N_{\text{PF}} \leftarrow 0$, $\rho \leftarrow 1.5$
$s^{\text{ini}} \leftarrow \text{OriginalTopology}(\mathscr{D}^{\text{rec}})$
$(\text{feasible}^{\text{ini}}, J^{\text{ini}}) \leftarrow \text{EvaluateSolution}(\mathscr{D}^{\text{rec}}, s^{\text{ini}})$
$N_{\text{PF}} \leftarrow N_{\text{PF}} + 1$
$S^0 \leftarrow [s^{\text{ini}}], \quad F^0 \leftarrow [F^{\text{ini}}]$
$s^{\text{mesh}} \leftarrow 1_{n_r}$ ▷ All branches closed
$S^{\text{power}} \leftarrow \text{EvaluateReferencePowerFlow}(\mathscr{D}^{\text{rec}}, s^{\text{mesh}})$ ▷ Outside the evaluation budget
$\Phi_\rho(x) \leftarrow \rho x - (\rho - 1)x^2$
$n_{\text{lig}} \leftarrow n_r - n_b + 1$
for $i = 2, \ldots, N^{\text{pop}}$ **do**
    $s \leftarrow 1_{n_r}$ ▷ All branches closed
    for $h = 1, \ldots, n_{\text{lig}}$ **do**
        $\Gamma_h \leftarrow \text{IdentifyCycle}(G, s, r)$
        Sort the branches in Γ_h by increasing (S_j^{power}, j)
        Let $(j_1, \ldots, j_q)$ denote the resulting order, where $q = |\Gamma_h|$
        for $\ell = 1, \ldots, q$ **do**
            $\pi_\ell \leftarrow \Phi_\rho\left(\frac{\ell}{q}\right) - \Phi_\rho\left(\frac{\ell - 1}{q}\right)$
        end for
        Draw $u \sim \mathscr{U}(0,1)$
        $\ell^\star \leftarrow \min\left\{\ell : u \leq \sum_{t=1}^{\ell} \pi_t\right\}$
        $s_{j_{\ell^\star}} \leftarrow 0$ ▷ Open the selected cycle branch
    end for
    $(\text{feasible}, J) \leftarrow \text{EvaluateSolution}(\mathscr{D}^{\text{rec}}, s)$
    $N_{\text{PF}} \leftarrow N_{\text{PF}} + 1$
    if feasible $= 1$ **then**
        $F \leftarrow J$
    else
        $F \leftarrow +\infty$
    end if
    $S^0 \leftarrow [S^0; s], \quad F^0 \leftarrow [F^0; F]$
end for
return S^0, F^0, and N_{PF}

Source: The author.

power ranking only guides the stochastic branch selection.

Each generated topology is evaluated using the fitness and constraint-handling procedure defined in Subsection 4.4. Electrically infeasible radial topologies and repeated topologies are retained in the initial population. An electrically infeasible topology is assigned $F^{\text{rec}}(s) = +\infty$. The process continues until the population contains N^{pop} members, as summarized in Algorithm 2.

Algorithm 3 - Generation of the initial population for distribution system restoration

Require: Restoration data $\mathscr{D}^{\text{rest}}$; connected post-fault graph $G^{\text{post}} = (\Omega_n, \Omega_b^{\text{post}})$; root node r; population size N^{pop}
Ensure: Initial population S^0; fitness vector F^0; number of power-flow evaluations N_{PF}

$S^0 \leftarrow \emptyset$, $F^0 \leftarrow \emptyset$, $N_{\text{PF}} \leftarrow 0$
$s^{\text{ini}} \leftarrow \text{PostFaultTopology}(\mathscr{D}^{\text{rest}})$
$(\text{feasible}^{\text{ini}}, J^{\text{ini}}) \leftarrow \text{EvaluateSolution}(\mathscr{D}^{\text{rest}}, s^{\text{ini}})$
$N_{\text{PF}} \leftarrow N_{\text{PF}} + 1$
if $\text{feasible}^{\text{ini}} = 1$ **then**
    $F^{\text{ini}} \leftarrow J^{\text{ini}}$
else
    $F^{\text{ini}} \leftarrow +\infty$
end if
$S^0 \leftarrow [s^{\text{ini}}], \quad F^0 \leftarrow [F^{\text{ini}}]$
for $i = 2, \ldots, N^{\text{pop}}$ **do**
    for $j = 1, \ldots, |\Omega_b^{\text{post}}|$ **do**
        Draw $\phi_j \sim \mathscr{U}(0,1)$
    end for
    $T \leftarrow \text{DeterministicPrim}(G^{\text{post}}, \phi, r)$
    $s \leftarrow \text{BinaryEdgeVector}(T, \Omega_b^{\text{post}})$
    $(\text{feasible}, J) \leftarrow \text{EvaluateSolution}(\mathscr{D}^{\text{rest}}, s)$
    $N_{\text{PF}} \leftarrow N_{\text{PF}} + 1$
    if $\text{feasible} = 1$ **then**
        $F \leftarrow J$
    else
        $F \leftarrow +\infty$
    end if
    $S^0 \leftarrow [S^0; s], \quad F^0 \leftarrow [F^0; F]$
end for
return S^0, F^0, and N_{PF}

Source: The author.

4.5.2 Initialization for distribution system restoration

For distribution system restoration, the initial population is generated from the post-fault graph after faulted components have been isolated. Random weights are assigned to the available candidate branches, and Prim's algorithm is applied to generate each radial solution proposal. Consequently, every generated topology is a spanning tree of the post-fault graph whenever that graph remains connected.

Each generated topology is evaluated using the restoration objective function and the corresponding electrical and operational constraints, as defined in the restoration application chapter. Electrically infeasible or repeated solution proposals are rejected and regenerated. This process continues until the population contains N^{pop} valid radial topologies. Therefore, although the initialization strategies differ between reconfiguration and restoration, both use Prim's algorithm as the constructive mechanism for generating radial solution proposals.

The restoration initialization procedure is summarized in Algorithm 3. The post-fault operating topology is assigned to the first population member, while the remaining members are generated by assigning random branch weights and applying Prim's algorithm.

4.6 COMPLETE WTPSO OPTIMIZATION PROCEDURE

Algorithm 4 summarizes the complete WTPSO procedure for distribution system reconfiguration and restoration. The general optimization structure is common to both applications, whereas the graph construction, initial-population generation, objective function, and problem-specific constraints are defined according to the application under consideration. The initialization procedures for reconfiguration and restoration are presented in Algorithms 2 and 3, respectively. The generation of each new radial topology is performed by the tier-weighted branch-priority mechanism described in Algorithm 1, while fitness evaluation and constraint handling follow the procedure defined in Subsection 4.4.

The tier-weighted mechanism employs an iteration-dependent inertia weight rather than a constant value. Following the linearly decreasing strategy adopted in Prastyo, Hidayat e Ardiyanto (2022), its value at iteration k is calculated as

$$w(k) = \max\left\{w_{\min},\ w_{\max} - k\left(\frac{w_{\max} - w_{\min}}{k_w}\right)\right\}. \tag{19}$$

Thus, $w(k)$ decreases linearly from $w_{\max}$ to $w_{\min}$ during the first k_w iterations and remains equal to $w_{\min}$ thereafter. Since $w(k)$ defines the interval bounds employed by the tier-weighted mechanism, these bounds are recalculated at each iteration using the current value of $w(k)$. Larger initial values promote exploration through greater interval overlap, whereas the progressive reduction of $w(k)$ decreases this overlap and increases the influence of promising solutions.

The maximum number of power-flow evaluations, $N_{\mathrm{PF}}^{\max}$, is adopted as the stopping criterion. This budget includes the evaluation of the N^{pop} initial population members and all candidate solutions generated during the iterative process.

The proposed tier-weighted mechanism is modular because the construction of new topologies is separated from the application-specific fitness evaluation. Consequently, the same optimization structure can be applied to both reconfiguration and restoration by supplying the corresponding graph, network data, objective function, and operational constraints. The following section discusses the incorporation of this mechanism into the EPSO.

4.7 MODULARITY OF THE WTPSO AND EXTENSION TO THE WTEPSO

The tier-weighted branch-priority mechanism introduced in the WTPSO is modular because the topology-construction operator is separated from the remaining components of the optimization procedure. Its function is to transform information from the current, personal-best, and global-best topologies into branch priorities, which are subsequently mapped by Prim's algorithm into a radial topology. Consequently, this constructive operator can be incorporated into other

Algorithm 4 - Complete WTPSO optimization procedure

Require: Application $a \in \{\text{rec}, \text{rest}\}$; connected application graph $G^a = (\Omega_n^a, \Omega_b^a)$; application data $\mathscr{D}^a$; root node r^a; population size N^{pop}; maximum number of power-flow evaluations $N_{\text{PF}}^{\max}$; inertia-transition iteration k_w; parameters $w_{\min}$, $w_{\max}$, c_1, and c_2; random seed ξ
Ensure: Best topology g^{best} and its fitness F_g^{best}

Initialize the pseudorandom generator using seed ξ
if $a = \text{rec}$ **then**
    $(S^0, F^0, N_{\text{PF}}) \leftarrow \text{InitialPopulationReconfiguration}\big(G^a, \mathscr{D}^a, r^a, N^{\text{pop}}\big)$ ▷ Algorithm 2
else
    $(S^0, F^0, N_{\text{PF}}) \leftarrow \text{InitialPopulationRestoration}\big(G^a, \mathscr{D}^a, r^a, N^{\text{pop}}\big)$ ▷ Algorithm 3
end if
for $i = 1, \ldots, N^{\text{pop}}$ **do**
    $(p_i^{\text{best}}, F_i^{\text{best}}) \leftarrow (s_i^0, F_i^0)$
end for
$i^\star \leftarrow \min\big(\arg\min_{1 \le i \le N^{\text{pop}}} F_i^{\text{best}}\big)$
$(g^{\text{best}}, F_g^{\text{best}}) \leftarrow (p_{i^\star}^{\text{best}}, F_{i^\star}^{\text{best}})$
$k \leftarrow 0$
while $N_{\text{PF}} < N_{\text{PF}}^{\max}$ **do**
    $w(k) \leftarrow \max\left\{w_{\min},\ w_{\max} - k\left(\dfrac{w_{\max} - w_{\min}}{k_w}\right)\right\}$
    for $i = 1, \ldots, N^{\text{pop}}$ **do**
        $s_i^{k+1} \leftarrow \text{TierWeightedTree}\big(G^a, s_i^k, p_i^{\text{best}}, g^{\text{best}}, w(k), c_1, c_2, r^a\big)$ ▷ Algorithm 1
        $(\text{feasible}_i^{k+1}, J_i^{k+1}) \leftarrow \text{EvaluateSolution}\big(\mathscr{D}^a, s_i^{k+1}\big)$
        $N_{\text{PF}} \leftarrow N_{\text{PF}} + 1$
        if $\text{feasible}_i^{k+1} = 1$ **then**
            $F_i^{k+1} \leftarrow J_i^{k+1}$
        else
            $F_i^{k+1} \leftarrow +\infty$
        end if
        if $F_i^{k+1} < F_i^{\text{best}}$ **then**
            $(p_i^{\text{best}}, F_i^{\text{best}}) \leftarrow (s_i^{k+1}, F_i^{k+1})$
        end if
    end for
    $i^\star \leftarrow \min\big(\arg\min_{1 \le i \le N^{\text{pop}}} F_i^{\text{best}}\big)$
    if $F_{i^\star}^{\text{best}} < F_g^{\text{best}}$ **then**
        $(g^{\text{best}}, F_g^{\text{best}}) \leftarrow (p_{i^\star}^{\text{best}}, F_{i^\star}^{\text{best}})$
    end if
    $k \leftarrow k + 1$
end while
return g^{best} and F_g^{best}

Source: The author.

compatible population-based optimization methods without modifying the application-specific objective function, constraint-handling procedure, initialization strategy, or stopping criterion.

Given this modularity, the tier-weighted mechanism is incorporated into the EPSO, yielding the weighted tier evolutionary particle swarm optimization (WTEPSO). The replication, strategic-parameter mutation, evaluation, and selection mechanisms of the EPSO are retained. However, the conventional velocity–position update used to generate new solution proposals is replaced by the tier-weighted branch-priority mechanism followed by Prim's algorithm. The resulting method therefore combines the evolutionary and self-adaptive characteristics of the EPSO with

the structure-preserving topology-construction mechanism introduced in the WTPSO.

The complete mathematical formulation of the WTEPSO is provided in Appendix A. The tier-weighted construction of each radial candidate is summarized in Algorithm 5, while the complete optimization procedure, including initialization, mutation, candidate generation, evaluation, and selection, is presented in Algorithm 6.

4.8 PARAMETER CALIBRATION VIA BAYESIAN OPTIMIZATION

The performance of metaheuristic algorithms depends on the selection of their control parameters, making parameter calibration an optimization problem in its own right (Roman *et al.*, 2016; Rüther; Rieck, 2024). In this work, BO is adopted as a common calibration procedure for the proposed WTPSO and WTEPSO, as well as for the metaheuristics employed as comparison methods. Calibration is performed independently for each algorithm, test system, and application $a \in \{\text{rec}, \text{rest}\}$.

BO is particularly suitable for computationally expensive black-box optimization problems (Frazier, 2018; Hildebrandt *et al.*, 2024). At each evaluation, the previously assessed parameter configurations and their corresponding objective values are used to update a Gaussian-process surrogate model. The expected-improvement-plus acquisition function then selects the next configuration by balancing exploration of the parameter space and exploitation of regions with promising predicted performance.

Because the evaluated metaheuristics are stochastic, each candidate parameter configuration θ is assessed over $R_{\text{cal}} = 15$ calibration runs. Let $J_v^a(\theta)$ denote the final application-specific objective value obtained in calibration run v. The criterion supplied to BO is

$$J_{\text{cal}}^a(\theta) = \overline{J}^a(\theta) + s_J^a(\theta) = \frac{1}{R_{\text{cal}}} \sum_{v=1}^{R_{\text{cal}}} J_v^a(\theta) + s_J^a(\theta), \tag{20}$$

where $\overline{J}^a(\theta)$ and $s_J^a(\theta)$ are, respectively, the sample mean and sample standard deviation of the objective values obtained over the calibration runs. Therefore, $J_{\text{cal}}^a(\theta)$ is a mean–dispersion criterion that favors parameter configurations providing both good average performance and low run-to-run variability. The standard deviation is used directly as a unit-weight variability penalty.

For $a = \text{rec}$, $J_v^a(\theta)$ corresponds to the final active-power-loss value obtained under the reconfiguration constraints. For $a = \text{rest}$, it corresponds to the final restoration objective value defined in the corresponding application chapter. In both cases, solution evaluation follows the application-specific objective function and constraint-handling procedure defined in Section 4.4.

Each BO run comprises 30 objective evaluations: 10 configurations from the initial design and 20 selected adaptively via the acquisition function. A fixed pseudorandom seed is used to

initialize each BO run. In addition, every candidate parameter configuration within a given calibration process is evaluated using the same fixed set of $R_{\text{cal}} = 15$ calibration seeds. Consequently, the empirical objective value obtained for a given parameter configuration is reproducible and is treated as deterministic by `bayesopt`.

After completing the 30 evaluations, the parameter configuration with the lowest observed value of $J^{a}_{\text{cal}}(\theta)$ is selected. The selected parameters are then fixed before the final comparative experiments that use random seeds disjoint from those used during calibration.

The algorithm-specific search domains, selected parameter configurations, population sizes, power-flow-evaluation budgets, and seed sets are reported in the corresponding reconfiguration and restoration application chapters. Within each test system and application, the compared methods use the same network data, power-flow procedure, electrical-feasibility criteria, and prescribed stopping budget.

5 APPLICATION TO DISTRIBUTION SYSTEM RECONFIGURATION

5.1 INTRODUCTION

Distribution system reconfiguration is a representative application for evaluating topology-oriented optimization methods, since it requires searching among alternative radial configurations while satisfying the network's electrical and operational constraints. It therefore provides an appropriate framework for assessing the solution-generation mechanisms introduced in Chapter 4.

This chapter applies the proposed WTPSO and WTEPSO to the reconfiguration problem aimed at minimizing active power losses. Their performance is compared with the EPSO, BPSO, and CE metaheuristics, while the solutions obtained from an MILP approximation are used as reference benchmarks. The comparative evaluation examines final solution quality, run-to-run variability, convergence as a function of power-flow evaluations and wall-clock time, and total computational time. Pairwise statistical comparisons are also conducted to assess the significance and magnitude of the observed differences.

The chapter first presents the mathematical formulation describing the physical, operational, and topological requirements of the reconfiguration problem. It then describes the problem-specific application of the metaheuristics, including the correspondence between the solution representation and the network branches, the construction of radial topologies, and their evaluation through power-flow calculations. Finally, the computational results are presented and discussed, including the calibrated control parameters, benchmark solutions, and comparative performance of the evaluated methods.

5.2 MATHEMATICAL FORMULATION OF THE RECONFIGURATION PROBLEM

Distribution system reconfiguration involves modifying the open or closed status of the available branches to minimize active power losses while maintaining a connected radial topology and satisfying the electrical and operational constraints. Because the problem combines binary topology decisions with nonlinear power-flow relations, it is initially represented as an mixed-integer nonlinear programming (MINLP).

Let Ω_n and Ω_b denote the sets of nodes and branches, respectively, and let n_{SE} denote the

substation node. For each branch $ij \in \Omega_b$, R_{ij}, X_{ij}, and Z_{ij} denote its resistance, reactance, and impedance magnitude, respectively, with $Z_{ij}^2 = R_{ij}^2 + X_{ij}^2$. The active and reactive demands at node i are denoted by P_i^D and Q_i^D, while P_i^G and Q_i^G represent the corresponding power injections.

The variables P_{ij} and Q_{ij} represent the active and reactive power flows through branch ij, while I_{ij}^{sqr} and V_i^{sqr} represent the squared branch-current and node-voltage magnitudes, respectively. The binary variables y_{ij}^+ and y_{ij}^- indicate whether branch ij is energized in the i-to-j or j-to-i direction. Therefore, $y_{ij}^+ + y_{ij}^-$ represents the energized status of branch ij. Based on the formulation presented in Borges, Franco e Rider (2014), the reconfiguration problem is initially expressed as follows:

$$\text{minimize} \quad \sum_{ij \in \Omega_b} R_{ij} I_{ij}^{\text{sqr}} \tag{21}$$

Subject to:

$$\sum_{ki \in \Omega_b} P_{ki} - \sum_{ij \in \Omega_b} \left(P_{ij} + R_{ij} I_{ij}^{\text{sqr}} \right) + P_i^G = P_i^D, \qquad \forall i \in \Omega_n \tag{22}$$

$$\sum_{ki \in \Omega_b} Q_{ki} - \sum_{ij \in \Omega_b} \left(Q_{ij} + X_{ij} I_{ij}^{\text{sqr}} \right) + Q_i^G = Q_i^D, \qquad \forall i \in \Omega_n \tag{23}$$

$$V_i^{\text{sqr}} - V_j^{\text{sqr}} = 2\left(R_{ij} P_{ij} + X_{ij} Q_{ij} \right) + Z_{ij}^2 I_{ij}^{\text{sqr}} + \zeta_{ij}, \qquad \forall ij \in \Omega_b \tag{24}$$

$$\zeta_{ij} \leq \left(\overline{V}^2 - \underline{V}^2 \right) \left(1 - y_{ij}^+ - y_{ij}^- \right), \qquad \forall ij \in \Omega_b \tag{25}$$

$$-\zeta_{ij} \leq \left(\overline{V}^2 - \underline{V}^2 \right) \left(1 - y_{ij}^+ - y_{ij}^- \right), \qquad \forall ij \in \Omega_b \tag{26}$$

$$V_j^{\text{sqr}} I_{ij}^{\text{sqr}} = P_{ij}^2 + Q_{ij}^2, \qquad \forall ij \in \Omega_b \tag{27}$$

$$\underline{V}^2 \leq V_i^{\text{sqr}} \leq \overline{V}^2, \qquad \forall i \in \Omega_n \tag{28}$$

$$0 \leq I_{ij}^{\text{sqr}} \leq \bar{I}_{ij}^2 \left(y_{ij}^+ + y_{ij}^- \right), \qquad \forall ij \in \Omega_b \tag{29}$$

$$P_{ij}^+ - P_{ij}^- = P_{ij}, \qquad \forall ij \in \Omega_b \tag{30}$$

$$0 \leq P_{ij}^+ \leq \overline{V}\, \bar{I}_{ij} y_{ij}^+, \qquad \forall ij \in \Omega_b \tag{31}$$

$$0 \leq P_{ij}^- \leq \overline{V}\, \bar{I}_{ij} y_{ij}^-, \qquad \forall ij \in \Omega_b \tag{32}$$

$$-\overline{V}\, \bar{I}_{ij} \left(y_{ij}^+ + y_{ij}^- \right) \leq Q_{ij} \leq \overline{V}\, \bar{I}_{ij} \left(y_{ij}^+ + y_{ij}^- \right), \qquad \forall ij \in \Omega_b \tag{33}$$

$$\sum_{ij \in \Omega_b} \left(y_{ij}^+ + y_{ij}^- \right) = |\Omega_n| - 1, \tag{34}$$

$$\sum_{ij \in \Omega_b} y_{ij}^+ + \sum_{ji \in \Omega_b} y_{ji}^- = 1, \qquad \forall j \in \Omega_n \setminus \{n_{\text{SE}}\} \tag{35}$$

$$y_{ij}^+ + y_{ij}^- \leq 1, \qquad \forall ij \in \Omega_b \tag{36}$$

$$y_{ij}^+, y_{ij}^- \in \{0, 1\}, \qquad \forall ij \in \Omega_b. \tag{37}$$

In model (21)–(37), $I_{ij}^{\mathrm{sqr}} = I_{ij}^2$ and $V_i^{\mathrm{sqr}} = V_i^2$. The objective function (21) minimizes active power losses. Constraints (22) and (23) enforce the nodal active- and reactive-power balances, while (24) represents the branch voltage drop. Constraints (25) and (26) bound the auxiliary variable ζ_{ij}, activating the voltage-drop relation when the branch is energized and relaxing it otherwise. The nonlinear relation among voltage, current, and power flow is imposed by (27). Voltage and current limits are enforced by (28) and (29), respectively. Constraint (30) decomposes the active-power flow into nonnegative directional components, whose activation is controlled by y_{ij}^{+} and y_{ij}^{-} through (31) and (32). The reactive-power flow is bounded by (33). Radiality is enforced by the tree-cardinality constraint (34), the unique-supply condition for every non-substation node in (35), and the mutually exclusive branch directions in (36). The binary domains of the directional variables are specified in (37).

The formulation is classified as an MINLP because (27) contains a product of continuous variables and quadratic power-flow terms. To obtain the MILP formulation used to compute the benchmark solutions, constraint (27) is replaced by a piecewise-linear approximation. Let N_v denote the number of voltage-discretization variables and W the number of blocks used in the piecewise-linear approximation.

$$\Delta^V = \frac{\overline{V}^2 - \underline{V}^2}{N_v + 1}, \qquad \Delta_{ij}^S = \frac{\overline{V}\,\overline{I}_{ij}}{W}, \qquad m_{ij,w}^S = (2w-1)\Delta_{ij}^S \tag{38}$$

$$\underline{V}^2 + \Delta^V \sum_{s=1}^{N_v} x_{j,s} \le V_j^{\mathrm{sqr}} \le \underline{V}^2 + \Delta^V \left(1 + \sum_{s=1}^{N_v} x_{j,s}\right), \qquad \forall j \in \Omega_n \tag{39}$$

$$x_{j,s} \le x_{j,s-1}, \qquad \forall j \in \Omega_n, \quad s = 2,\ldots,N_v \tag{40}$$

$$x_{j,s} \in \{0,1\}, \qquad \forall j \in \Omega_n, \quad s = 1,\ldots,N_v \tag{41}$$

$$0 \le P_{ij,s}^c \le \Delta^V \overline{I}_{ij}^2 x_{j,s}, \qquad \forall ij \in \Omega_b, \quad s = 1,\ldots,N_v \tag{42}$$

$$P_{ij,s}^c \le \Delta^V I_{ij}^{\mathrm{sqr}}, \qquad \forall ij \in \Omega_b, \quad s = 1,\ldots,N_v \tag{43}$$

$$P_{ij,s}^c \ge \Delta^V I_{ij}^{\mathrm{sqr}} - \Delta^V \overline{I}_{ij}^2 (1 - x_{j,s}), \qquad \forall ij \in \Omega_b, \quad s = 1,\ldots,N_v \tag{44}$$

$$\left(\underline{V}^2 + \frac{\Delta^V}{2}\right) I_{ij}^{\mathrm{sqr}} + \sum_{s=1}^{N_v} P_{ij,s}^c = \sum_{w=1}^{W} m_{ij,w}^S \left(\Delta_{ij,w}^P + \Delta_{ij,w}^Q\right), \qquad \forall ij \in \Omega_b \tag{45}$$

$$P_{ij}^{+} + P_{ij}^{-} = \sum_{w=1}^{W} \Delta_{ij,w}^P, \qquad \forall ij \in \Omega_b \tag{46}$$

$$Q_{ij}^{+} - Q_{ij}^{-} = Q_{ij}, \qquad \forall ij \in \Omega_b \tag{47}$$

$$Q_{ij}^{+} + Q_{ij}^{-} = \sum_{w=1}^{W} \Delta_{ij,w}^{Q}, \qquad \forall ij \in \Omega_b \tag{48}$$

$$Q_{ij}^{+}, Q_{ij}^{-} \geq 0, \qquad \forall ij \in \Omega_b \tag{49}$$

$$0 \leq \Delta_{ij,w}^{P} \leq \Delta_{ij}^{S}, \qquad \forall ij \in \Omega_b, \quad w = 1, \ldots, W \tag{50}$$

$$0 \leq \Delta_{ij,w}^{Q} \leq \Delta_{ij}^{S}, \qquad \forall ij \in \Omega_b, \quad w = 1, \ldots, W. \tag{51}$$

Equation (38) defines the voltage-discretization step, the width of the piecewise-linear power blocks, and their corresponding slopes. Constraints (39)–(44) identify the voltage interval and linearize the correction terms associated with the product $V_j^{\mathrm{sqr}} I_{ij}^{\mathrm{sqr}}$. Equation (45) replaces the nonlinear equality (27) by combining the voltage discretization with piecewise-linear approximations of the squared active and reactive power flows. Constraints (46)–(51) define the corresponding nonnegative flow components and bounded block variables. The approximation resolution is controlled by N_v and W, with finer discretizations increasing the model size.

The model comprising (21)–(26), (28)–(37), and (38)–(51) constitutes the MILP approximation implemented in AMPL and solved with CPLEX to obtain the benchmark solutions used in this chapter. The adopted values of N_v and W are reported with the computational settings in Section 5.4.

5.3 APPLICATION OF THE METAHEURISTICS TO THE RECONFIGURATION PROBLEM

As illustrated in Fig. 1, each solution proposal is represented by a binary branch-status vector whose entries follow the fixed ordering of the available branches in Ω_b. For branch ij, the corresponding status is equivalent to $y_{ij}^{+} + y_{ij}^{-}$ in the mathematical formulation: a value of 1 indicates an energized branch, whereas a value of 0 indicates an open branch. Consequently, the zero-valued entries of the solution vector directly define the open-switch configuration.

Each candidate topology is evaluated through the EvaluateSolution$(\mathscr{D}^{\mathrm{rec}}, s)$ operation defined in Section 4.4. An AC power flow is performed using the branch statuses represented by s. If the power flow converges and the electrical and operational requirements of the reconfiguration model are satisfied, the active-power losses defined by (21) are assigned as the candidate fitness. Otherwise, the topology is classified as electrically infeasible and assigned infinite fitness according to (14). In particular, the voltage and current limits are those defined in (28) and (29), respectively.

The WTPSO and WTEPSO were applied to the reconfiguration problem using the complete optimization procedures presented in Algorithms 4 and 6, respectively. The comparative EPSO implementation, based on Miranda e Fonseca (2002b), updates continuous branch-weight vectors

through its evolutionary operators and supplies the resulting weights to Prim's algorithm. The CE method, adapted from Sebaa, Gelen e Nouri (2019), samples branch-weight vectors from an adaptive probability distribution, constructs radial topologies using Prim's algorithm, and updates the distribution based on the elite solutions. Therefore, the WTPSO, WTEPSO, EPSO, and CE satisfy the topological requirements of (34)–(36) through their constructive spanning-tree representation. The BPSO implementation, based on Hizarci, Demirel e Turkay (2022), uses a sigmoid transfer function to generate binary branch-status vectors. Since this operation does not preserve radiality by construction, each resulting configuration is checked for connectivity and for the presence of exactly $|\Omega_n| - 1$ energized branches. Nonradial configurations are rejected before the power-flow calculation and assigned infinite fitness; no radiality-repair procedure is applied.

To ensure a controlled comparison, all methods use the reconfiguration initialization procedure defined in Algorithm 2, together with the same network data, AC power-flow routine, objective function, electrical-feasibility criteria, and maximum power-flow-evaluation budget $N_{\mathrm{PF}}^{\max}$. Therefore, the methods differ primarily in the search mechanism used to generate new candidate topologies. Their control parameters are calibrated according to the common BO protocol defined in Section 4.8.

5.4 RESULTS

This section presents the computational results obtained for the 33-, 84-, 136-, and 415-node distribution systems. The results are organized into three parts: parameter calibration and experimental settings, benchmark solutions obtained using the MILP approximation, and the comparative performance of the evaluated metaheuristics.

5.4.1 Parameter calibration and experimental settings

The common BO procedure defined in Section 4.8 was applied independently to each metaheuristic and test system. For the reconfiguration application, $J_{\nu}^{\mathrm{rec}}(\theta)$ corresponds to the final active-power loss obtained in calibration run ν for parameter configuration θ. Each BO run was initialized with the pseudorandom seed $\xi_{\mathrm{BO}} = 84001$, and every candidate configuration was evaluated using the fixed calibration-seed set $\mathscr{S}_{\mathrm{cal}}^{\mathrm{rec}} = \{841001, \ldots, 841015\}$. The search domains for the EPSO, BPSO, and CE parameters were selected to encompass values commonly adopted in their original and related studies (Miranda; Fonseca, 2002b; Hizarci; Demirel; Turkay, 2022; Sebaa; Gelen; Nouri, 2019). The domains of $w_{\min}$, $w_{\max}$, c_1, c_2, and k_w for the proposed WTPSO were defined according to the parameter roles and admissibility conditions described in Section 4.3. The constraint $w_{\min} \leq w_{\max}$ was imposed, and k_w was treated as an integer variable. For the WTEPSO and EPSO, the mutation rate τ and communication probability cp

Table 3 - Parameter search intervals adopted for the BO calibration of the metaheuristics applied to distribution system reconfiguration.

Algorithm	Parameter	Search interval
WTPSO	$w_{\min}$	$[0,1]$
	$w_{\max}$	$[0,1]$
	c_1	$[0,0.5]$
	c_2	$[0,0.5]$
	k_w	$\{1,2,\ldots,100\}$
WTEPSO	τ	$[0,1]$
	cp	$[0,1]$
EPSO	τ	$[0,1]$
	cp	$[0,1]$
BPSO	w	$[0,1]$
	$V_{\max}$	$[0,6]$
	c_{1i}	$[0,2]$
	c_{1f}	$[2,4]$
CE	σ	$[0,1]$
	β	$[0,1]$
	ε	$[0,0.20]$

Source: The author.

were calibrated, while the number of population replicas was fixed at $rr = 1$. The same search domains were adopted for the parameters shared by these two methods. For the BPSO, w, $V_{\max}$, c_{1i}, and c_{1f} were calibrated, with $V_{\min} = -V_{\max}$. For the CE, the sample size was fixed at $L = N^{\text{pop}}$, and the number of elite samples was calculated as $N_{\text{elite}} = \text{round}(\varepsilon L)$; consequently, only σ, β, and ε were calibrated. The resulting search domains are summarized in Table 3.

After completing the calibration, the parameter configuration with the lowest observed value of $J_{\text{cal}}^{\text{rec}}(\theta)$ was selected separately for each algorithm and test system. The selected parameters, together with the population size N^{pop} and the maximum power-flow-evaluation budget $N_{\text{PF}}^{\max}$, are reported in Table 4.

For the final comparison, each metaheuristic was executed 50 times for each test system. The seed sets assigned to the WTPSO, WTEPSO, EPSO, BPSO, and CE were $\{6001,\ldots,6050\}$, $\{6051,\ldots,6100\}$, $\{6101,\ldots,6150\}$, $\{6151,\ldots,6200\}$, and $\{6201,\ldots,6250\}$, respectively. These sets were mutually disjoint and were also disjoint from $\mathscr{S}_{\text{cal}}^{\text{rec}}$.

The metaheuristics were implemented in MATLAB R2021b. All simulations were performed on a computer equipped with a 2.20-GHz Intel Core i7-8750H processor and 16 GB of RAM. The technical data of the test systems are available in Baran e Wu (1989), Chiou, Chang e Su (2005), Mantovani, Casari e Romero (2000), Agustin (1998).

Table 4 - Parameters for the WTPSO, WTEPSO, EPSO, BPSO, and CE approaches for the 33-, 84-, 136-, and 415-node test systems.

Test system	WTPSO	EPSO	BPSO	CE	WTEPSO
33-node	$w_{\min} = 0.80$	$\tau = 0.88$	$w = 1$	$L = 100$	$\tau = 0.30$
	$w_{\max} = 0.86$	$cp = 0.28$	$V_{\min} = -4.24$	$\varepsilon = 0.11$	$cp = 0.89$
	$c_1 = 0.10$	$rr = 1$	$V_{\max} = 4.24$	$N_{elite} = 11$	$rr = 1$
	$c_2 = 0.03$		$c_{1i} = 0.71$	$\sigma = 0.95$	
	$k_w = 4$		$c_{1f} = 2.32$	$\beta = 0.09$	
			$N^{\text{pop}} = 100$, $N_{\text{PF}}^{\max} = 5100$		
84-node	$w_{\min} = 0.90$	$\tau = 1$	$w = 1$	$L = 105$	$\tau = 0.64$
	$w_{\max} = 0.92$	$cp = 0.15$	$V_{\min} = -5.63$	$\varepsilon = 0.11$	$cp = 1.00$
	$c_1 = 0.19$	$rr = 1$	$V_{\max} = 5.63$	$N_{elite} = 12$	$rr = 1$
	$c_2 = 0.12$		$c_{1i} = 0.14$	$\sigma = 0.72$	
	$k_w = 25$		$c_{1f} = 2.56$	$\beta = 0.09$	
			$N^{\text{pop}} = 105$, $N_{\text{PF}}^{\max} = 10605$		
136-node	$w_{\min} = 0.84$	$\tau = 0.48$	$w = 0.41$	$L = 200$	$\tau = 0.51$
	$w_{\max} = 0.91$	$cp = 0.12$	$V_{\min} = -4.90$	$\varepsilon = 0.05$	$cp = 0.96$
	$c_1 = 0.15$	$rr = 1$	$V_{\max} = 4.90$	$N_{elite} = 10$	$rr = 1$
	$c_2 = 0.05$		$c_{1i} = 0.74$	$\sigma = 0.34$	
	$k_w = 2$		$c_{1f} = 2.88$	$\beta = 0.02$	
			$N^{\text{pop}} = 200$, $N_{\text{PF}}^{\max} = 80000$		
415-node	$w_{\min} = 0.61$	$\tau = 0.93$	$w = 0.41$	$L = 200$	$\tau = 0.36$
	$w_{\max} = 0.99$	$cp = 0.15$	$V_{\min} = -4.90$	$\varepsilon = 0.13$	$cp = 1.00$
	$c_1 = 0.21$	$rr = 1$	$V_{\max} = 4.90$	$N_{elite} = 25$	$rr = 1$
	$c_2 = 4.74 \times 10^{-4}$		$c_{1i} = 0.74$	$\sigma = 0.67$	
	$k_w = 34$		$c_{1f} = 2.88$	$\beta = 0.11$	
			$N^{\text{pop}} = 200$, $N_{\text{PF}}^{\max} = 80000$		

Source: The author.

5.4.2 Benchmark results from the MILP formulation

The MILP approximation defined by (21)–(26), (28)–(37), and (38)–(51) was implemented in AMPL and solved using IBM ILOG CPLEX version 22.1.1. For all test systems, $N_v = 0$ and $W = 50$ were adopted. Thus, the voltage–current product was approximated using the midpoint of the admissible squared-voltage interval, while the squared active- and reactive-power flows were represented using 50 piecewise-linear blocks. A relative optimality gap of 0.001% was imposed. Table 5 reports the resulting open-switch configurations, active-power losses, and total solution times for the 33-, 84-, 136-, and 415-node systems. These results are used as benchmarks for the metaheuristic comparison.

Table 5 - Benchmark results obtained with the MILP approximation for the 33-, 84-, 136-, and 415-node test systems.

Test system	Open switches	Power losses [kW]	Time [s]
33-node	7, 9, 14, 32, 37	139.55	0.36
84-node	7, 13, 34, 39, 42, 55, 62 72, 83, 86, 89, 90, 92	469.88	0.82
136-node	7, 35, 51, 90, 96, 106, 118 126, 135, 137, 138, 141, 142 144, 145, 146, 147, 148, 150 151, 155	280.19	4.66
415-node	22, 51, 104, 166, 208, 223 292, 308, 316, 325, 373, 395 402, 405, 406, 411, 415, 416 417, 418, 419, 421, 422, 424 425, 426, 427, 428, 429, 430 431, 433, 434, 435, 437, 438 439, 440, 442, 443, 444, 445 447, 448, 450, 451, 452, 457 460, 463, 465, 466, 467, 468 469, 470, 471, 472, 473	581.90	88968.23

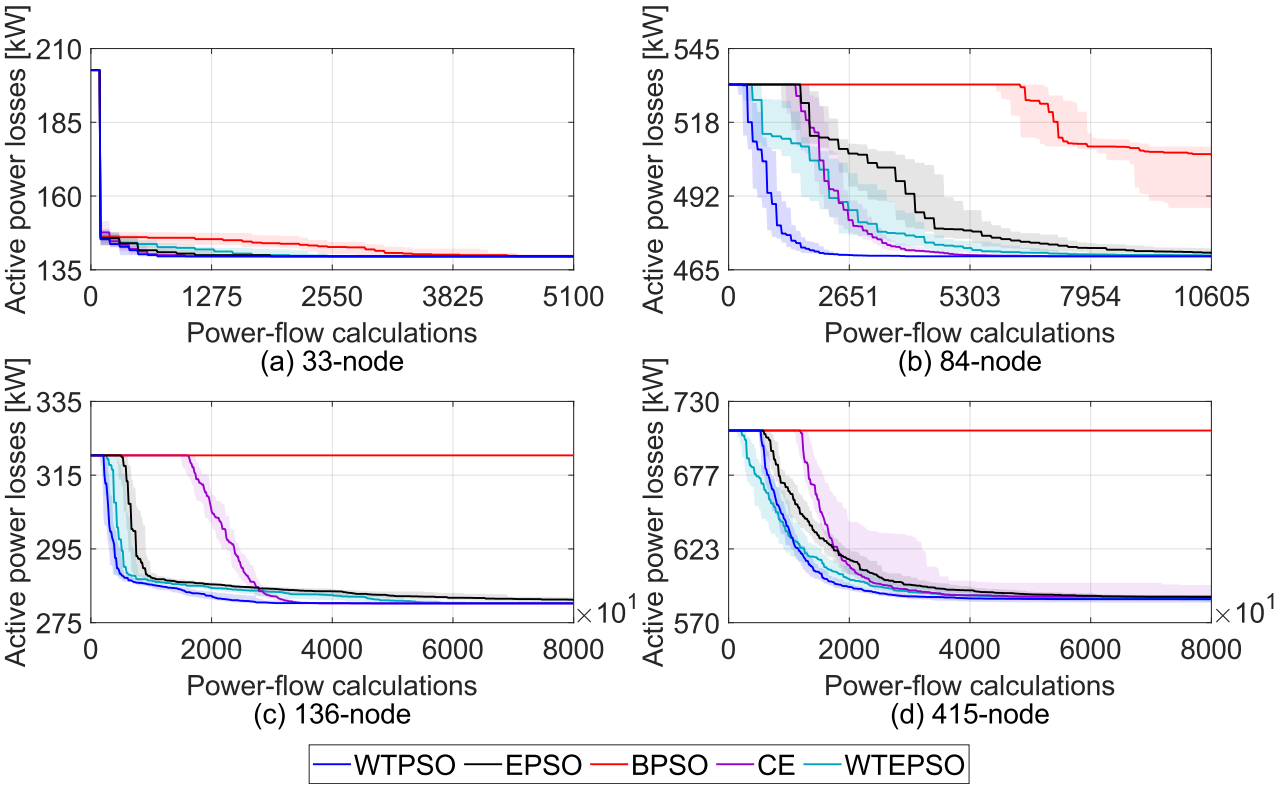
Source: The author.

5.4.3 Comparative analysis of the metaheuristics

The comparative results are examined from two complementary perspectives. First, solution quality and convergence behavior are analyzed under the common power-flow-evaluation budget. Subsequently, the computational efficiency of the metaheuristics is assessed using cumulative and total wall-clock times.

Figure 5 compares the convergence behavior of the evaluated metaheuristics under the common power-flow-evaluation budget. For the 33-node system, all methods rapidly approach the same low-loss region, although the BPSO requires more evaluations to reach its final level. Both proposed methods, WTPSO and WTEPSO, achieve rapid initial reductions and stabilize near the reference solution. For the 84-node system, the WTPSO reaches the lowest-loss region with the fewest power-flow evaluations. The WTEPSO also progressively approaches this region and converges faster than the EPSO, whereas the BPSO remains at substantially higher losses. The CE exhibits a competitive convergence trajectory, although the WTPSO reaches the final low-loss region earlier. For the 136-node system, the WTPSO and WTEPSO exhibit the most rapid initial reductions and remain close throughout the remainder of the evaluation budget. The EPSO and CE require more evaluations to approach a similar loss range, while the BPSO shows no relevant improvement. For the 415-node system, the two proposed methods again provide rapid initial reductions and stabilize in the lowest-loss region observed in the figure. The

Figure 5 - Median best-so-far active-power losses as a function of the number of power-flow calculations for the WTPSO, EPSO, BPSO, CE, and WTEPSO approaches over 50 independent runs. The shaded regions represent the interquartile ranges. Results are shown for the (a) 33-node, (b) 84-node, (c) 136-node, and (d) 415-node test systems.

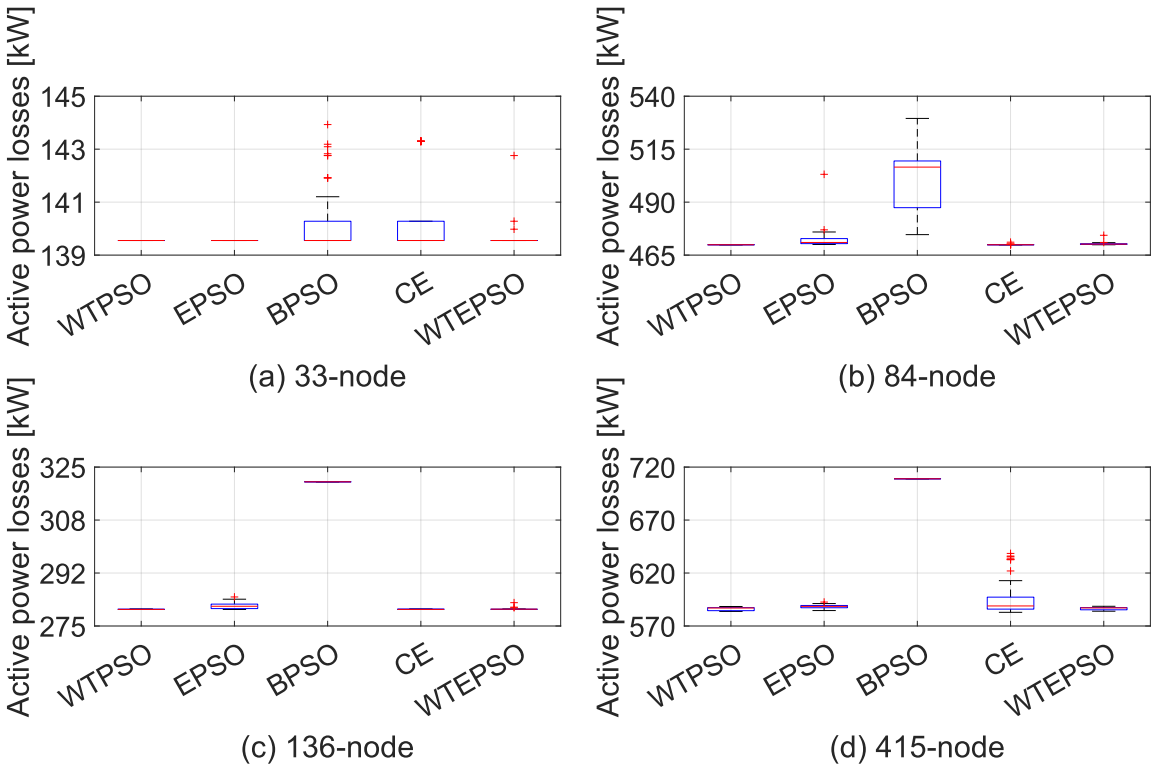


Source: The author.

EPSO and CE improve more gradually, with the CE also presenting greater run-to-run variability during part of the search. In contrast, the BPSO remains at the same high-loss level throughout the evaluation budget. These convergence profiles are complemented by the final-solution distributions and descriptive statistics presented next.

The final-solution distributions shown in Fig. 6 and summarized in Table 6 complement the convergence profiles by showing the solution quality and run-to-run variability obtained at the end of the prescribed power-flow-evaluation budget. For the 33-node system, the median losses of all methods coincide with the reference value reported in Table 5. The WTPSO and EPSO attain this value without observable dispersion. The WTEPSO also remains concentrated at the reference value, although its mean and standard deviation indicate occasional higher-loss solutions. The BPSO and CE present greater variability and more pronounced upper-tail observations. For the 84-node system, the WTPSO reproduces the reference loss of 469.88 kW in every run. The CE presents the same median and interquartile range, but its nonzero mean and standard deviation indicate occasional higher-loss results. The WTEPSO remains close to

Figure 6 - Box plots of the final active-power losses obtained by the WTPSO, EPSO, BPSO, CE, and WTEPSO approaches over 50 independent runs under the same power-flow-evaluation budget. Results are shown for the (a) 33-node, (b) 84-node, (c) 136-node, and (d) 415-node test systems.



Source: The author.

the reference value, with a median of 470.19 kW and limited dispersion. The EPSO presents a higher median and greater variability, whereas the BPSO produces the highest losses and the widest interquartile range. For the 136-node system, the distributions of the WTPSO, CE, and WTEPSO remain close to, but slightly above, the reference loss of 280.19 kW. The WTPSO presents the lowest mean and shares the lowest median with the CE, while also exhibiting limited dispersion. The WTEPSO presents a similarly concentrated distribution, although with a slightly higher mean and standard deviation. The EPSO results are moderately higher and more dispersed, while the BPSO consistently remains at a substantially higher loss level. For the 415-node system, none of the evaluated methods reaches the reference loss of 581.90 kW. Nevertheless, the WTPSO and WTEPSO provide the most favorable final distributions. The WTPSO presents the lowest mean and median losses, whereas the WTEPSO presents a slightly lower standard deviation. The EPSO results are moderately higher, while the pronounced upper tail and outliers of the CE increase both its mean and standard deviation. Although the BPSO shows no dispersion, this behavior reflects repeated convergence to the same high-loss solution rather than robustness near the reference solution.

To determine whether the differences observed in the convergence profiles and final-loss

Table 6 - Descriptive statistics of the final active-power losses obtained by the WTPSO, EPSO, BPSO, CE, and WTEPSO algorithms over 50 independent runs. Means and standard deviations are reported together with the medians and the first and third quartiles.

Test system	Algorithm	Mean ± SD [kW]	Median [Q_1, Q_3] [kW]
33-node	WTPSO	139.55 ± 0.00	139.55 [139.55, 139.55]
	EPSO	139.55 ± 0.00	139.55 [139.55, 139.55]
	BPSO	140.25 ± 1.24	139.55 [139.55, 140.28]
	CE	140.73 ± 2.19	139.55 [139.55, 140.28]
	WTEPSO	139.64 ± 0.47	139.55 [139.55, 139.55]
84-node	WTPSO	469.88 ± 0.00	469.88 [469.88, 469.88]
	EPSO	472.25 ± 4.72	470.97 [470.42, 472.80]
	BPSO	499.46 ± 14.82	506.53 [487.39, 509.44]
	CE	469.94 ± 0.18	469.88 [469.88, 469.88]
	WTEPSO	470.30 ± 0.64	470.19 [470.01, 470.40]
136-node	WTPSO	280.25 ± 0.05	280.22 [280.22, 280.30]
	EPSO	281.42 ± 1.05	281.21 [280.48, 281.89]
	BPSO	320.36 ± 0.00	320.36 [320.36, 320.36]
	CE	280.28 ± 0.07	280.22 [280.22, 280.34]
	WTEPSO	280.33 ± 0.31	280.30 [280.22, 280.30]
415-node	WTPSO	586.15 ± 1.57	586.99 [584.48, 587.35]
	EPSO	588.18 ± 1.77	588.54 [587.23, 589.37]
	BPSO	708.94 ± 0.00	708.94 [708.94, 708.94]
	CE	596.86 ± 17.12	588.93 [585.93, 597.24]
	WTEPSO	586.52 ± 1.33	587.08 [585.29, 587.37]

Source: The author.

distributions are statistically supported, Tables 7 and 8 report the pairwise comparisons using the proposed WTPSO and WTEPSO, respectively, as control algorithms. For each control algorithm, Holm's correction was applied over the three comparisons performed within each test system.

For the 33-node system, no statistically significant difference is detected between the WTPSO and EPSO, with $\delta = 0$. In contrast, the WTPSO produces significantly lower losses than the BPSO and CE, with negative effect sizes and confidence intervals excluding zero. For the 84-node system, all three comparisons are significant. Complete separation is observed relative to the EPSO and BPSO ($\delta = -1$), whereas the smaller effect relative to the CE is consistent with their close descriptive distributions. For the 136-node system, the WTPSO produces significantly lower losses than all three comparison methods, with a large effect relative to the EPSO, complete separation relative to the BPSO, and a substantial effect relative to the CE. The same general behavior is observed in the 415-node system, where all comparisons favor the WTPSO; complete separation is again observed relative to the BPSO.

The comparisons using the WTEPSO as the control algorithm also support most of the

Table 7 - Two-sided Mann–Whitney test results ($\alpha = 0.05$) for final active-power losses, with WTPSO as the control algorithm. The p-values were adjusted using Holm's correction over the three comparisons within each test system. Cliff's δ is reported with its 95% bootstrap confidence interval. Negative effect sizes favor the WTPSO.

Test system	Comparison	p_{Holm}	Cliff's δ [95% CI]
33-node	WTPSO vs EPSO	1.000	0.000 [0.000, 0.000]
	WTPSO vs BPSO	1.11×10^{-5}	-0.360 [-0.500, -0.240]
	WTPSO vs CE	3.13×10^{-5}	-0.320 [-0.460, -0.200]
84-node	WTPSO vs EPSO	9.90×10^{-20}	-1.000 [-1.000, -1.000]
	WTPSO vs BPSO	9.90×10^{-20}	-1.000 [-1.000, -1.000]
	WTPSO vs CE	9.52×10^{-4}	-0.200 [-0.320, -0.100]
136-node	WTPSO vs EPSO	3.91×10^{-14}	-0.879 [-0.959, -0.777]
	WTPSO vs BPSO	4.67×10^{-20}	-1.000 [-1.000, -1.000]
	WTPSO vs CE	1.61×10^{-5}	-0.491 [-0.681, -0.284]
415-node	WTPSO vs EPSO	5.19×10^{-8}	-0.646 [-0.794, -0.477]
	WTPSO vs BPSO	9.93×10^{-20}	-1.000 [-1.000, -1.000]
	WTPSO vs CE	5.93×10^{-5}	-0.466 [-0.670, -0.249]

Source: The author.

patterns observed in the descriptive results. For the 33-node system, no statistically significant difference is detected between the WTEPSO and EPSO, whereas the WTEPSO produces significantly lower losses than the BPSO and CE. For the 84-node system, the WTEPSO produces significantly lower losses than the EPSO and BPSO, with complete separation relative to the latter. However, the positive effect size relative to the CE indicates that the CE yields significantly lower losses in this system. For the 136-node system, the WTEPSO produces significantly lower losses than the EPSO and BPSO, while no statistically significant difference is detected relative to the CE, with the corresponding confidence interval including zero. In the 415-node system, all three comparisons are significant and favor the WTEPSO, with complete separation relative to the BPSO.

Taken together, the convergence profiles, descriptive statistics, and inferential comparisons show that both proposed methods provide competitive solution quality under the adopted evaluation budgets. The WTPSO presents the most consistent statistical advantage across the evaluated systems. The WTEPSO also performs favorably relative to the EPSO and BPSO, while its comparative performance relative to the CE depends on the test system.

Following the solution-quality analysis under the common power-flow-evaluation budget, the computational efficiency of the metaheuristics is assessed using cumulative and total wall-clock times. Figure 7 complements the analysis based on power-flow evaluations by relating the median best-so-far losses to the actual elapsed time. For the 33-node system, all methods approach the same low-loss region, although the WTPSO reaches it in a comparatively short elapsed time. The WTEPSO also attains the same final region but follows a longer temporal trajectory. For

Table 8 - Two-sided Mann–Whitney test results ($\alpha = 0.05$) for final active-power losses, with WTEPSO as the control algorithm. The p-values were adjusted using Holm's correction over the three comparisons within each test system. Cliff's δ is reported with its 95% bootstrap confidence interval. Negative effect sizes favor the WTEPSO.

Test system	Comparison	p_{Holm}	Cliff's δ [95% CI]
33-node	WTEPSO vs EPSO	0.082	0.060 [0.000, 0.140]
	WTEPSO vs BPSO	6.74×10^{-4}	−0.305 [−0.455, −0.159]
	WTEPSO vs CE	0.001	−0.272 [−0.411, −0.127]
84-node	WTEPSO vs EPSO	4.03×10^{-10}	−0.726 [−0.855, −0.571]
	WTEPSO vs BPSO	2.05×10^{-17}	−1.000 [−1.000, −1.000]
	WTEPSO vs CE	1.10×10^{-10}	0.720 [0.572, 0.854]
136-node	WTEPSO vs EPSO	3.26×10^{-11}	−0.766 [−0.893, −0.613]
	WTEPSO vs BPSO	2.59×10^{-20}	−1.000 [−1.000, −1.000]
	WTEPSO vs CE	0.274	−0.124 [−0.355, 0.114]
415-node	WTEPSO vs EPSO	4.94×10^{-7}	−0.599 [−0.770, −0.407]
	WTEPSO vs BPSO	9.93×10^{-20}	−1.000 [−1.000, −1.000]
	WTEPSO vs CE	5.46×10^{-4}	−0.402 [−0.625, −0.164]

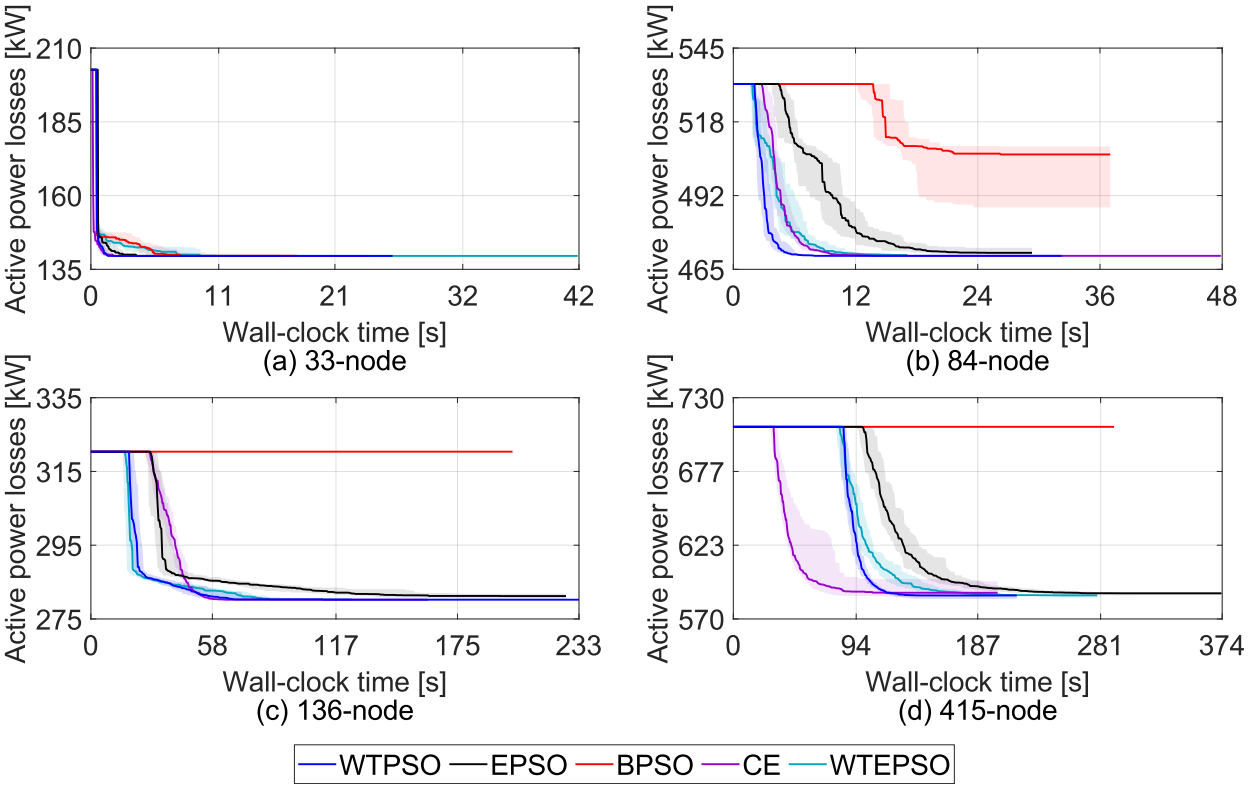
Source: The author.

the 84-node system, the WTPSO presents the fastest reduction toward the lowest-loss region, followed by the WTEPSO and CE. The EPSO improves more gradually, whereas the BPSO remains at substantially higher losses. For the 136-node system, the WTPSO and WTEPSO exhibit the earliest reductions and approach the lowest-loss region within relatively short elapsed times. The CE subsequently reaches a similar region, while the EPSO improves more slowly and the BPSO shows no relevant reduction. For the 415-node system, the CE presents the fastest initial decrease but also greater run-to-run variability, as indicated by its wider interquartile region. The WTPSO and WTEPSO subsequently approach the lowest observed loss region, whereas the EPSO requires more elapsed time and the BPSO remains at a high-loss solution.

Figure 8 shows the distributions of the total wall-clock times required to exhaust the prescribed power-flow-evaluation budget. These total runtimes complement the convergence profiles by quantifying the computational cost of completing the entire evaluation budget.

For the 33-node system, the WTPSO presents the lowest median runtime, whereas the WTEPSO requires the longest total execution time. For the 84-node system, the WTEPSO presents the lowest median runtime, followed by the WTPSO, while the remaining methods require moderately longer times. In the 136-node system, the WTEPSO again presents the lowest median runtime, followed by the CE and BPSO. The WTPSO requires more time than these methods but less than the EPSO. However, the relatively short runtime of the BPSO does not translate into competitive solution quality because it remains at a substantially higher-loss solution. For the 415-node system, the WTPSO presents the lowest median runtime and a relatively concentrated distribution, followed by the CE. The WTEPSO requires more time than

Figure 7 - Median best-so-far active-power losses as a function of cumulative wall-clock time for the WTPSO, EPSO, BPSO, CE, and WTEPSO approaches over 50 independent runs. The shaded regions represent the interquartile ranges. Each profile is displayed up to the maximum observed runtime of the corresponding method. Results are shown for the (a) 33-node, (b) 84-node, (c) 136-node, and (d) 415-node test systems.



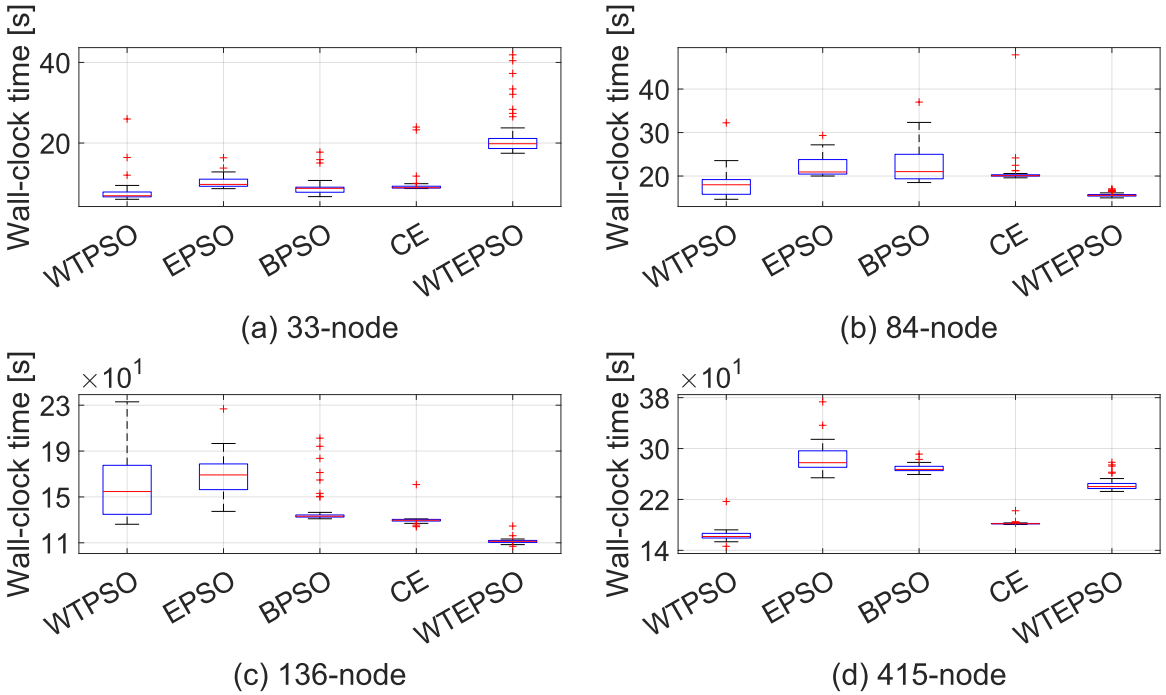
Source: The author.

these two methods but less than the EPSO and BPSO. These descriptive runtime differences are examined statistically in the following tables.

To determine whether the differences observed in the total-runtime distributions are statistically supported, Tables 9 and 10 report pairwise comparisons using the WTPSO and WTEPSO as control algorithms, respectively. All Holm-adjusted comparisons are statistically significant, and all corresponding confidence intervals exclude zero.

For the 33-node system, the WTPSO requires significantly less time than the EPSO, BPSO, and CE, with large negative effect sizes. The same behavior is observed in the 84-node system. For the 136-node system, the WTPSO is significantly faster than the EPSO, although the effect is comparatively smaller. Conversely, the positive effect sizes obtained relative to the BPSO and CE indicate that these methods require less time than the WTPSO. In the 415-node system, the WTPSO is significantly faster than all three comparison methods. Complete separation is observed relative to the EPSO and BPSO, while the comparison with the CE is close to complete

Figure 8 - Box plots of the total wall-clock times required by the WTPSO, EPSO, BPSO, CE, and WTEPSO approaches to complete the same prescribed power-flow-evaluation budget over 50 independent runs. Results are shown for the (a) 33-node, (b) 84-node, (c) 136-node, and (d) 415-node test systems.



Source: The author.

Table 9 - Two-sided Mann–Whitney test results ($\alpha = 0.05$) for total wall-clock times, with WTPSO as the control algorithm. The p-values were adjusted using Holm's correction over the three comparisons within each test system. Cliff's δ is reported with its 95% bootstrap confidence interval. Negative effect sizes favor WTPSO.

Test system	Comparison	p_{Holm}	Cliff's δ [95% CI]
33-node	WTPSO vs EPSO	2.09×10^{-12}	-0.834 $[-0.951, -0.686]$
	WTPSO vs BPSO	1.32×10^{-6}	-0.562 $[-0.741, -0.361]$
	WTPSO vs CE	1.71×10^{-10}	-0.754 $[-0.903, -0.570]$
84-node	WTPSO vs EPSO	1.99×10^{-12}	-0.834 $[-0.944, -0.698]$
	WTPSO vs BPSO	2.82×10^{-10}	-0.745 $[-0.869, -0.596]$
	WTPSO vs CE	7.15×10^{-9}	-0.672 $[-0.848, -0.478]$
136-node	WTPSO vs EPSO	0.015	-0.282 $[-0.501, -0.058]$
	WTPSO vs BPSO	7.17×10^{-5}	0.480 [0.257, 0.687]
	WTPSO vs CE	1.37×10^{-11}	0.803 [0.648, 0.934]
415-node	WTPSO vs EPSO	2.12×10^{-17}	-1.000 $[-1.000, -1.000]$
	WTPSO vs BPSO	2.12×10^{-17}	-1.000 $[-1.000, -1.000]$
	WTPSO vs CE	1.35×10^{-16}	-0.960 $[-1.000, -0.880]$

Source: The author.

separation.

Table 10 - Two-sided Mann–Whitney test results ($\alpha = 0.05$) for total wall-clock times, with WTEPSO as the control algorithm. The p-values were adjusted using Holm's correction over the three comparisons within each test system. Cliff's δ is reported with its 95% bootstrap confidence interval. Negative effect sizes favor WTEPSO.

Test system	Comparison	p_{Holm}	Cliff's δ [95% CI]
33-node	WTEPSO vs EPSO	2.12×10^{-17}	$1.000\ [1.000, 1.000]$
	WTEPSO vs BPSO	2.12×10^{-17}	$0.998\ [0.990, 1.000]$
	WTEPSO vs CE	8.86×10^{-16}	$0.934\ [0.829, 1.000]$
84-node	WTEPSO vs EPSO	2.12×10^{-17}	$-1.000\ [-1.000, -1.000]$
	WTEPSO vs BPSO	2.12×10^{-17}	$-1.000\ [-1.000, -1.000]$
	WTEPSO vs CE	2.12×10^{-17}	$-1.000\ [-1.000, -1.000]$
136-node	WTEPSO vs EPSO	2.12×10^{-17}	$-1.000\ [-1.000, -1.000]$
	WTEPSO vs BPSO	2.12×10^{-17}	$-1.000\ [-1.000, -1.000]$
	WTEPSO vs CE	2.12×10^{-17}	$-0.999\ [-1.000, -0.995]$
415-node	WTEPSO vs EPSO	8.50×10^{-16}	$-0.944\ [-0.994, -0.872]$
	WTEPSO vs BPSO	1.82×10^{-14}	$-0.890\ [-0.993, -0.766]$
	WTEPSO vs CE	2.12×10^{-17}	$1.000\ [1.000, 1.000]$

Source: The author.

The runtime behavior of the WTEPSO shows a stronger dependence on the test system. For the 33-node system, the positive effect sizes indicate that the WTEPSO requires significantly more time than all three comparison methods. For the 84-node system, all comparisons show complete separation in favor of the WTEPSO. A similar result is obtained for the 136-node system, with complete or nearly complete separation relative to the EPSO, BPSO, and CE. For the 415-node system, the WTEPSO is significantly faster than the EPSO and BPSO, but the positive effect size relative to the CE indicates that the CE requires less total execution time.

The runtime results must be interpreted together with the corresponding solution quality. The WTPSO exhibits favorable computational performance on the 33-, 84-, and 415-node systems, whereas its relative runtime on the 136-node system depends on the comparison method. The WTEPSO achieves particularly favorable runtimes on the 84- and 136-node systems, but takes longer on the 33-node system and more time than the CE on the 415-node system. Therefore, the computational advantage of each proposed method depends on the test-system size and should be considered jointly with the final-loss distributions.

6 APPLICATION TO DISTRIBUTION SYSTEM SERVICE RESTORATION

6.1 INTRODUCTION

Distribution system service restoration is a representative application for evaluating topology-oriented optimization methods under post-fault operating conditions. Following the isolation of a permanent fault, the restoration process requires selecting additional switching actions to reconnect as much affected demand as possible while satisfying the network's electrical, operational, and topological requirements. In addition to radiality and connectivity, candidate restoration plans must comply with voltage and current limits, substation capacities, and the requirement that a single real substation supply each energized component. The problem, therefore, provides an appropriate framework for assessing the adaptability of the solution-generation mechanisms introduced in Chapter 4.

This chapter applies the proposed WTPSO and WTEPSO, together with the EPSO, to the radial service restoration problem. The objective is to minimize the weighted nonrestored demand and the costs associated with opening normally closed switches and closing normally open switches. The solutions obtained from an MISOCP formulation are adopted as benchmark values. The comparative evaluation considers solution quality, robustness, convergence behavior, and computational effort over multiple independent runs and different fault scenarios.

The chapter first presents the mathematical formulation describing the electrical, operational, radiality, connectivity, and substation-assignment requirements of the restoration problem. It then describes the problem-specific application of the metaheuristics, including the augmented post-fault network, the representation of real and artificial lines, the constructive generation of radial restoration plans, and their evaluation through power-flow calculations. Finally, the computational results are presented and discussed for the 53- and 417-node distribution systems, including the calibrated parameters, the benchmark restoration plans obtained with the MISOCP formulation, and the comparative performance of the evaluated metaheuristics.

6.2 MATHEMATICAL FORMULATION OF THE RADIAL SERVICE RESTORATION PROBLEM

Distribution system service restoration comprises the set of actions performed after the isolation of a permanent fault and before the repair of the faulted section. During this restorative state, switching operations are performed to reconnect as much load as possible while preserving the electrical, operational, and topological requirements of the distribution system. In this work, the service restoration problem is restricted to radial operating configurations. Accordingly, the objective is to minimize the weighted nonrestored demand and the costs associated with changes in the status of normally open and normally closed switches. The formulation adopted in this work is a reduced version of the MISOCP model proposed in Vargas *et al.* (2021).

Let $\mathscr{N}^D$ denote the set of demand nodes, $\mathscr{N}^S$ the set of real substation nodes, and $\mathscr{N}^R$ the set of real nodes, excluding the artificial substation. The set $\mathscr{N}$ contains the demand nodes, the real substations, and the artificial substation. Moreover, $\mathscr{S}^F$ represents the set of sections affected by the fault, and S_i identifies the section containing node i. The set of real lines is denoted by $\mathscr{L}$, whereas $\mathscr{L}^O$ and $\mathscr{L}^C$ contain the lines whose switches are normally open and normally closed, respectively. The set $\mathscr{L}^H$ contains the artificial lines connecting the artificial substation to the sections that may remain nonrestored. The augmented set of real and artificial lines is given by $\mathscr{L}^U = \mathscr{L} \cup \mathscr{L}^H$. For each real line $ij \in \mathscr{L}$, the parameters R_{ij}, X_{ij}, and Z_{ij} denote its resistance, reactance, and impedance magnitude. The active and reactive demands at node i are denoted by P_i^D and Q_i^D, respectively. The variables P_{ij} and Q_{ij} represent the active and reactive power flows in line ij, while I_{ij}^{sqr} and V_i^{sqr} represent the squared current and voltage magnitudes. The active and reactive power supplied by a real substation are denoted by P_i^{SE} and Q_i^{SE}. The binary variable w_{ij} is equal to one when line ij is in service and zero when it is open. The binary variable y_i characterizes the restoration state of node i: $y_i = 0$ indicates an energized node, whereas $y_i = 1$ indicates a nonrestored node. The auxiliary variable ζ_{ij} decouples the voltage-drop equation when line ij is open.

The radial service restoration problem is formulated as follows:

$$\text{minimize} \quad \sum_{\substack{i \in \mathscr{N}^D \\ S_i \notin \mathscr{S}^F}} \sigma_i P_i^D y_i + \sum_{ij \in \mathscr{L}^O} \tau_{ij} w_{ij} + \sum_{ij \in \mathscr{L}^C} \eta_{ij}(1 - w_{ij}) \tag{52}$$

Subject to:

$$\sum_{ki \in \mathscr{L}} P_{ki} - \sum_{ij \in \mathscr{L}} \left(P_{ij} + R_{ij} I_{ij}^{\text{sqr}} \right) + P_i^{SE} = P_i^D (1 - y_i), \qquad \forall i \in \mathscr{N}^R \tag{53}$$

$$\sum_{ki \in \mathscr{L}} Q_{ki} - \sum_{ij \in \mathscr{L}} \left(Q_{ij} + X_{ij} I_{ij}^{\text{sqr}} \right) + Q_i^{SE} = Q_i^D (1 - y_i), \qquad \forall i \in \mathscr{N}^R \tag{54}$$

$$V_i^{\mathrm{sqr}} - V_j^{\mathrm{sqr}} + \zeta_{ij} = 2\left(R_{ij}P_{ij} + X_{ij}Q_{ij}\right) + Z_{ij}^2 I_{ij}^{\mathrm{sqr}}, \qquad \forall ij \in \mathscr{L} \quad (55)$$

$$V_j^{\mathrm{sqr}} I_{ij}^{\mathrm{sqr}} \geq P_{ij}^2 + Q_{ij}^2, \qquad \forall ij \in \mathscr{L} \quad (56)$$

$$|\zeta_{ij}| \leq \left(\overline{V}^2 - \underline{V}^2\right)(1 - w_{ij}), \qquad \forall ij \in \mathscr{L} \quad (57)$$

$$\underline{V}^2 \leq V_i^{\mathrm{sqr}} \leq \overline{V}^2, \qquad \forall i \in \mathscr{N}^D \quad (58)$$

$$0 \leq I_{ij}^{\mathrm{sqr}} \leq \overline{I}_{ij}^2 w_{ij}, \qquad \forall ij \in \mathscr{L} \quad (59)$$

$$|P_{ij}| \leq \overline{V}\,\overline{I}_{ij} w_{ij}, \qquad \forall ij \in \mathscr{L} \quad (60)$$

$$|Q_{ij}| \leq \overline{V}\,\overline{I}_{ij} w_{ij}, \qquad \forall ij \in \mathscr{L} \quad (61)$$

$$(P_i^{SE})^2 + (Q_i^{SE})^2 \leq \left(\overline{S_i^{SE}}\right)^2. \qquad \forall i \in \mathscr{N}^S \quad (62)$$

The first term of (52) quantifies the weighted active demand that cannot be restored. The demand within the faulted sections is excluded because the fault-isolation procedure imposes its disconnection and cannot be modified by the restoration plan. The second term penalizes the closing of normally open switches, while the third term penalizes the opening of normally closed switches. Thus, the objective function simultaneously favors load restoration and a reduced number of switching operations. Constraints (53) and (54) impose the active and reactive power balances at each real node. Constraint (55) represents the voltage drop along a real line. When $w_{ij} = 1$, constraint (57) forces $\zeta_{ij} = 0$, and the voltage-drop relation is enforced. When $w_{ij} = 0$, the auxiliary variable allows the voltage magnitudes at the terminal nodes to be decoupled. Constraint (56) is the second-order cone representation relating the squared voltage and current magnitudes to the active and reactive power flows. The voltage limits at the demand nodes are imposed by (58). Constraint (59) limits the line current according to its operational state. Similarly, (60) and (61) bound the active and reactive power flows, respectively, and set them to zero when the line is open. The apparent-power capacity of each real substation is imposed by (62). For lines without switches, w_{ij} is fixed at one.

Following the artificial network representation adopted by Vargas *et al.* (2021), an artificial substation is introduced and connected through artificial lines to the sections that may remain nonrestored. This construction separates the energized network supplied by the real substations from the nonrestored portion connected to the artificial substation. The variables f_{ij}^f and g_i^f denote the artificial flow and artificial injection used to impose connectivity. These variables do not represent electrical power or distributed generation. The radiality and connectivity conditions are given by:

$$\sum_{ij \in \mathscr{L}^U} w_{ij} = |\mathscr{N}^D|, \qquad (63)$$

$$\sum_{ki \in \mathscr{L}^U} f_{ki}^f - \sum_{ij \in \mathscr{L}^U} f_{ij}^f + g_i^f = y_i, \qquad \forall i \in \mathscr{N} \quad (64)$$

$$|f^f_{ij}| \leq |\mathscr{N}| w_{ij}, \qquad \forall ij \in \mathscr{L}^U \quad (65)$$

$$f^f_{ij} \geq 0, \qquad \forall ij \in \mathscr{L}^H \quad (66)$$

$$\sum_{ki \in \mathscr{L}^U} w_{ki} + \sum_{ij \in \mathscr{L}^U} w_{ij} \geq 1, \qquad \forall i \in \mathscr{N}^D \quad (67)$$

$$|y_i - y_j| \leq 1 - w_{ij}, \qquad \forall ij \in \mathscr{L} \quad (68)$$

$$w_{ij} \in \{0,1\}, \qquad \forall ij \in \mathscr{L}^U \quad (69)$$

$$y_i \in \{0,1\}. \qquad \forall i \in \mathscr{N} \quad (70)$$

In the general formulation of Vargas *et al.* (2021), the number of closed real and artificial lines may exceed $|\mathscr{N}^D|$ when temporary operational loops are allowed. In the present work, the number of loops is fixed at zero. Therefore, (63) requires exactly $|\mathscr{N}^D|$ lines to be in service. Combined with the connectivity constraints, this equality produces a radial topology. Constraint (64) represents the artificial flow balance. The artificial injection g^f_i is fixed at zero at every node except the artificial substation. If $y_i = 1$, a unit artificial demand is assigned to node i, requiring a path between its section and the artificial substation. Hence, nodes that cannot be restored belong to the artificial network. Constraint (65) allows artificial flow only through lines with status equal to 1. Constraint (66) establishes the orientation of the flow leaving the artificial substation. The fencing constraint (67) ensures that each demand node has at least one incident real or artificial line in service. Finally, (68) prevents a closed real line from connecting nodes with different restoration states. Therefore, energized and nonrestored portions remain separated. The artificial substation and all real substations are maintained at an energized state, with their corresponding y_i variables fixed at zero. The lines required to isolate a faulted section are fixed open, and the nodes belonging to that section are fixed as nonrestored. Nodes that remain energized after fault isolation are fixed at $y_i = 0$, whereas only the affected downstream sections are considered for reconnection.

When multiple substations are present, radiality alone does not explicitly guarantee that an energized component is supplied by only one substation. Therefore, an additional artificial network is associated with each real substation. These networks reproduce the topology of the real network and identify the substation supplying each energized node. The binary variable $y^c_{i,s}$ is equal to one when energized node i is assigned to substation s. The binary variable $w^c_{ij,s}$ associates an energized real line ij with the artificial network of substation s. The continuous variables $f^c_{ij,s}$ and $g^c_{i,s}$ represent the corresponding artificial flow and injection:

$$\sum_{ki \in \mathscr{L}} f^c_{ki,s} - \sum_{ij \in \mathscr{L}} f^c_{ij,s} + g^c_{i,s} = y^c_{i,s}, \qquad \forall i \in \mathscr{N}^R,\ \forall s \in \mathscr{N}^S \quad (71)$$

$$|f^c_{ij,s}| \leq |\mathscr{N}| w^c_{ij,s}, \qquad \forall ij \in \mathscr{L},\ \forall s \in \mathscr{N}^S \quad (72)$$

$$\sum_{s \in \mathcal{N}^S} w^c_{ij,s} = w_{ij}, \qquad \forall ij \in \mathcal{L} \tag{73}$$

$$\sum_{s \in \mathcal{N}^S} y^c_{i,s} = 1 - y_i, \qquad \forall i \in \mathcal{N}^R \tag{74}$$

$$|y^c_{i,s} - y^c_{j,s}| \leq 1 - w_{ij}, \qquad \forall ij \in \mathcal{L},\ \forall s \in \mathcal{N}^S:\ S_i \neq S_j \tag{75}$$

$$y^c_{i,s} = y^c_{j,s}, \qquad \forall ij \in \mathcal{L},\ \forall s \in \mathcal{N}^S:\ S_i = S_j \tag{76}$$

$$w^c_{ij,s} = w^c_{kl,s}, \qquad \forall ij,kl \in \mathcal{L}.\ \forall s \in \mathcal{N}^S:\ S_i = S_k,\ S_j = S_l \tag{77}$$

The artificial injections and the substation assignment variables are fixed according to

$$g^c_{i,s} = 0, \qquad \forall i \in \mathcal{N}^R \setminus \mathcal{N}^S,\ \forall s \in \mathcal{N}^S \tag{78}$$

$$g^c_{i,s} = 0, \qquad \forall i, s \in \mathcal{N}^S : i \neq s \tag{79}$$

$$y^c_{i,s} = 0, \qquad \forall i, s \in \mathcal{N}^S : i \neq s \tag{80}$$

$$y^c_{s,s} = 1, \qquad \forall s \in \mathcal{N}^S \tag{81}$$

$$y^c_{i,s} \in \{0,1\}, \qquad \forall i \in \mathcal{N}^R,\ \forall s \in \mathcal{N}^S \tag{82}$$

$$w^c_{ij,s} \in \{0,1\}, \qquad \forall ij \in \mathcal{L},\ \forall s \in \mathcal{N}^S. \tag{83}$$

Constraint (71) imposes the flow balance in the artificial network associated with each real substation. Constraints (72) and (73) ensure that an in-service real line is assigned to exactly one substation and can carry artificial flow only in the corresponding artificial network. Constraint (74) assigns each energized node to exactly one real substation. If $y_i = 1$, node i is nonrestored and all its assignment variables are zero. If $y_i = 0$, exactly one variable $y^c_{i,s}$ is equal to one. Constraints (75) and (76) require nodes connected by an in-service line, or belonging to the same section, to be supplied by the same substation. Constraint (77) maintains a consistent substation assignment for lines connecting the same pair of sections. Constraints (78) and (79) prevent artificial injections at demand nodes and at substations that do not correspond to the artificial network under consideration. Constraints (80) and (81) fix the assignment of the real substation nodes. Collectively, these constraints prevent the interconnection of different substations and ensure that a single real substation supplies each energized radial component.

The resulting formulation is a mixed-integer second-order cone programming (MISOCP). Its discrete variables determine the line states, restoration states, and substation assignments, whereas its continuous variables describe the electrical operation and the auxiliary connectivity flows. The second-order cone constraint (56) and the convex substation capacity constraint (62) preserve the MISOCP structure. In this work, the formulation is used to obtain benchmark solutions for assessing the metaheuristic algorithms. The corresponding benchmark results are presented in Section 6.4.

6.3 APPLICATION OF THE METAHEURISTICS TO THE SERVICE RESTORATION PROBLEM

Based on the comparative assessment conducted for the reconfiguration problem, the WTPSO, WTEPSO, and EPSO were selected for application to the service restoration problem, as they provided the best overall performance. The WTPSO and WTEPSO follow the complete optimization procedures presented in Algorithms 4 and 6, respectively, using the restoration-specific initialization procedure defined in Algorithm 3. Their general search mechanisms remain unchanged; therefore, this section describes only the problem-specific adaptations required to represent, construct, and evaluate solution proposals for service restoration.

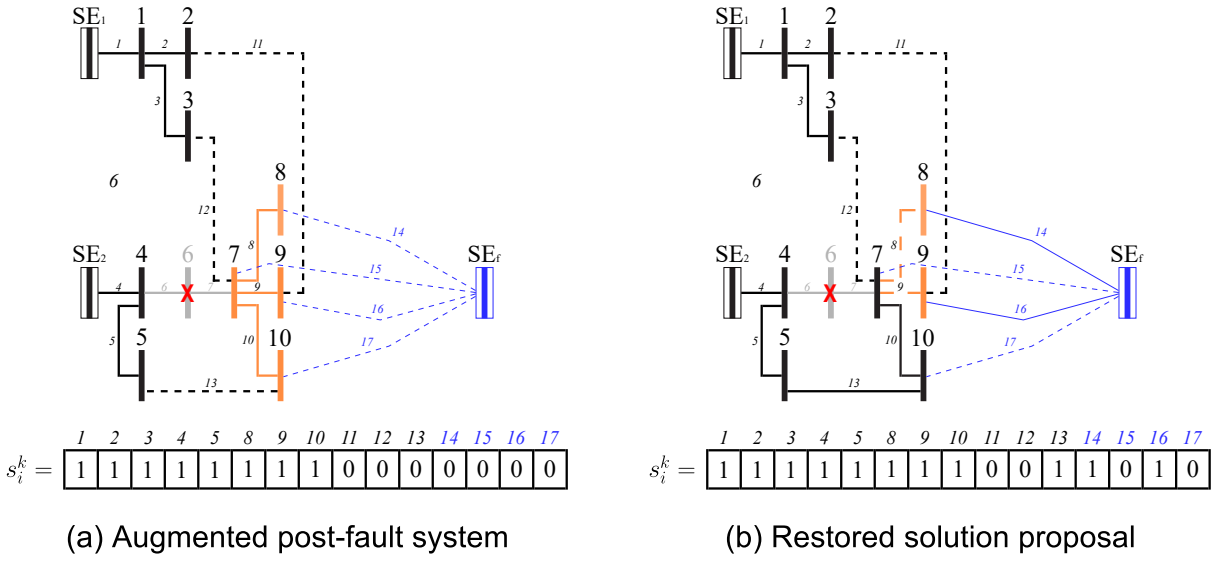
Following fault isolation, the lines required to isolate the faulted section are fixed open and excluded from the optimization decisions. The remaining real lines, together with the artificial lines introduced in Section 6.2, define the augmented post-fault network used by the metaheuristics. Every solution proposal is represented by a binary vector whose positions follow a fixed ordering of these lines. For a real line, a value equal to one indicates that the line is in service, whereas a value equal to zero indicates that it is open. For an artificial line, a value equal to one associates the corresponding nonrestored section with the artificial substation. Artificial lines do not represent physical lines or switching operations and do not carry electrical power.

Figure 9 illustrates this representation. The real substations and the initially energized portion of the network are represented in black. The faulted section is shown in gray, and the red cross indicates the fault location. The sections affected by the fault and considered during restoration are highlighted in orange. The artificial substation and its associated lines are represented in blue. Each position of the vector shown below the network corresponds to the line identified immediately above it.

Figure 9(a) represents the physical state of the system immediately after fault isolation and before any restorative switching action is performed. Section 6 contains the permanent fault and is isolated by opening lines 6 and 7. Since the fault-isolation procedure imposes the states of these lines, they are excluded from the solution vector s_i^k, which explains the nonconsecutive numbering of its entries. As a result, sections 7, 8, 9, and 10 constitute the affected portion of the network considered for restoration. The dashed blue lines 14, 15, 16, and 17 indicate the artificial connection associated with each affected section. Thus, the vector includes the status of all real and artificial lines considered in the augmented post-fault network.

Figure 9(b) presents a restored solution proposal. Real line 13 is selected, reconnecting sections 7 and 10 to substation SE_2. Sections 8 and 9 remain disconnected from the real substations and are therefore classified as nonrestored. Artificial lines 14 and 16 are selected to associate these sections with the artificial substation SE_f. Conversely, artificial lines 15 and 17 remain unselected because their corresponding sections, 7 and 10, have been restored through

Figure 9 - Illustrative test system and binary encoding of the restoration process: (a) post-fault isolated system and correspondence between the affected sections and the artificial lines; and (b) restored solution proposal.



Source: The author.

the real system. Thus, the restoration state of a section is determined from its connectivity rather than solely from the status of its incident real lines. A section connected to a real substation is considered restored and corresponds to $y_i = 0$ in the mathematical formulation. A section associated with the artificial substation is considered nonrestored and corresponds to $y_i = 1$. Consequently, the solution vector simultaneously represents the real switching configuration and identifies the demand that remains nonrestored.

Solution proposals are generated using the same constructive radial-topology strategy adopted for the reconfiguration problem, now applied to the augmented post-fault network. The WTPSO and WTEPSO assign line weights using their respective weighting mechanisms, whereas the EPSO evolves the line-weight vectors according to its replication, mutation, and selection procedures. For all three algorithms, Prim's algorithm constructs a radial topology from these weights. During this construction, the real and artificial substations are temporarily represented by a common root node. After the topology has been generated, the substations are separated again. The resulting configuration is a radial forest in which each component is associated with one real or artificial substation. This procedure guarantees radiality and connectivity, prevents the interconnection of different real substations, and provides the metaheuristic counterpart of the topological requirements established in (63)–(83).

Each solution proposal is evaluated using the objective function defined in (52). The weighted nonrestored demand is calculated from the sections associated with the artificial substation. As in the mathematical formulation, the demand located inside the faulted section is excluded because

it cannot be restored before the fault has been repaired. The remaining terms account for the closing of normally open switches and the opening of normally closed switches. Artificial lines are not included in the switching cost. After identifying the restored and nonrestored sections, a power-flow analysis is performed for the radial components supplied by the real substations. The resulting voltage magnitudes, line loadings, and substation power injections are used to verify the operational requirements defined in (53)–(62). If the power flow converges and all operational limits are satisfied, the fitness is equal to the objective function value obtained from (52). Otherwise, the solution proposal is classified as infeasible.

All solution proposals generated by the WTPSO, WTEPSO, and EPSO are evaluated using the same objective function, power-flow procedure, and feasibility criteria. Within each fault scenario, the algorithms use the same population size, maximum number of iterations, and stagnation limit. A run terminates when either the maximum number of iterations $k_{\max}$ is reached or no strict improvement in the global-best objective value is observed for $k_{\text{stg}}^{\max}$ consecutive iterations. The stagnation counter is reset to zero whenever the global-best solution is improved and is incremented otherwise. Consequently, the algorithms may perform different numbers of power-flow evaluations before termination; these differences are explicitly examined in the computational-effort analysis.

6.4 RESULTS

This section presents a statistical evaluation of the WTPSO, WTEPSO, and EPSO algorithms applied to the radial service restoration problem. Their results are compared with the benchmark solutions obtained using the MISOCP formulation presented in (52)–(83). All three metaheuristics were implemented using the common solution representation and evaluation procedure described in Section 6.3. The MISOCP formulation was implemented in the AMPL modeling language and solved using the CPLEX solver (version 22.1.1), whereas the metaheuristics were implemented in MATLAB R2021b. Each algorithm was executed 50 times for every fault scenario to account for its stochastic behavior.

The experiments consider the 53- and 417-node distribution systems. The 53-node system comprises 50 load nodes and three substations located at nodes 101, 102, and 104, with nominal capacities of 33400, 30000, and 22000 kVA, respectively. Its total active and reactive demands are 45668.70 kW and 22118.24 kVAr, respectively, and its nominal voltage is 13.8 kV. The voltage magnitude limits adopted in this work are 0.95 and 1.00 p.u. The 417-node system has three substations located at nodes 415, 416, and 417 and operates at a nominal voltage of 10.0 kV. Under normal operating conditions, its total active and reactive demands are 27372.30 kW and 13237.00 kVAr, respectively. The minimum and maximum voltage magnitude limits adopted in the experiments are 0.90 and 1.00 p.u. The complete load, branch, initial switch-status, and equipment-capacity data for both test systems can be obtained from the website of the Laboratory

of Power Systems Planning (LaPSEE), under "Downloads"[1]. For the 53-node system, two fault scenarios are analyzed: a permanent fault in section 14 and simultaneous permanent faults in sections 11, 14, and 21. For the 417-node system, permanent faults in sections 92 and 208 are considered separately.

The common BO procedure defined in Section 4.8 was applied independently to each metaheuristic and fault scenario. For the restoration application, $J_{\nu}^{\mathrm{rest}}(\theta)$ denotes the final restoration objective value obtained in calibration run ν for parameter configuration θ. Each BO run was initialized with the pseudorandom seed $\xi_{\mathrm{BO}} = 84001$, and every candidate parameter configuration was evaluated using the fixed calibration-seed set $\mathscr{S}_{\mathrm{cal}}^{\mathrm{rest}} = \{841001, \ldots, 841015\}$. The resulting control parameters adopted in the final experiments are presented in Table 11.

For the final comparison, each metaheuristic was executed 50 times for each fault scenario. The seed sets assigned to the WTPSO, WTEPSO, and EPSO were $\{6001, \ldots, 6050\}$, $\{6051, \ldots, 6100\}$, and $\{6101, \ldots, 6150\}$, respectively. These sets were mutually disjoint and were also disjoint from $\mathscr{S}_{\mathrm{cal}}^{\mathrm{rest}}$.

Performance was evaluated in terms of solution quality, robustness, convergence behavior, and computational effort. Solution quality and robustness were assessed using the minimum, mean, median, maximum, and standard deviation of the objective function values obtained over the independent runs. The nonrestored active demand, percentage of restored load, and number of switching operations were also analyzed to provide an operational interpretation of the solutions. Computational effort was evaluated by the number of power-flow calculations and the total computational time. To further examine the variability among runs, the best- and worst-performing solutions were analyzed individually, including their operational performance and representative switching plans. The following subsections present the benchmark results and the comparative performance analysis of the metaheuristics.

6.4.1 Benchmark results from the MISOCP formulation

The MISOCP formulation presented in (52)–(83) was solved for each fault scenario, and the solutions were adopted as benchmarks for the subsequent assessment of the metaheuristics. Table 12 summarizes the restoration performance in terms of switching operations, active load curtailment, percentage of restored load, objective function value, and computational time. The corresponding switching plans and the nodes that remain nonrestored are reported in Table 13. The switching operations required to isolate the faulted sections are imposed before the restoration problem is solved and are therefore not included in the reported number of operations. Consequently, the values in both tables account only for the additional opening and closing actions that define the restoration plan. Similarly, the nonrestored-node column lists only nodes

[1] `http://www.feis.unesp.br/#!/lapsee`

Table 11 - Parameter settings of the WTPSO, WTEPSO, and EPSO for the service restoration scenarios.

Test system	Fault section	WTPSO	WTEPSO	EPSO
53-node	14	$w_{\min} = 0.67$	$\tau = 0.25$	$\tau = 0.51$
		$w_{\max} = 1$	$cp = 0.94$	$cp = 1.00$
		$c_1 = 0.21$	$rr = 1$	$rr = 1$
		$c_2 = 0.01$		
		$k_w = 48$		
		$N^{\text{pop}} = 150$, $k_{\max} = 700$, $k_{\text{stg}}^{\max} = 80$		
53-node	11,14,21	$w_{\min} = 0.66$	$\tau = 0.56$	$\tau = 0.033$
		$w_{\max} = 1$	$cp = 0.45$	$cp = 0.24$
		$c_1 = 0.22$	$rr = 1$	$rr = 1$
		$c_2 = 0.04$		
		$k_w = 78$		
		$N^{\text{pop}} = 150$, $k_{\max} = 700$, $k_{\text{stg}}^{\max} = 80$		
417-node	92	$w_{\min} = 0.63$	$\tau = 0.80$	$\tau = 0.83$
		$w_{\max} = 0.81$	$cp = 1.00$	$cp = 0.19$
		$c_1 = 0.24$	$rr = 1$	$rr = 1$
		$c_2 = 0.039$		
		$k_w = 21$		
		$N^{\text{pop}} = 200$, $k_{\max} = 700$, $k_{\text{stg}}^{\max} = 80$		
417-node	208	$w_{\min} = 0.65$	$\tau = 0.60$	$\tau = 0.99$
		$w_{\max} = 0.73$	$cp = 0.99$	$cp = 0.16$
		$c_1 = 0.25$	$rr = 1$	$rr = 1$
		$c_2 = 0.07$		
		$k_w = 23$		
		$N^{\text{pop}} = 200$, $k_{\max} = 700$, $k_{\text{stg}}^{\max} = 80$		

Source: The author.

that remain de-energized after restoration; nodes located within the faulted sections are isolated and excluded from this list and the load curtailment term of the objective function.

In Table 12 the objective value of $US\$\ 48515$ for the fault in section 14 comprises $US\$\ 48510$ associated with 4851 kW of nonrestored demand and $US\$\ 5$ associated with five restorative switching operations. The remaining objective values follow the same calculation. For the single fault in section 14 of the 53-node system, the benchmark solution performs five switching operations: three openings and two closings. These actions restore 40.17% of the demand affected by the fault isolation process, while 4851 kW remain curtailed. Nodes 15, 16, 41, 46, and 47 cannot be reconnected without violating the problem's operational requirements. The corresponding objective value is $US\$\ 48515$, obtained in 5.94 s. The simultaneous faults in

Table 12 - Benchmark restoration performance obtained with the MISOCP mathematical model.

Test system	Fault section	Switching operations	Active load curtailment $[kW]$	Active load restored $[\%]$	Objective value $[US\$]$	Time [s]
53-node	14	5	4851.00	40.17	48515	5.94
	11,14,21	11	8316.00	57.45	83171	11.25
417-node	92	5	21.00	99.27	215	1249.69
	208	6	0	100	6	1212.02

Source: The author.

Table 13 - Benchmark switching plans obtained with the MISOCP mathematical model.

Test system	Faulted section	Switches opened	Switches closed	Nonrestored nodes
53-node	14	16-40, 42-41, 47-42	35-40, 28-50	15, 16, 41, 46, 47
	11, 14, 21	22-9, 45-12, 32-39, 33-39, 16-40	13-12, 18-17, 104-22, 8-33, 35-40, 10-38	15, 16, 32, 41, 42, 46, 47, 48, 49, 50
417-node	92	3-20, 58-20	88-89, 85-244, 20-33	87
	208	90-370, 345-346	160-180, 125-128, 369-370, 280-281	–

Source: The author.

sections 11, 14, and 21 affect a larger portion of the 53-node system and require eleven restorative switching operations. The resulting configuration restores 57.45% of the demand eligible for restoration, while 8316 kW remain curtailed. The benchmark objective value is $US\$$ 83171, and the solution is obtained in 11.25 s.

For the 417-node system, the fault in section 92 results in five switching operations. The proposed plan restores all affected nodes except node 87, limits active load curtailment to 21 kW, and achieves a restored load percentage of 99.27%. The resulting objective value is $US\$$ 215. For the fault in section 208, six switching operations are sufficient to reconnect all the demand affected by the fault isolation. Hence, no node remains de-energized, active load curtailment is zero, and the restored load percentage reaches 100%. In this case, the objective value of $US\$$ 6 is determined exclusively by the switching operations. The computational times for the 417-node scenarios are 1249.69 and 1212.02 s, respectively, which are considerably higher than those obtained for the 53-node system. This increase reflects the larger number of binary switching decisions and electrical constraints associated with the larger network.

These benchmark results provide the reference objective values and restoration plans used to assess the solutions obtained by the metaheuristics. The following subsection examines both the quality of these solutions and their consistency across independent runs.

Table 14 - Descriptive statistics of the objective-function values obtained by the WTPSO, WTEPSO, and EPSO algorithms for the service restoration problem under different fault scenarios over 50 independent runs.

Test system	Faulted section	Algorithm	Mean [US$]	Median [US$]	Std [US$]	$P^{\min}$ [US$]	$P^{\max}$ [US$]
53-node	14	WTPSO	49014	48515	1994.8	48515	56830
		WTEPSO	49346	48515	2519.8	48515	56830
		EPSO	51675	48515	4077.0	48515	56831
53-node	11, 14, 21	WTPSO	85360	83864	2586.0	83171	89406
		WTEPSO	84876	83864	2477.4	83171	92875
		EPSO	85513	83864	2902.2	83171	92180
417-node	92	WTPSO	636.94	217	866.74	215	3379
		WTEPSO	2686.30	2117.5	2639.6	217	13260
		EPSO	3169.6	2569.5	2007.1	436	10415
417-node	208	WTPSO	63.36	10	226.83	6	1231
		WTEPSO	1425.90	19	2529.60	6	12654
		EPSO	2086.5	1387	2273.70	20	10897

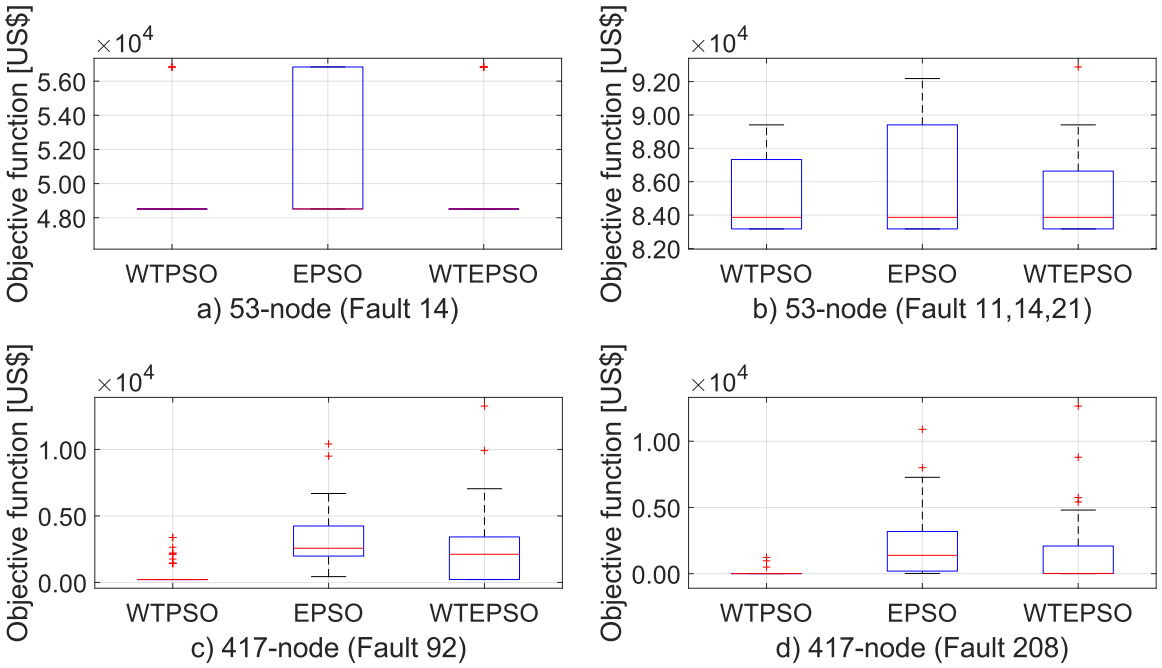
Source: The author.

6.4.2 Solution quality and robustness

The solution quality and robustness of the metaheuristics were evaluated over 50 independent runs for each fault scenario. Table 14 presents the mean, median, standard deviation, minimum, and maximum objective-function values obtained by each method. The minimum values are compared with the reference values provided by the MISOCP model in Table 12.

For the 53-node system, the proposed WTPSO and WTEPSO, as well as the EPSO, reached the benchmark objective value at least once under both fault scenarios. For the single fault at section 14, the WTPSO achieved the lowest mean and standard deviation, while all three algorithms presented the same median and minimum values. For the simultaneous faults at sections 11, 14, and 21, the WTEPSO obtained the lowest mean and standard deviation, whereas the WTPSO presented the smallest maximum value. For the 417-node system, the differences among the methods were more pronounced. The proposed WTPSO met the benchmark objective for both fault scenarios and achieved the lowest mean, median, standard deviation, and maximum values. The proposed WTEPSO also reached the benchmark value for the fault at section 208 and obtained a solution close to the benchmark for the fault at section 92, with a minimum value of *US*$ 217 compared with the reference value of *US*$ 215. However, its larger standard deviations indicate greater variability in these scenarios. The EPSO did not meet the benchmark for either fault scenario in the 417-node system and exhibited higher average objective function values. Overall, the proposed approaches achieved the lowest values for the large-scale system, with the WTPSO showing the most consistent performance across the evaluated restoration scenarios.

Figure 10 - Box plots of the objective function values obtained from 50 independent runs of the WTPSO, EPSO, and WTEPSO algorithms for the service restoration problem under the following fault scenarios: (a) 53-node system, section 14; (b) 53-node system, sections 11, 14, and 21; (c) 417-node system, section 92; and (d) 417-node system, section 208.



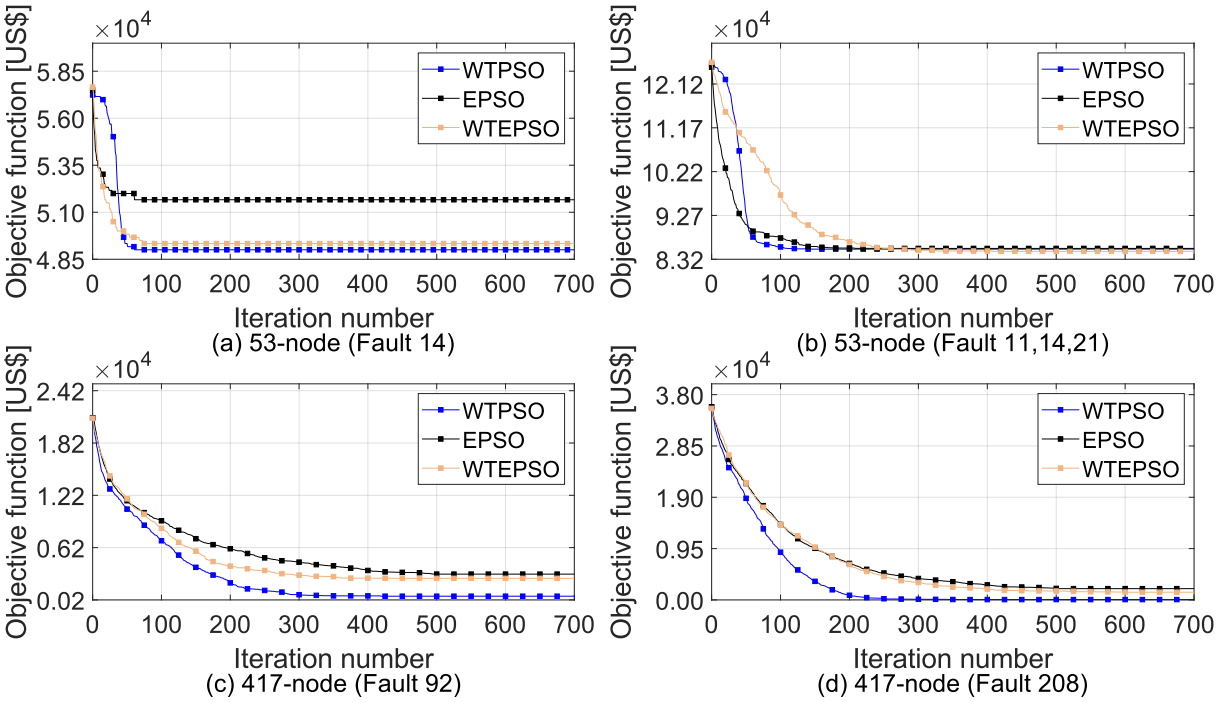
Source: The author.

Figure 10 complements the descriptive statistics by illustrating the distribution of the objective function values obtained over the 50 independent runs. For the 53-node system with a fault at section 14, the WTPSO and WTEPSO exhibit compact distributions concentrated near the benchmark value, whereas the EPSO shows greater dispersion. For the simultaneous faults at sections 11, 14, and 21, the three methods present similar median values, with the WTEPSO showing slightly lower overall variability, although the differences among the algorithms are relatively small. For the 417-node system, the differences among the algorithms become more evident. The WTPSO exhibits the most concentrated distributions and the lowest medians across both fault scenarios. For the fault at section 208, the WTEPSO also reaches the benchmark value and presents a lower median than the EPSO, although some runs produce considerably higher objective-function values. Overall, the box plots confirm the consistency of the proposed WTPSO, while the proposed WTEPSO remains competitive but exhibits greater variability for the larger test system.

6.4.3 Convergence behavior

Figure 11 presents the average convergence behavior of the evaluated metaheuristics for the service restoration problem. For the 53-node system with a fault at section 14, the proposed

Figure 11 - Average convergence profiles of the WTPSO, EPSO, and WTEPSO algorithms over 50 independent runs for the service restoration problem under the following fault scenarios: (a) 53-node system, section 14; (b) 53-node system, sections 11, 14, and 21; (c) 417-node system, section 92; and (d) 417-node system, section 208.



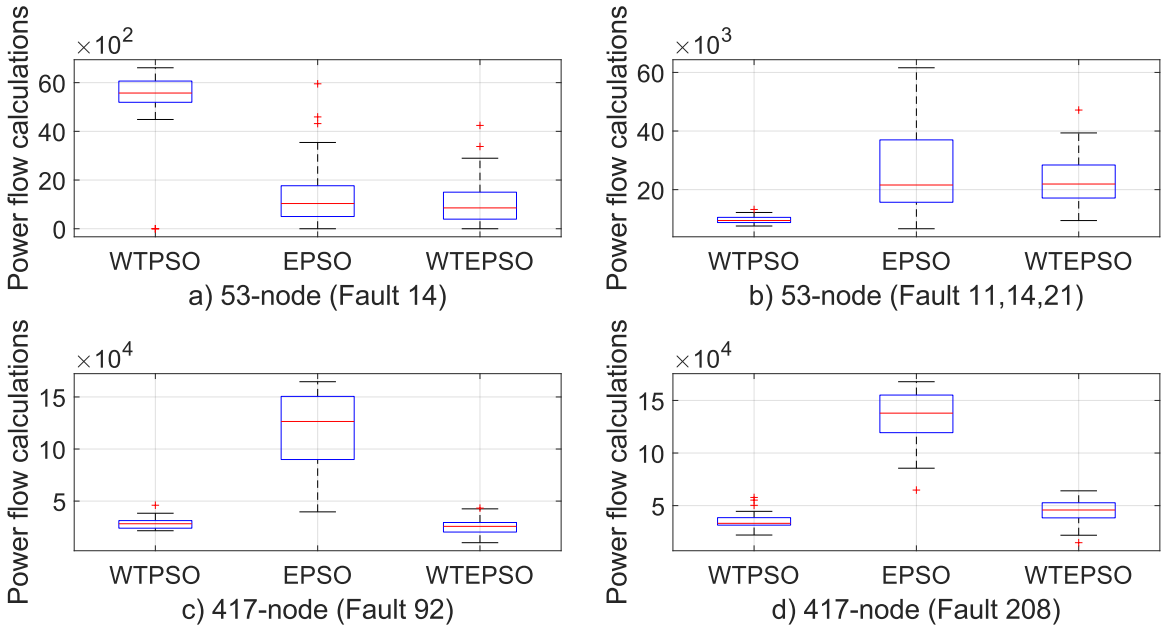
Source: The author.

WTPSO and WTEPSO rapidly reduce the objective-function value and stabilize at similar levels, with the WTPSO attaining a slightly lower final average. The EPSO also converges rapidly but stabilizes at a higher value. For the simultaneous faults at sections 11, 14, and 21, the WTPSO exhibits the fastest initial reduction, whereas the WTEPSO follows a more gradual trajectory and reaches the lowest final average value. For the 417-node system, the WTPSO converges more rapidly and attains the lowest final average value for both fault scenarios. The WTEPSO converges more gradually but finishes below the EPSO in both cases. These convergence profiles are consistent with the descriptive statistics reported in Table 14.

6.4.4 Computational effort

The computational effort of the evaluated metaheuristics is analyzed in Figs. 12 and 13, which show the distributions of the number of power flow calculations and computation times, respectively. For the 53-node system with a fault at section 14, the proposed WTPSO requires more power flow calculations than the WTEPSO and EPSO. For the simultaneous faults at sections 11, 14, and 21, however, the WTPSO presents the lowest median and the most compact distribution. For the 417-node system, both proposed approaches require substantially fewer

Figure 12 - Box plots of the number of power flow calculations performed over 50 independent runs of the WTPSO, EPSO, and WTEPSO algorithms for the service restoration problem under the following fault scenarios: (a) 53-node, section 14; (b) 53-node system, sections 11, 14, and 21; (c) 417-node system, section 92; and (d) 417-node system, section 208.



Source: The author.

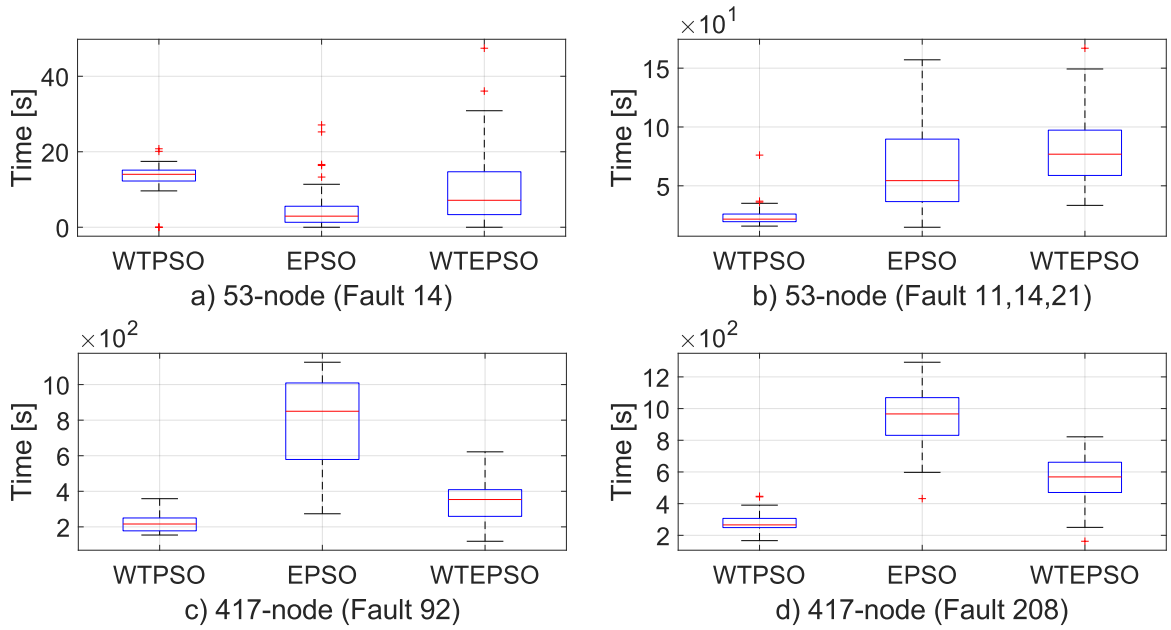
power flow calculations than the EPSO. The WTEPSO presents a slightly lower median for the fault at section 92, whereas the WTPSO requires fewer calculations for the fault at section 208.

As shown in Fig. 13, the EPSO presents the lowest median computation time for the 53-node system with a fault at section 14, followed by the WTEPSO. For the simultaneous faults, the WTPSO exhibits the lowest and most concentrated computation times. For both fault scenarios in the 417-node system, the WTPSO presents the lowest median time, while the WTEPSO requires less time than the EPSO. The differences between the relative rankings based on computation time and power-flow calculations indicate that execution time also depends on each algorithm's internal operations. Overall, the WTPSO presents the lowest computational effort for the more demanding scenarios, while the WTEPSO remains less computationally demanding than the EPSO for the 417-node system.

6.4.5 Best- and worst-case restoration solutions

To examine the range of outcomes produced by the stochastic algorithms, the best- and worst-performing solutions observed across the 50 independent runs are analyzed individually. For each algorithm and fault scenario, the best solution is defined as the run with the minimum objective function value, and the worst solution as the run with the maximum value. When more

Figure 13 - Box plots of the computation times obtained over 50 independent runs of the WTPSO, EPSO, and WTEPSO algorithms for the service restoration problem under the following fault scenarios: (a) 53-node system, section 14; (b) 53-node system, sections 11, 14, and 21; (c) 417-node system, section 92; and (d) 417-node system, section 208.



Source: The author.

than one run achieves the same minimum or maximum objective-function value, the switching plan from one of these runs is reported as a representative solution. Tables 15 and 16 present, respectively, the operational performance and switching plans associated with the best solutions.

The best-case results in Table 15 show that for both fault scenarios in the 53-node system, the three metaheuristics achieve the objective values of the MISOCP model. They also reproduce the corresponding load curtailment, the restored load percentage, the number of switching operations, and the switching plans. For the 417-node system with a fault at section 92, the proposed WTPSO matches the benchmark objective value of $US\$$ 215, with five switching operations and 99.27% of the active load restored, although its switching plan differs from the reference topology. The WTEPSO restores the same load but requires two additional switching operations, resulting in an objective value of $US\$$ 217. The EPSO obtains a higher objective value of $US\$$ 436 and restores 98.54% of the load. For the fault at section 208, both proposed approaches reach the benchmark value of $US\$$ 6, restoring the entire load with six switching operations, although they produce switching plans that differ from the reference plan. The EPSO also restores 100% of the load but requires 20 switching operations. Overall, the WTPSO reaches the benchmark objective value in all four scenarios, while the WTEPSO does so in three scenarios and the EPSO in the two scenarios of the 53-node system.

Although the best-case results demonstrate the algorithms' ability to produce high-quality

Table 15 - Performance of the best service restoration solution obtained by the WTPSO, WTEPSO, and EPSO algorithms over 50 independent runs under different fault scenarios.

Test system	Fault section	Algorithm	Switching operations	Active load curtailment $[kW]$	Active load restored $[\%]$	Objective value $[US\$]$
53-node	14	WTPSO	5	4851.00	40.17	48515
		WTEPSO	5	4851.00	40.17	48515
		EPSO	5	4851.00	40.17	48515
53-node	11,14,21	WTPSO	11	8316.00	57.45	83171
		WTEPSO	11	8316.00	57.45	83171
		EPSO	11	8316.00	57.45	83171
417-node	92	WTPSO	5	21.00	99.27	215
		WTEPSO	7	21.00	99.27	217
		EPSO	15	42.10	98.54	436
417-node	208	WTPSO	6	0	100	6
		WTEPSO	6	0	100	6
		EPSO	20	0	100	20

Source: The author.

restoration plans, they do not characterize their sensitivity to stochastic variation. For this reason, Tables 17 and 18 report the operational performance and switching plans associated with the worst solutions observed across the 50 independent runs.

The worst-case results in Table 17 show that, for the 53-node system with a fault at section 14, the three algorithms restore 29.92% of the active load, compared with 40.17% in the benchmark solution. The WTPSO and WTEPSO obtain an objective value of $US\$$ 56830, while the EPSO obtains $US\$$ 56831. For the simultaneous faults at sections 11, 14, and 21, the WTPSO presents the closest worst-case result to the benchmark, with an objective value of $US\$$ 89406 and 54.26% of the load restored. The EPSO and WTEPSO obtain higher objective values and lower restored load percentages in this scenario. The differences are more pronounced for the 417-node system. For the fault at section 92, the worst solution obtained by the WTPSO restores 88.32% of the load, whereas the EPSO and WTEPSO restore 63.99% and 54.15%, respectively, compared with 99.27% in the benchmark solution. For the fault at section 208, the WTPSO retains a restored load percentage of 97.59%, while the EPSO and WTEPSO obtain 78.48% and 75.00%, respectively. The corresponding switching plans in Table 18 reflect these differences through additional nonrestored nodes and, particularly for the larger system, an increased number of switching operations. Overall, the WTPSO presents the lowest or tied-lowest worst-case objective value in all evaluated scenarios, whereas the WTEPSO exhibits greater sensitivity to stochastic variation in the 417-node system.

Table 16 - Switching plans corresponding to the best service restoration solutions obtained by the WTPSO, WTEPSO, and EPSO algorithms over 50 independent runs for each fault scenario.

Test system	Faulted section	Algorithm	Switches opened	Switches closed	Nonrestored nodes
53-node	14	WTPSO	16-40, 42-41, 47-42	35-40, 28-50	15, 16, 41, 46, 47
		WTEPSO	16-40, 42-41, 47-42	35-40, 28-50	15, 16, 41, 46, 47
		EPSO	16-40, 42-41, 47-42	35-40, 28-50	15, 16, 41, 46, 47
53-node	11, 14, 21	WTPSO	22-9, 45-12, 32-39, 33-39, 16-40	13-12, 18-17, 104-22, 8-33, 35-40, 10-38	15, 16, 32, 41, 42, 46, 47, 48, 49, 50
		WTEPSO	22-9, 45-12, 32-39, 33-39, 16-40	13-12, 18-17, 104-22, 8-33, 35-40, 10-38	15, 16, 32, 41, 42, 46, 47, 48, 49, 50
		EPSO	22-9, 45-12, 32-39, 33-39, 16-40	13-12, 18-17, 104-22, 8-33, 35-40, 10-38	15, 16, 32, 41, 42, 46, 47, 48, 49, 50
417-node	92	WTPSO	3-20, 58-20	88-89, 384-68, 20-33	87
		WTEPSO	3-20, 58-20 18-5	384-68, 88-89, 20-33, 7-3	87
		EPSO	68-93, 54-24, 2-17, 2-14, 2-13, 25-35, 77-59, 58-20	384-68, 41-43, 88-89, 66-384, 34-47, 20-33, 7-3	2, 87, 93
417-node	208	WTPSO	90-370, 283-282	259-261, 125-128, 293-236, 280-281	–
		WTEPSO	73-77, 283-282	359-251, 125-128, 293-236, 280-281	–
		EPSO	59-70, 78-79, 47-21, 57-149, 253-254, 283-282, 77-59, 58-20, 281-282	61-60, 259-261, 36-45, 85-244, 359-251, 230-231, 280-281, 66-252, 27-31, 293-236, 149-138	–

Source: The author.

Table 17 - Performance of the worst service restoration solution obtained by the WTPSO, WTEPSO, and EPSO algorithms over 50 independent runs under different fault scenarios.

Test system	Fault section	Algorithm	Switching operations	Active load curtailment $[kW]$	Active load restored $[\%]$	Objective value $[US\$]$
53-node	14	WTPSO	4	5682.2	29.92	56830
		WTEPSO	4	5682.2	29.92	56830
		EPSO	5	5682.2	29.92	56831
53-node	11,14,21	WTPSO	9	8939.7	54.26	89406
		WTEPSO	13	9286.2	52.48	92875
		EPSO	11	9216.9	52.84	92180
417-node	92	WTPSO	8	337.10	88.32	3379
		WTEPSO	21	1323.9	54.15	13260
		EPSO	17	1039.8	63.99	10415
417-node	208	WTPSO	11	122	97.59	1231
		WTEPSO	41	1261.3	75.00	12654
		EPSO	21	1087.3	78.48	10897

Source: The author.

Table 18 - Switching plans corresponding to the worst service restoration solutions obtained by the WTPSO, WTEPSO, and EPSO algorithms over 50 independent runs for each fault scenario.

Test system	Faulted section	Algorithm	Switches opened	Switches closed	Nonrestored nodes
53-node	14	WTPSO	16-40, 48-42,	35-40, 28-50	15, 16, 41, 42, 46, 47
		WTEPSO	16-40, 48-42,	35-40, 28-50	15, 16, 41, 42, 46, 47
		EPSO	16-40, 48-42, 46-47	35-40, 28-50	15, 16, 41, 42, 46, 47
53-node	11, 14, 21	WTPSO	22-9, 45-12, 39-38, 35-34,	13-12, 18-17, 104-22, 8-33, 10-38	15, 16, 35, 36, 40, 41, 42, 46, 47, 48, 49, 50
		WTEPSO	20-19, 22-9, 45-12, 38-44, 33-39, 48-42, 49-48	13-12, 18-17, 104-22, 8-33, 10-38, 28-50	15, 16, 20, 40, 41, 42, 44, 45, 46, 47, 48
		EPSO	22-9, 45-12, 39-38, 34-33, 50-49	13-12, 18-17, 104-22, 8-33, 10-38, 28-50	15, 16, 34, 35, 36, 40, 41, 42, 46, 47, 48, 49
417-node	92	WTPSO	64-67, 8-9, 37-32, 25-35	384-68, 42-37, 88-89, 20-33	35, 38, 41 87
		WTEPSO	89-67, 52-56, 20-44, 35-38, 6-7, 2-14, 19-8, 14-16, 37-32, 12-15, 86-91, 10-88, 60-58, 24-29, 67-68	61-60, 42-37, 85-244, 20-33, 7-3, 3-10,	2, 4, 5, 6, 12, 13, 14, 16, 17, 18, 19, 25, 27, 29, 32, 34, 35, 38, 41, 44, 56, 87, 88, 89, 91
		EPSO	56-27, 17-18, 19-8, 32-44, 4-12, 110-84, 10-11, 25-35,	85-244, 27-31, 20-33, 7-3, 107-103, 3-10	2, 4, 11, 12, 13, 14, 15, 16, 17, 19, 32, 35,

			58-62, 58-20, 15-11		37, 38, 41, 58, 60, 86, 87, 91
417-node	208	WTPSO	63-61, 71-63, 253-254, 21-72, 234-233	61-60, 39-30, 359-251, 280-281, 293-236, 230-228	63
		WTEPSO	76-72, 51-52, 81-76, 73-80, 65-71, 79-83, 63-61, 78-79, 48-50, 277-279, 279-280, 37-32, 57-149, 57-125, 160-129, 154-156, 161-172, 251-360, 254-255, 21-72, 77-78, 257-259, 383-370, 281-235, 21-57	61-60, 42-37, 39-30, 160-180, 125-128, 143-150, 369-370, 66-252, 176-179, 148-57, 66-384, 75-81, 27-31, 293-236, 146-149, 230-228	43, 48, 63, 71, 76, 78, 79, 80, 82, 255, 259, 277, 278, 279, 280
		EPSO	72-73, 79-83, 63-61, 64-67, 279-280, 21-50, 253-254, 21-72, 40-47, 257-259, 46-42, 21-49, 234-233	384-68, 61-60, 36-45, 42-37, 382-383, 230-231, 280-281, 148-57, 66-384, 27-31, 293-236	43, 46, 48, 50, 72, 74, 75, 76, 81, 259, 277, 278, 279

Source: The author.

Overall, the results show that the proposed approaches can produce high-quality restoration plans for both test systems. The WTPSO provides the most consistent balance between solution quality and computational effort, while the WTEPSO also reaches benchmark or near-benchmark solutions but exhibits greater variability for the larger system. These results support the applicability of the proposed topology-based search mechanisms to the service restoration problem.

7 CONCLUSIONS AND FUTURE WORKS

7.1 CONCLUSIONS

This thesis proposed an interval-based weighting mechanism for discrete, topology-dependent optimization in radial distribution systems. The study showed that the information contained in the current, individual-best, and global-best solutions can be translated into branch-selection priorities without conventional velocity and position updates. Combined with Prim's algorithm, this mechanism generates radial candidate topologies directly, avoiding transfer functions and radiality-repair procedures. This formulation led to the proposed WTPSO and was subsequently incorporated into the evolutionary framework of the EPSO, yielding the WTEPSO.

The application to distribution system reconfiguration and service restoration demonstrated the modularity of the proposed mechanism. The same optimization core was retained across both problems, with application-specific adaptations to the network graph, initialization procedure, solution representation, objective evaluation, and feasibility verification. Accordingly, the proposed approaches maintain a common and relatively simple algorithmic structure despite the different objectives, operating conditions, and constraints of the two applications.

For distribution system reconfiguration, the proposed approaches were compared with the EPSO, BPSO, and CE, using the MILP approximation as the reference. The results showed that the WTPSO and WTEPSO consistently produced high-quality radial configurations under the adopted power-flow-evaluation budgets. The WTPSO provided the most favorable overall balance among solution quality, robustness, convergence behavior, and computational effort. The WTEPSO also produced competitive final solutions, with distributions that remained close to those obtained by the WTPSO; however, its relative computational efficiency depended on the size of the test system.

For service restoration, the proposed approaches were compared with the EPSO, using solutions from an MISOCP formulation as references. Both approaches produced high-quality and operationally feasible restoration plans under the evaluated fault conditions. In their best runs, the WTPSO attained the reference objective value in all four evaluated scenarios, whereas the WTEPSO attained it in three scenarios and remained close in the fourth. The WTPSO exhibited the most consistent performance, achieved the lowest mean and median objective

values for the 417-node system, and maintained better solution quality in its least-favorable runs. The WTEPSO remained competitive and required less computational effort than the EPSO for the 417-node system, although it exhibited greater run-to-run variability in the more demanding scenarios.

Taken together, these findings support the central hypothesis that swarm information can be reformulated through interval-based branch priorities and used to guide constructive searches in topology-dependent discrete problems. The objectives of the thesis were therefore achieved within the scope of the evaluated systems, mathematical models, fault scenarios, operating constraints, and computational budgets. The evidence obtained also provides a basis for extending the proposed approaches to larger and previously unseen systems, uncertain and time-varying operating conditions, distributed energy resources, multiobjective formulations, and more detailed operational models.

7.2 FUTURE WORKS

Based on the findings obtained and the opportunities identified during the development of this thesis, the following research directions are proposed:

1. **Sequential and dynamic service restoration.** The restoration formulation can be extended from determining a final network topology to optimizing the complete sequence of switching operations. This extension should verify radiality and electrical feasibility after every operation and may consider energy not supplied, restoration time, critical-load priorities, switching precedence, and manual or remotely controlled devices.

2. **Uncertainty and active distribution networks.** The proposed approaches can be extended to stochastic or robust formulations that account for uncertainties in demand, renewable generation, fault duration, and component availability. Distributed generation, energy storage systems, controllable loads, and microgrids may also be incorporated into multiperiod reconfiguration and restoration problems.

3. **Extension to other combinatorial problems.** The interval-based weighting principle may be investigated in other topologies and combinatorial optimization problems for which a compatible constructive procedure is available. Such studies should examine which properties of the representation and construction mechanism are required to preserve meaningful information exchange among the current, personal-best, and global-best solutions.

REFERENCES

AGUSTIN, J. L. B. *Aplicación de algoritmos genéticos al diseño óptimo de sistemas de distribución de energía eléctrica*. Tese (Doutorado) — Universidad de Zaragoza, Zaragoza, Spain, 1998.

BABUKARTHIK, R.; DHASARATHAN, C.; KUMAR, M.; SHANKAR, A.; THAKUR, S.; CHENG, X. A novel approach for multi-constraints knapsack problem using cluster particle swarm optimization. *Computers & Electrical Engineering*, Amsterdam, Netherlands, v. 96, p. 107399, 2021. ISSN 0045-7906.

BARAN, M.; WU, F. Network reconfiguration in distribution systems for loss reduction and load balancing. *IEEE Transactions on Power Delivery*, Piscataway, v. 4, n. 2, p. 1401–1407, 1989.

BEHBAHANI, M. R.; JALILIAN, A.; BAHMANYAR, A.; ERNST, D. Comprehensive review on static and dynamic distribution network reconfiguration methodologies. *IEEE Access*, Piscataway, NJ, USA, v. 12, p. 9510–9525, 2024.

BEHBAHANI, M. R.; JALILIAN, A.; BAHMANYAR, A.; ERNST, D. Comprehensive review on static and dynamic distribution network reconfiguration methodologies. *IEEE Access*, Piscataway, NJ, USA, v. 12, p. 9510–9525, 2024.

BEHESHTI, Z. A time-varying mirrored S-shaped transfer function for binary particle swarm optimization. *Information Sciences*, Amsterdam, Netherlands, v. 512, p. 1503–1542, 2020. ISSN 0020-0255.

BEHESHTI, Z. A novel X-shaped binary particle swarm optimization. *Soft Computing*, Berlin, Germany, v. 25, n. 4, p. 3013–3042, fev. 2021. ISSN 1433-7479.

BEHESHTI, Z. UTF: Upgrade transfer function for binary meta-heuristic algorithms. *Applied Soft Computing*, Amsterdam, Netherlands, v. 106, p. 107346, 2021. ISSN 1568-4946.

BISCHL, B.; BINDER, M.; LANG, M.; PIELOK, T.; RICHTER, J.; COORS, S.; THOMAS, J.; ULLMANN, T.; BECKER, M.; BOULESTEIX, A.-L.; DENG, D.; LINDAUER, M. Hyperparameter optimization: Foundations, algorithms, best practices, and open challenges. *Wiley Interdisciplinary Reviews: Data Mining and Knowledge Discovery*, Hoboken, NJ, USA, v. 13, n. 2, p. e1484, 2023.

BORGES, M. C. O.; FRANCO, J. F.; RIDER, M. J. Optimal reconfiguration of electrical distribution systems using mathematical programming. *Journal of Control, Automation and Electrical Systems*, New York, NY, USA, v. 25, n. 1, p. 103–111, 2014. Disponível em: https://doi.org/10.1007/s40313-013-0070-x.

BOSISIO, A.; BERIZZI, A.; LUPIS, D.; MOROTTI, A.; IANNARELLI, G.; GRECO, B. A tabu-search-based algorithm for distribution network restoration to improve reliability and

resiliency. *Journal of Modern Power Systems and Clean Energy*, Nanjing, China, v. 11, n. 1, p. 302–311, 2023.

CAMPOVERDE, E. L.; TORRES, S. P.; OCHOACORREA, D.; GIRALDO, J. S. Service restoration in distribution systems considering priority customers and microgrids. *Electric Power Systems Research*, Amsterdam, Netherlands, v. 237, p. 110988, 2024.

CHIOU, J.-P.; CHANG, C.-F.; SU, C.-T. Variable scaling hybrid differential evolution for solving network reconfiguration of distribution systems. *IEEE Transactions on Power Systems*, Piscataway, NJ, USA, v. 20, n. 2, p. 668–674, 2005.

ÇIMEN, M. E.; GARIP, Z.; BOZ, A. F. Comparison of metaheuristic optimization algorithms with a new modified Deb feasibility constraint handling technique. *Turkish Journal of Electrical Engineering and Computer Sciences*, Ankara, Türkiye, v. 29, p. 3270–3289, 2021.

CIVANLAR, S.; GRAINGER, J.; YIN, H.; LEE, S. Distribution feeder reconfiguration for loss reduction. *IEEE Transactions on Power Delivery*, Piscataway, NJ, USA, v. 3, n. 3, p. 1217–1223, 1988.

EL-FERGANY, A. A. Reviews, challenges, and insights on computational methods for network reconfigurations in smart electricity distribution networks. *Archives of Computational Methods in Engineering*, Dordrecht, Netherlands, v. 31, p. 1233–1253, 2024.

FRAZIER, P. I. A tutorial on Bayesian optimization. *arXiv preprint arXiv:1807.02811*, Ithaca, NY, USA, 2018.

GAUTAM, M.; BHUSAL, N.; BENIDRIS, M.; LOUIS, S. J. A spanning tree-based genetic algorithm for distribution network reconfiguration. In: *2020 IEEE Industry Applications Society Annual Meeting*. Detroit, MI, USA: [s.n.], 2020. p. 1–6.

GEREZ, C.; SILVA, L. I.; BELATI, E. A.; FILHO, A. J. S.; COSTA, E. C. M. Distribution network reconfiguration using selective firefly algorithm and a load flow analysis criterion for reducing the search space. *IEEE Access*, Piscataway, NJ, USA, v. 7, p. 67874–67888, 2019.

GERI, A.; MACCIONI, M.; MELONI, C.; NATI, L.; PALAZZOLI, A. Power distribution network configuration applying the corridor method. *Computers & Industrial Engineering*, Amsterdam, Netherlands, v. 186, p. 109709, 2023. ISSN 0360-8352.

GONÇALVES, J. F.; RESENDE, M. G. C. Biased random-key genetic algorithms for combinatorial optimization. *Journal of Heuristics*, New York, NY, USA, v. 17, n. 5, p. 487–525, 2011.

GUO, S. S.; WANG, J. S.; GUO, M. W. Z-shaped transfer functions for binary particle swarm optimization algorithm. *Computational Intelligence and Neuroscience*, London, United Kingdom, v. 2020, p. 6502807, 2020.

HILDEBRANDT, S.; NUNES, S.; FRANKE, M.; SAND, G. Studies on a Bayesian optimization based approach to tune hyperparameters of matheuristics. In: *Learning and Intelligent Optimization*. Ischia Island, Italy: Springer Nature Switzerland, 2024. p. 203–217.

HIZARCI, H.; DEMIREL, O.; TURKAY, B. E. Distribution network reconfiguration using

time-varying acceleration coefficient assisted binary particle swarm optimization. *Engineering Science and Technology, an International Journal*, Amsterdam, Netherlands, v. 35, p. 101230, 2022. ISSN 2215-0986.

HOUSSEIN, E. H.; GAD, A. G.; HUSSAIN, K.; SUGANTHAN, P. N. Major advances in particle swarm optimization: Theory, analysis, and application. *Swarm and Evolutionary Computation*, Amsterdam, Netherlands, v. 63, p. 100868, 2021. ISSN 2210-6502.

IGDER, M. A.; LIANG, X. Service restoration using deep reinforcement learning and dynamic microgrid formation in distribution networks. *IEEE Transactions on Industry Applications*, Piscataway, NJ, USA, v. 59, n. 5, p. 5453–5472, 2023.

IGDER, M. A.; LIANG, X.; MITOLO, M. Service restoration through microgrid formation in distribution networks: A review. *IEEE Access*, Piscataway, NJ, USA, v. 10, p. 46618–46632, 2022.

JACOB, R. A.; PAUL, S.; CHOWDHURY, S.; GEL, Y. R.; ZHANG, J. Real-time outage management in active distribution networks using reinforcement learning over graphs. *Nature Communications*, London, United Kingdom, v. 15, p. 4766, 2024.

JIN, X.; WEI, B.; DENG, L.; YANG, S.; ZHENG, J.; WANG, F. An adaptive pyramid PSO for high-dimensional feature selection. *Expert Systems with Applications*, Amsterdam, Netherlands, v. 257, p. 125084, 2024. ISSN 0957-4174.

JOSHI, M.; GYANCHANDANI, M.; WADHVANI, D. R. Analysis of genetic algorithm, particle swarm optimization and simulated annealing on benchmark functions. In: *2021 5th International Conference on Computing Methodologies and Communication (ICCMC)*. Erode, Tamil Nadu, India: [s.n.], 2021. p. 1152–1157.

KENNEDY, J.; EBERHART, R. Particle swarm optimization. In: *Proceedings of ICNN'95 - International Conference on Neural Networks*. Perth, WA, Australia: [s.n.], 1995. v. 4, p. 1942–1948 vol.4.

KENNEDY, J.; EBERHART, R. A discrete binary version of the particle swarm algorithm. In: *1997 IEEE International Conference on Systems, Man, and Cybernetics. Computational Cybernetics and Simulation*. Orlando, FL, USA: [s.n.], 1997. v. 5, p. 4104–4108 vol.5.

KERCKHOVE, S.; D'HULST, R.; HERTEM, D. V. Low voltage reconfiguration: A comparison of metaheuristic and mathematical programming approaches. *Electric Power Systems Research*, Amsterdam, Netherlands, v. 237, p. 110823, 2024.

KRAMER, O. A review of constraint-handling techniques for evolution strategies. *Applied Computational Intelligence and Soft Computing*, Cairo, Egypt, v. 2010, p. 1–11, 2010.

KULKARNI, A. J.; MEZURA-MONTES, E.; WANG, Y.; GANDOMI, A. H.; KRISHNASAMY, G. (Ed.). *Constraint Handling in Metaheuristics and Applications*. Singapore: Springer, 2021. ISBN 978-981-33-6710-4.

KUMAR, L.; BHARTI, K. K. A novel hybrid BPSO–SCA approach for feature selection. *Natural Computing*, Dordrecht, Netherlands, v. 20, n. 1, p. 39–61, mar. 2021. ISSN 1572-9796.

LAGAROS, N. D.; KOURNOUTOS, M.; KALLIORAS, N. A.; NORDAS, A. N. Constraint handling techniques for metaheuristics: A state-of-the-art review and new variants. *Optimization and Engineering*, Cham, Switzerland, v. 24, p. 2251–2298, 2023.

LANDEROS, A.; KOZIEL, S.; ABDEL-FATTAH, M. F. Distribution network reconfiguration using feasibility-preserving evolutionary optimization. *Journal of Modern Power Systems and Clean Energy*, Nanjing, China, v. 7, n. 3, p. 589–598, 2019.

LI, A.-D.; XUE, B.; ZHANG, M. Improved binary particle swarm optimization for feature selection with new initialization and search space reduction strategies. *Applied Soft Computing*, Amsterdam, Netherlands, v. 106, p. 107302, 2021. ISSN 1568-4946.

LI, X.; FANG, W.; ZHU, S. An improved binary quantum-behaved particle swarm optimization algorithm for knapsack problems. *Information Sciences*, Amsterdam, Netherlands, v. 648, p. 119529, 2023. ISSN 0020-0255.

LI, X.; FANG, W.; ZHU, S.; ZHANG, X. An adaptive binary quantum-behaved particle swarm optimization algorithm for the multidimensional knapsack problem. *Swarm and Evolutionary Computation*, Amsterdam, Netherlands, v. 86, p. 101494, 2024. ISSN 2210-6502.

LUO, L.; MA, J.; WANG, H.; LUO, S. Optimal network reconfiguration using beetle antennae search based on the Prim algorithm. In: *2020 35th Youth Academic Annual Conference of Chinese Association of Automation (YAC)*. Zhanjiang, China: [s.n.], 2020. p. 656–660.

MACEDO, M.; SIQUEIRA, H.; FIGUEIREDO, E.; SANTANA, C.; LIRA, R. C.; GOKHALE, A.; BASTOS-FILHO, C. Overview on binary optimization using swarm-inspired algorithms. *IEEE Access*, Piscataway, NJ, USA, v. 9, p. 149814–149858, 2021.

MAHDAVI, M.; ALHELOU, H. H.; BAGHERI, A.; DJOKIC, S. Z.; RAMOS, R. A. V. A comprehensive review of metaheuristic methods for the reconfiguration of electric power distribution systems and comparison with a novel approach based on efficient genetic algorithm. *IEEE Access*, Piscataway, NJ, USA, v. 9, p. 122872–122906, 2021.

MAHDAVI, M.; ALHELOU, H. H.; GOPI, P.; HOSSEINZADEH, N. Importance of radiality constraints formulation in reconfiguration problems. *IEEE Systems Journal*, Piscataway, NJ, USA, v. 17, n. 4, p. 6710–6723, 2023.

MAHDAVI, M.; ALHELOU, H. H.; HATZIARGYRIOU, N. D.; JURADO, F. Reconfiguration of electric power distribution systems: Comprehensive review and classification. *IEEE Access*, Piscataway, NJ, USA, v. 9, p. 118502–118527, 2021.

MANTOVANI, J.; CASARI, F.; ROMERO, R. Reconfiguração de sistemas de distribuicao radiais utilizando o critério de queda de tensão. *Controle and Automação*, Campinas, SP, Brazil, v. 11, p. 150–159, 2000.

MARINI, F.; WALCZAK, B. Particle swarm optimization (PSO). A tutorial. *Chemometrics and Intelligent Laboratory Systems*, Amsterdam, Netherlands, v. 149, p. 153–165, 2015. ISSN 0169-7439.

MENDOZA, J.; LOPEZ, R.; MORALES, D.; LOPEZ, E.; DESSANTE, P.; MORAGA, R. Minimal loss reconfiguration using genetic algorithms with restricted population and addressed

operators: Real application. *IEEE Transactions on Power Systems*, Piscataway, NJ, USA, v. 21, n. 2, p. 948–954, 2006.

MIRANDA, V.; FONSECA, N. EPSO – best-of-two-worlds meta-heuristic applied to power system problems. In: *Proceedings of the 2002 Congress on Evolutionary Computation. CEC'02 (Cat. No.02TH8600)*. Honolulu, HI, USA: [s.n.], 2002. v. 2, p. 1080–1085 vol.2.

MIRANDA, V.; FONSECA, N. EPSO-evolutionary particle swarm optimization, a new algorithm with applications in power systems. In: *IEEE/PES Transmission and Distribution Conference and Exhibition*. Yokohama, Japan: [s.n.], 2002. v. 2, p. 745–750 vol.2.

MIRANDA, V.; KEKO, H.; DUQUE, Á. J. Stochastic star communication topology in evolutionary particle swarms (EPSO). *International Journal of Computational Intelligence Research*, Delhi, India, v. 4, n. 2, p. 105–116, 2008.

MIRJALILI, S.; ZHANG, H.; MIRJALILI, S.; CHALUP, S.; NOMAN, N. A novel U-shaped transfer function for binary particle swarm optimisation. In: NAGAR, A. K.; DEEP, K.; BANSAL, J. C.; DAS, K. N. (Ed.). *Soft Computing for Problem Solving 2019*. Singapore: Springer Singapore, 2020. p. 241–259.

PRASTYO, P. H.; HIDAYAT, R.; ARDIYANTO, I. Enhancing sentiment classification performance using hybrid query expansion ranking and binary particle swarm optimization with adaptive inertia weights. *ICT Express*, Seoul, Republic of Korea, v. 8, n. 2, p. 189–197, 2022. ISSN 2405-9595.

PRIM, R. C. Shortest connection networks and some generalizations. *Bell System Technical Journal*, New York, NY, USA, v. 36, n. 6, p. 1389–1401, 1957.

RAHIMI, I.; GANDOMI, A. H.; CHEN, F.; MEZURA-MONTES, E. A review on constraint handling techniques for population-based algorithms: From single-objective to multi-objective optimization. *Archives of Computational Methods in Engineering*, Dordrecht, Netherlands, v. 30, n. 3, p. 2181–2209, 2023.

ROMAN, I.; CEBERIO, J.; MENDIBURU, A.; LOZANO, J. A. Bayesian optimization for parameter tuning in evolutionary algorithms. In: *Proceedings of the IEEE Congress on Evolutionary Computation (CEC)*. Vancouver, BC, Canada: [s.n.], 2016. p. 4839–4845.

RÜTHER, C.; RIECK, J. A bayesian optimization approach for tuning a grouping genetic algorithm for solving practically oriented pickup and delivery problems. *Logistics*, Basel, Switzerland, v. 8, n. 14, 2024.

SALCEDO-SANZ, S. A survey of repair methods used as constraint handling techniques in evolutionary algorithms. *Computer Science Review*, Amsterdam, Netherlands, v. 3, n. 3, p. 175–192, 2009.

SEBAA, K.; GELEN, A.; NOURI, H. Crossentropy method for distribution power systems reconfiguration. *Engineering Reports*, Hoboken, NJ, USA, v. 1, n. 3, p. e12052, 2019.

SILVEIRA, C. L. B.; TABARES, A.; FARIA, L. T.; FRANCO, J. F. Mathematical optimization versus metaheuristic techniques: A performance comparison for reconfiguration of distribution systems. *Electric Power Systems Research*, Amsterdam, Netherlands, v. 196, p. 107272, 2021.

ISSN 0378-7796.

SOUZA, E. S.; ROMERO, R.; FRANCO, J. F. Restoration of electrical distribution systems using a relaxed mathematical model. *Journal of Control, Automation and Electrical Systems*, New York, NY, USA, v. 29, n. 2, p. 259–269, 2018.

SUDHAKAR, T. D.; PRASAD, H. Optimal service reconfiguration and restoration of network using cuckoo-search and Prim's algorithms. In: *2023 3rd International Conference on Pervasive Computing and Social Networking (ICPCSN)*. Salem, Tamil Nadu, India: [s.n.], 2023. p. 660–666.

SUN, J.; XU, W.; FANG, W.; CHAI, Z. Quantum-behaved particle swarm optimization with binary encoding. In: BELICZYNSKI, B.; DZIELINSKI, A.; IWANOWSKI, M.; RIBEIRO, B. (Ed.). *Adaptive and Natural Computing Algorithms*. Berlin, Heidelberg: Springer Berlin Heidelberg, 2007. p. 376–385. ISBN 978-3-540-71618-1.

SUN, S.; LI, G.; CHEN, C.; BIAN, Y.; BIE, Z. A novel formulation of radiality constraints for resilient reconfiguration of distribution systems. *IEEE Transactions on Smart Grid*, Piscataway, NJ, USA, v. 14, n. 2, p. 1337–1340, 2023.

VARGAS, R.; MACEDO, L. H.; HOME-ORTIZ, J. M.; ROMERO, R. Optimal restoration of distribution systems considering temporary closed-loop operation. *IEEE Systems Journal*, Piscataway, NJ, USA, v. 15, n. 4, p. 5483–5494, 2021.

VARGAS, R.; ROMERO, R.; FRANCO, J. F. Biased random-key genetic algorithm applied to the optimal reconfiguration of radial distribution systems. In: *2018 IEEE PES Transmission & Distribution Conference and Exhibition – Latin America (T&D-LA)*. Lima, Peru: [s.n.], 2018. p. 1–5.

WANG, Y.; XU, Y.; LI, J.; HE, J.; WANG, X. On the radiality constraints for distribution system restoration and reconfiguration problems. *IEEE Transactions on Power Systems*, Piscataway, NJ, USA, v. 35, n. 4, p. 3294–3296, 2020.

ZYL, J.-P. van; ENGELBRECHT, A. P. Set-based particle swarm optimisation: A review. *Mathematics*, Basel, Switzerland, v. 11, n. 13, p. 2980, 2023.

APPENDIX A - FORMULATION OF THE WEIGHTED TIER EVOLUTIONARY PARTICLE SWARM OPTIMIZATION (WTEPSO)

A.1 MOTIVATION

The interval-based weighting mechanism proposed in this work was designed as a modular component. Although its main formulation is presented within the WTPSO, the same mechanism can be incorporated into other population-based metaheuristics, provided that their learning components can be associated with the current, personal-best, and global-best solution proposals. To demonstrate this modularity, this appendix presents an adaptation of the proposed weighting mechanism to the evolutionary particle swarm optimization (EPSO). The objective is not to develop an unrelated metaheuristic, but to show how the parameters governing the interval bounds can be replaced by the evolutionary weights of the EPSO, while preserving the original branch-selection and radial-topology generation mechanisms.

Furthermore, the proposed adaptation is motivated by the discrete nature of topology optimization problems in distribution systems, encompassing both reconfiguration and service restoration. Although the EPSO provides self-adaptive search capabilities by evolving its strategic parameters, its original velocity-position update mechanism was conceived for continuous optimization problems (Miranda; Fonseca, 2002a; Miranda; Fonseca, 2002b). In contrast, the proposed interval-based weighting mechanism replaces the conventional particle update process with a qualitative strategy specifically designed to generate radial topologies in discrete search spaces.

Therefore, the resulting WTEPSO combines the self-adaptive capabilities of the EPSO with a topology-generation mechanism tailored to distribution-system applications, potentially improving the balance between exploration and exploitation in combinatorial search spaces.

A.2 OVERVIEW OF EPSO

The EPSO, originally proposed by Miranda and Fonseca (Miranda; Fonseca, 2002a; Miranda; Fonseca, 2002b), combines concepts from PSO and evolution strategies by incorporating social interaction among particles and self-adaptive parameters that govern their movement. Unlike conventional PSO (Kennedy; Eberhart, 1995), in which the inertia weight and the cognitive and social coefficients are externally specified, the EPSO treats these coefficients as strategic parameters that evolve throughout the optimization process. As a result, each particle is charac-

terized not only by its position in the search space but also by a set of strategic parameters that determine its search behavior. The algorithm is composed of five main stages:

1. Replication, in which each particle generates a copy; in the implementation adopted in this work, the replication rate is $rr = 1$;
2. Mutation, in which the strategic parameters associated with the copied particle are modified according to a stochastic process;
3. Reproduction, in which new solution proposals are generated using both the original and mutated strategic parameters;
4. Evaluation, in which the resulting solution proposals are assessed through the objective function;
5. Selection, in which the proposals generated using the original and mutated strategic parameters are compared, and the better proposal is retained together with its associated strategic parameters.

Through this mutation-and-selection process, the strategic parameters associated with successful solution proposals are propagated to subsequent iterations. This self-adaptive mechanism enables each particle to dynamically adjust its search behavior, making the EPSO particularly well-suited for integration with the proposed interval-based weighting mechanism.

The following section presents the mathematical equations governing the mutation of the strategic parameters and the generation of new solution proposals in the EPSO.

A.3 MAIN EQUATIONS OF EPSO

In the EPSO, each particle is associated with a set of strategic parameters that evolve throughout the optimization process. These parameters determine the contributions of inertia, individual learning, collective learning, and the perturbation applied to the global-best solution. Consequently, the optimization process evolves both the solution proposals and the parameters that generate them. The formulation adopted in this work follows the original EPSO framework proposed by Miranda e Fonseca (2002a), Miranda e Fonseca (2002b) and includes a fourth strategic parameter associated with the perturbation of the global best (Miranda; Keko; Duque, 2008).

Let

$$\mathbf{w}_i^k = \left[w_{i,1}^k, w_{i,2}^k, w_{i,3}^k, w_{i,4}^k \right], \qquad \forall i \in \{1, \ldots, N^{\text{pop}}\} \tag{84}$$

denote the vector of strategic parameters associated with particle i at iteration k, where:

- $w_{i,1}^k$ is the inertia weight, associated with the inertia component;
- $w_{i,2}^k$ is the memory weight, associated with the cognitive component;
- $w_{i,3}^k$ is the cooperation weight, associated with the social component;
- $w_{i,4}^k$ controls the perturbation applied to the global best solution.

During the mutation stage, the strategic parameters evolve according to

$$w_{i,q}^{k,\text{new}} = w_{i,q}^k + \tau \cdot N(0,1), \qquad \forall i \in \{1,\ldots,N^{\text{pop}}\}, \forall q \in \{1,\ldots,4\}, \tag{85}$$

where τ is the mutation rate and $N(0,1)$ denotes a Gaussian random variable with zero mean and unit variance.

Subsequently, the global best solution is perturbed according to

$$g_i^{\text{best,new}} = g^{\text{best}} + w_{i,4}^{k,\text{new}} \cdot N(0,1), \qquad \forall i \in \{1,\ldots,N^{\text{pop}}\} \tag{86}$$

thus introducing additional diversity into the search process.

The particle velocity is then updated as

$$v_i^{k+1} = w_{i,1}^{k,\text{new}} v_i^k + w_{i,2}^{k,\text{new}} \left[p_i^{\text{best}} - s_i^k\right] + w_{i,3}^{k,\text{new}} \left[g_i^{\text{best,new}} - s_i^k\right], \quad \forall i \in \{1,\ldots,N^{\text{pop}}\} \tag{87}$$

while the particle position is computed as

$$s_i^{k+1} = s_i^k + v_i^{k+1}, \qquad \forall i \in \{1,\ldots,N^{\text{pop}}\} \tag{88}$$

These equations describe the conventional continuous velocity–position update mechanism of the EPSO. The strategic parameters are independently mutated and subsequently retained or discarded during the selection stage based on the quality of the solution proposals they generate.

In the proposed WTEPSO, the conventional velocity–position update equations (87) and (88) are not directly applied. Instead, the evolutionary weights defined above are used to compute

the interval bounds from which the branch weights are sampled. Prim's algorithm then uses these weights to construct new radial solution proposals, as described in the following sections.

A.4 WEIGHTED TIER EVOLUTIONARY PARTICLE SWARM OPTIMIZATION (WTEPSO)

The interval-based weighting mechanism proposed in this work was originally formulated using the inertia weight w and the cognitive and social coefficients c_1 and c_2 of the conventional PSO. Since the EPSO replaces these fixed parameters with evolutionary weights that vary throughout the optimization process, the proposed mechanism can be naturally incorporated into the EPSO framework by establishing a correspondence between the parameters of both methods.

More specifically, the inertia weight and the cognitive and social coefficients of the original WTPSO formulation are replaced by the mutated weights associated with each particle:

$$w \longrightarrow w_{i,1}^{k,\text{new}}, \tag{89}$$

$$c_1 \longrightarrow w_{i,2}^{k,\text{new}}, \tag{90}$$

$$c_2 \longrightarrow w_{i,3}^{k,\text{new}}. \tag{91}$$

Consequently, the interval-based weighting mechanism becomes particle- and iteration-dependent. The parameter $w_{i,1}^{k,\text{new}}$ regulates the degree of overlap among the intervals and, therefore, the stochasticity of the branch-selection process. Similarly, $w_{i,2}^{k,\text{new}}$ determines the influence of the personal best solution p_i^{best}, while $w_{i,3}^{k,\text{new}}$ determines the influence of the perturbed global best solution $g^{\text{best,new}}$.

To preserve valid interval bounds, the strategic parameters are maintained within the following admissible ranges:

$$0 \leq w_{i,1}^{k,\text{new}}, w_{i,4}^{k,\text{new}} \leq 1, \qquad \forall i \in \{1,\ldots,N^{\text{pop}}\} \tag{92}$$

$$0 \leq w_{i,2}^{k,\text{new}}, w_{i,3}^{k,\text{new}} \leq 0.5, \qquad \forall i \in \{1,\ldots,N^{\text{pop}}\} \tag{93}$$

For each solution proposal i, the WTEPSO generates two candidate topologies at each iteration: one using the current strategic parameters $\mathbf{w}_i^k$ and another using the mutated strategic parameters $\mathbf{w}_i^{k,\text{new}}$. Since the interval calculations are identical in both cases, the following equations are presented only for the mutated parameters. After evaluation, the better candidate and its associated strategic parameters are retained during the selection stage.

In the conventional continuous EPSO, the fourth strategic parameter controls the perturbation

of the global-best position, as expressed in (86). However, because the solution proposals considered in this work are binary vectors representing branch operating states, the global-best topology cannot be perturbed directly via vector addition. Instead, the perturbation is performed in the space of the continuous branch weights associated with the global-best topology.

Let $\rho^{g,k}$ denote the branch-weight vector associated with the global-best topology at iteration k. For each particle i, this vector is perturbed according to

$$\widetilde{\rho}_{ij}^{g,k} = \rho_j^{g,k} + w_{i,4}^{k,\text{new}} \eta_{ij}^k, \qquad \forall i \in \{1,\ldots,N^{\text{pop}}\}, \quad j = 1,\ldots,n_r. \tag{94}$$

where $\eta_{ij}^k \sim \mathcal{N}(0,1)$ is an independent Gaussian random variable and j denotes the branch index.

The perturbed global-best topology associated with particle i is then obtained as

$$g_i^{\text{best,new}} = \text{Prim}\left(\widetilde{\rho}_i^{g,k}\right), \qquad \forall i \in \{1,\ldots,N^{\text{pop}}\} \tag{95}$$

where $\text{Prim}(\cdot)$ returns the binary branch-status vector corresponding to the minimum spanning tree obtained using Prim's algorithm (Prim, 1957).

Before computing the interval bounds, a stochastic communication mechanism is applied to the perturbed global-best topology. Let

$$\chi_{ij}^k \sim \text{Bernoulli}(cp), \tag{96}$$

$$g_{ij}^{\text{best,new,comm}} = \chi_{ij}^k g_{ij}^{\text{best,new}}, \qquad \forall i \in \{1,\ldots,N^{\text{pop}}\}, \quad j = 1,\ldots,n_r. \tag{97}$$

where $cp \in [0,1]$ is the communication probability (Miranda; Keko; Duque, 2008). Therefore, the operating state of each branch in the perturbed global-best topology is used by particle i with probability cp.

Therefore, the interval assigned to each branch is determined from its operating state in the current solution proposal s_i^k, the personal-best solution p_i^{best}, and the communicated perturbed global-best information $g_i^{\text{best,new,comm}}$. The corresponding interval-bound expressions are presented in the following section.

A.5 COMPUTATION OF INTERVAL BOUNDS

The intervals adopted in the WTEPSO follow the same structure introduced in Section 4.2 for the original WTPSO. The interval assigned to each branch depends on its operating state in the current solution proposal s_i^k, the personal-best solution p_i^{best}, and the communicated perturbed global-best information $g_i^{\text{best,new,comm}}$. The parameter $m \in \{1,2,3,4\}$ preserves the interpretation adopted in the original WTPSO. Specifically, $m = 1$ indicates that the branch is closed in all three cases, $m = 2$ that it is closed in two cases, $m = 3$ that it is closed in only one case, and $m = 4$ that it is open in all three cases. For $m = 2$ and $m = 3$, the interval bounds also depend on the specific solutions in which the branch is closed.

Since the strategic parameters of the EPSO evolve for each particle and iteration, the corresponding interval bounds also become particle- and iteration-dependent. The lower and upper bounds associated with the inertia component are given by

$$e_{i,m}^{w} = (m-1)\cdot\left(1 - w_{i,1}^{k,\text{new}}\right), \qquad \forall i \in \{1,\ldots,N^{\text{pop}}\}, \forall m \in \{1,2,3,4\} \tag{98}$$

$$f_{i,m}^{w} = (m-1)\cdot\left(1 - w_{i,1}^{k,\text{new}}\right) + 1, \qquad \forall i \in \{1,\ldots,N^{\text{pop}}\}, \forall m \in \{1,2,3,4\} \tag{99}$$

where $w_{i,1}^{k,\text{new}}$ controls the degree of overlap among the intervals and, consequently, the stochasticity of the branch-weighting process.

The final interval bounds are obtained by incorporating the memory and cooperation weights, $w_{i,2}^{k,\text{new}}$ and $w_{i,3}^{k,\text{new}}$, while preserving the logical structure defined for the original WTPSO. The three binary entries considered for branch b_j are its operating states in the current solution s_i^k, the individual-best solution p_i^{best}, and the communicated perturbed global-best information $g_i^{\text{best,new,comm}}$. Accordingly, the following expressions are considered.

•Branch b_j closed in all the current solution proposals: $(s_{ij}^k, p_{ij}^{\text{best}}, g_{ij}^{\text{best,new,comm}}) = (1,1,1)$.

$$[e_{i,1}, f_{i,1}] = \left[e_{i,1}^{w}, f_{i,1}^{w} - \left(w_{i,2}^{k,\text{new}} + w_{i,3}^{k,\text{new}}\right)\right], \qquad \forall i \in \{1,\ldots,N^{\text{pop}}\} \tag{100}$$

•Branch b_j closed in two current solution proposals:

a)s_i^k *and* p_i^{best}*:* $(s_{ij}^k, p_{ij}^{\text{best}}, g_{ij}^{\text{best,new,comm}}) = (1,1,0)$.

$$[e_{i,2a}, f_{i,2a}] = \left[e_{i,2}^{w} + w_{i,3}^{k,\text{new}}, f_{i,2}^{w} - w_{i,2}^{k,\text{new}}\right], \qquad \forall i \in \{1,\ldots,N^{\text{pop}}\} \tag{101}$$

b)s_i^k *and* $g_i^{\text{best,new,comm}}$*:* $(s_{ij}^k, p_{ij}^{\text{best}}, g_{ij}^{\text{best,new,comm}}) = (1,0,1)$.

$$[e_{i,2b}, f_{i,2b}] = \left[e_{i,2}^w + w_{i,2}^{k,\text{new}}, f_{i,2}^w - w_{i,3}^{k,\text{new}}\right], \qquad \forall i \in \{1,\ldots,N^{\text{pop}}\} \tag{102}$$

c)p_i^{best} *and* $g_i^{\text{best,new,comm}}$*:* $(s_{ij}^k, p_{ij}^{\text{best}}, g_{ij}^{\text{best,new,comm}}) = (0,1,1)$.

$$[e_{i,2c}, f_{i,2c}] = \left[e_{i,2}^w, f_{i,2}^w - \left(w_{i,2}^{k,\text{new}} + w_{i,3}^{k,\text{new}}\right)\right] \qquad \forall i \in \{1,\ldots,N^{\text{pop}}\} \tag{103}$$

•Branch b_j closed in only one current solution proposal:

a)s_i^k*:* $(s_{ij}^k, p_{ij}^{\text{best}}, g_{ij}^{\text{best,new,comm}}) = (1,0,0)$.

$$[e_{i,3a}, f_{i,3a}] = \left[e_{i,3}^w + \left(w_{i,2}^{k,\text{new}} + w_{i,3}^{k,\text{new}}\right), f_{i,3}^w\right], \qquad \forall i \in \{1,\ldots,N^{\text{pop}}\} \tag{104}$$

b)p_i^{best}*:* $(s_{ij}^k, p_{ij}^{\text{best}}, g_{ij}^{\text{best,new,comm}}) = (0,1,0)$.

$$[e_{i,3b}, f_{i,3b}] = \left[e_{i,3}^w + w_{i,2}^{k,\text{new}}, f_{i,3}^w - w_{i,3}^{k,\text{new}}\right], \qquad \forall i \in \{1,\ldots,N^{\text{pop}}\} \tag{105}$$

$$\tag{106}$$

c)$g_i^{\text{best,new,comm}}$*:* $(s_{ij}^k, p_{ij}^{\text{best}}, g_{ij}^{\text{best,new,comm}}) = (0,0,1)$.

$$[e_{i,3c}, f_{i,3c}] = \left[e_{i,3}^w + w_{i,3}^{k,\text{new}}, f_{i,3}^w - w_{i,2}^{k,\text{new}}\right] \qquad \forall i \in \{1,\ldots,N^{\text{pop}}\} \tag{107}$$

•Branch b_j open in all the current solution proposals: $(s_{ij}^k, p_{ij}^{\text{best}}, g_{ij}^{\text{best,new,comm}}) = (0,0,0)$.

$$[e_{i,4}, f_{i,4}] = \left[e_{i,4}^w + \left(w_{i,2}^{k,\text{new}} + w_{i,3}^{k,\text{new}}\right), f_{i,4}^w\right], \qquad \forall i \in \{1,\ldots,N^{\text{pop}}\} \tag{108}$$

After determining the lower and upper interval bounds, a weight is generated for each branch using the same procedure described in Section 4.2. Prim's algorithm then uses the resulting branch-weight vector to construct the new radial solution proposal.

Algorithm 5 summarizes the tier-weighted construction operator employed by the WTEPSO. To use the same operator for the two candidates generated by each particle, let $\widehat{\mathbf{w}}_i^k$ denote either the current strategic-parameter vector $\mathbf{w}_i^k$ or its mutated counterpart $\mathbf{w}_i^{k,\text{new}}$. The algorithm is therefore called twice for each particle: once with $\widehat{\mathbf{w}}_i^k = \mathbf{w}_i^k$ and once with $\widehat{\mathbf{w}}_i^k = \mathbf{w}_i^{k,\text{new}}$. The resulting candidate topologies and their associated strategic parameters are subsequently evaluated and compared during the selection stage.

Algorithm 5 replaces the conventional velocity–position update during the reproduction stage. The operator is applied using both the current and mutated strategic-parameter vectors, producing two radial candidate topologies for each particle. After their application-specific fitness values have been evaluated, the candidate with the better fitness is retained together with

Algorithm 5 - Tier-weighted construction of a radial topology for the WTEPSO

Require: Connected graph $G = (\Omega_n, \Omega_b)$ with ordered branches $\Omega_b = (b_1, \ldots, b_{n_r})$; root node r; binary vectors s_i^k and p_i^{best}; global-best branch-weight vector $\rho^{g,k}$; strategic-parameter vector $\widehat{\mathbf{w}}_i^k = [\widehat{w}_{i,1}^k, \widehat{w}_{i,2}^k, \widehat{w}_{i,3}^k, \widehat{w}_{i,4}^k]$; communication probability cp

Ensure: New binary radial candidate topology s_i^{k+1} and its sampled branch-priority vector ϕ_i^k

for $j = 1, \ldots, n_r$ **do**
  Draw $\eta_{ij}^k \sim \mathcal{N}(0,1)$
  $\widetilde{\rho}_{ij}^{g,k} \leftarrow \rho_j^{g,k} + \widehat{w}_{i,4}^k \eta_{ij}^k$
end for
$\widetilde{T}_i^{g,k} \leftarrow \text{DeterministicPrim}\left(G, \widetilde{\rho}_i^{g,k}, r\right)$
$g_i^{\text{best,new}} \leftarrow \text{BinaryEdgeVector}\left(\widetilde{T}_i^{g,k}, \Omega_b\right)$
for $j = 1, \ldots, n_r$ **do**
  Draw $\chi_{ij}^k \sim \text{Bernoulli}(cp)$
  $g_{ij}^{\text{best,new,comm}} \leftarrow \chi_{ij}^k g_{ij}^{\text{best,new}}$
end for
for $m = 1, \ldots, 4$ **do**
  $[e_{i,m}^w, f_{i,m}^w] \leftarrow \left[(m-1)(1-\widehat{w}_{i,1}^k), (m-1)(1-\widehat{w}_{i,1}^k)+1\right]$
end for
for $j = 1, \ldots, n_r$ **do**
  $(x, p, g) \leftarrow \left(s_{ij}^k, p_{ij}^{\text{best}}, g_{ij}^{\text{best,new,comm}}\right)$
  if $(x,p,g) = (1,1,1)$ **then**
    $\alpha \leftarrow 1, \quad [e_{i,\alpha}, f_{i,\alpha}] \leftarrow \left[e_{i,1}^w, f_{i,1}^w - \left(\widehat{w}_{i,2}^k + \widehat{w}_{i,3}^k\right)\right]$
  else if $(x,p,g) = (1,1,0)$ **then**
    $\alpha \leftarrow 2\text{a}, \quad [e_{i,\alpha}, f_{i,\alpha}] \leftarrow \left[e_{i,2}^w + \widehat{w}_{i,3}^k, f_{i,2}^w - \widehat{w}_{i,2}^k\right]$
  else if $(x,p,g) = (1,0,1)$ **then**
    $\alpha \leftarrow 2\text{b}, \quad [e_{i,\alpha}, f_{i,\alpha}] \leftarrow \left[e_{i,2}^w + \widehat{w}_{i,2}^k, f_{i,2}^w - \widehat{w}_{i,3}^k\right]$
  else if $(x,p,g) = (0,1,1)$ **then**
    $\alpha \leftarrow 2\text{c}, \quad [e_{i,\alpha}, f_{i,\alpha}] \leftarrow \left[e_{i,2}^w, f_{i,2}^w - \left(\widehat{w}_{i,2}^k + \widehat{w}_{i,3}^k\right)\right]$
  else if $(x,p,g) = (1,0,0)$ **then**
    $\alpha \leftarrow 3\text{a}, \quad [e_{i,\alpha}, f_{i,\alpha}] \leftarrow \left[e_{i,3}^w + \left(\widehat{w}_{i,2}^k + \widehat{w}_{i,3}^k\right), f_{i,3}^w\right]$
  else if $(x,p,g) = (0,1,0)$ **then**
    $\alpha \leftarrow 3\text{b}, \quad [e_{i,\alpha}, f_{i,\alpha}] \leftarrow \left[e_{i,3}^w + \widehat{w}_{i,2}^k, f_{i,3}^w - \widehat{w}_{i,3}^k\right]$
  else if $(x,p,g) = (0,0,1)$ **then**
    $\alpha \leftarrow 3\text{c}, \quad [e_{i,\alpha}, f_{i,\alpha}] \leftarrow \left[e_{i,3}^w + \widehat{w}_{i,3}^k, f_{i,3}^w - \widehat{w}_{i,2}^k\right]$
  else
    $\alpha \leftarrow 4, \quad [e_{i,\alpha}, f_{i,\alpha}] \leftarrow \left[e_{i,4}^w + \left(\widehat{w}_{i,2}^k + \widehat{w}_{i,3}^k\right), f_{i,4}^w\right]$
  end if
  Draw $u_{ij}^k \sim \mathcal{U}(0,1)$
  $\phi_{ij}^k \leftarrow e_{i,\alpha} + (f_{i,\alpha} - e_{i,\alpha})\, u_{ij}^k$
end for
$T_i^{k+1} \leftarrow \text{DeterministicPrim}\left(G, \phi_i^k, r\right)$
  Prim rule: an edge is eligible if exactly one endpoint belongs to the partial tree; among eligible edges, select the one with the lexicographically smallest pair (ϕ_{ij}^k, j).
$s_i^{k+1} \leftarrow \text{BinaryEdgeVector}\left(T_i^{k+1}, \Omega_b\right)$
return s_i^{k+1} and ϕ_i^k

Source: The author.

its associated strategic parameters. Thus, the WTEPSO preserves the replication, mutation, and selection principles inherited from the EPSO, while replacing arithmetic particle motion with

structure-preserving topology generation.

A.6 COMPLETE WTEPSO OPTIMIZATION PROCEDURE

Algorithm 6 summarizes the complete WTEPSO procedure. The initial populations for reconfiguration and restoration are generated according to Algorithms 2 and 3, respectively. Each candidate radial topology is generated using the tier-weighted construction operator presented in Algorithm 5, while fitness evaluation and constraint handling follow the procedure defined in Subsection 4.4.

For each particle, two candidates are generated: one using the current strategic-parameter vector and another using its mutated counterpart. For compactness, let $\mathscr{H} = \{\text{cur}, \text{mut}\}$ denote these two candidates. The operation MutateStrategicParameters$(\mathbf{w}_i^k, \tau)$ implements the mutation rule in (85). The operation EvaluateFitness$(\mathscr{D}^a, s)$ returns the application-specific objective value when the candidate is feasible and $+\infty$ otherwise. As in the complete WTPSO procedure, the maximum number of power-flow evaluations, $N_{\text{PF}}^{\max}$, is adopted as the stopping criterion.

When a candidate is retained during the selection stage, its sampled branch-priority vector $\phi_{i,h}^k$ is stored as ρ_i^{k+1}. If the retained topology updates the personal or global best, the same vector is stored as $\rho_i^{p,\text{best}}$ or $\rho^{g,k+1}$, respectively.

The WTEPSO preserves the replication, strategic-parameter mutation, competition, individual memory, and global information sharing mechanisms inherited from the EPSO. However, the conventional velocity–position update is replaced by the tier-weighted topology-construction operator and Prim's algorithm. When the candidate generated with the mutated strategic parameters has lower fitness, its topology, strategic parameters, and branch-priority vector are retained. Otherwise, the candidate generated using the current strategic parameters is preserved.

A.7 FINAL REMARKS

This appendix presents the proposed WTEPSO formulation, which integrates the tier-weighted mechanism of the WTPSO into the evolutionary framework of the EPSO. The parameters w, c_1, and c_2 of the original WTPSO are replaced by the particle-specific inertia, memory, and cooperation parameters of the EPSO. A fourth strategic parameter controls the perturbation applied to the branch-weight vector associated with the global-best topology. Through mutation and selection, these parameters evolve independently for each particle, making the topology-construction mechanism both particle- and iteration-dependent.

In the WTEPSO, the conventional velocity–position update employed during the reproduction stage of the EPSO is replaced by the tier-weighted generation of branch priorities. These

Algorithm 6 - Complete WTEPSO optimization procedure

Require: Application $a \in \{\text{rec}, \text{rest}\}$; connected graph G^a; application data $\mathscr{D}^a$; root node r^a; N^{pop}; $N_{\text{PF}}^{\max}$; parameters τ and cp; random seed ξ
Ensure: Best topology g^{best} and its fitness F_g^{best}

Initialize the pseudorandom generator using seed ξ
if $a = \text{rec}$ **then**
  $(S^0, F^0, N_{\text{PF}}) \leftarrow \text{InitialPopulationReconfiguration}\big(G^a, \mathscr{D}^a, r^a, N^{\text{pop}}\big)$ ▷ Algorithm 2
else
  $(S^0, F^0, N_{\text{PF}}) \leftarrow \text{InitialPopulationRestoration}\big(G^a, \mathscr{D}^a, r^a, N^{\text{pop}}\big)$ ▷ Algorithm 3
end if
for $i = 1, \ldots, N^{\text{pop}}$ **do**
  Draw $w_{i,1}^0, w_{i,4}^0 \sim \mathscr{U}(0,1)$ and $w_{i,2}^0, w_{i,3}^0 \sim \mathscr{U}(0, 0.5)$
  $(p_i^{\text{best}}, F_i^{\text{best}}) \leftarrow (s_i^0, F_i^0)$
  $\rho_i^{p,\text{best}} \leftarrow \mathbf{1} - p_i^{\text{best}}$
end for
$i^\star \leftarrow \min\big(\arg\min_{1 \le i \le N^{\text{pop}}} F_i^{\text{best}}\big)$
$(g^{\text{best}}, F_g^{\text{best}}, \rho^{g,0}) \leftarrow (p_{i^\star}^{\text{best}}, F_{i^\star}^{\text{best}}, \rho_{i^\star}^{p,\text{best}})$
$k \leftarrow 0$
while $N_{\text{PF}} < N_{\text{PF}}^{\max}$ **do**
  for $i = 1, \ldots, N^{\text{pop}}$ **do**
    $\widehat{\mathbf{w}}_{i,\text{cur}}^k \leftarrow \mathbf{w}_i^k$
    $\widehat{\mathbf{w}}_{i,\text{mut}}^k \leftarrow \text{MutateStrategicParameters}\big(\mathbf{w}_i^k, \tau\big)$ ▷ Equation (85)
    for $h \in \mathscr{H}$ **do**
      $(s_{i,h}^{k+1}, \phi_{i,h}^k) \leftarrow \text{TierWeightedTree}\big(G^a, s_i^k, p_i^{\text{best}}, \rho^{g,k}, \widehat{\mathbf{w}}_{i,h}^k, cp, r^a\big)$ ▷ Algorithm 5
      $F_{i,h}^{k+1} \leftarrow \text{EvaluateFitness}\big(\mathscr{D}^a, s_{i,h}^{k+1}\big)$ ▷ Subsection 4.4
    end for
    $N_{\text{PF}} \leftarrow N_{\text{PF}} + 2$
    if $F_{i,\text{mut}}^{k+1} < F_{i,\text{cur}}^{k+1}$ **then**
      $h_i^\star \leftarrow \text{mut}$
    else
      $h_i^\star \leftarrow \text{cur}$
    end if
    $(s_i^{k+1}, F_i^{k+1}, \rho_i^{k+1}, \mathbf{w}_i^{k+1}) \leftarrow (s_{i,h_i^\star}^{k+1}, F_{i,h_i^\star}^{k+1}, \phi_{i,h_i^\star}^k, \widehat{\mathbf{w}}_{i,h_i^\star}^k)$
    if $F_i^{k+1} < F_i^{\text{best}}$ **then**
      $(p_i^{\text{best}}, F_i^{\text{best}}, \rho_i^{p,\text{best}}) \leftarrow (s_i^{k+1}, F_i^{k+1}, \rho_i^{k+1})$
    end if
  end for
  $i^\star \leftarrow \min\big(\arg\min_{1 \le i \le N^{\text{pop}}} F_i^{\text{best}}\big)$
  if $F_{i^\star}^{\text{best}} < F_g^{\text{best}}$ **then**
    $(g^{\text{best}}, F_g^{\text{best}}, \rho^{g,k+1}) \leftarrow (p_{i^\star}^{\text{best}}, F_{i^\star}^{\text{best}}, \rho_{i^\star}^{p,\text{best}})$
  else
    $\rho^{g,k+1} \leftarrow \rho^{g,k}$
  end if
  $k \leftarrow k + 1$
end while
return g^{best} and F_g^{best}

Source: The author.

priorities are sampled using information from the current topology, the personal-best topology, and the communicated perturbed global-best topology. Prim's algorithm then maps the resulting branch-priority vector into a radial candidate topology. For each particle, candidates generated using the current and mutated strategic parameters are evaluated, and the better candidate is retained

together with its associated strategic parameters and branch-priority vector. Thus, the proposed formulation combines the self-adaptive mechanisms of the EPSO with the structure-preserving topology construction introduced in the WTPSO.

The WTEPSO is applied to the distribution system reconfiguration and service restoration problems in Chapters 5 and 6, respectively. Its performance is evaluated and compared with the WTPSO, EPSO, BPSO, and CE using the numerical results presented in those chapters.

APPENDIX B - SCIENTIFIC PRODUCTION

•**Morán, John Peñaloza**; Romero, Rubén; Carvalho, Leonel; Soares, Tiago; Pinto, Tiago; Macedo, Leonardo H. "A Novel Particle Swarm Optimization Formulation for Distribution System Reconfiguration." *Swarm and Evolutionary Computation*, 2026. Manuscript under second review.

•**J. P. Morán** et al. "Sizing Distributed Energy Resources for Energy Communities." In: *2025 21st International Conference on the European Energy Market (EEM)*, Lisbon, Portugal, 2025, pp. 1–6. doi: 10.1109/EEM64765.2025.11050218.

•I. Araujo, R. Teixeira, **J. P. Morán**, T. Pinto, and J. Baptista. "Application of Time Series Clustering for Improving Forecasts in Energy Markets." In: *2025 21st International Conference on the European Energy Market (EEM)*, Lisbon, Portugal, 2025, pp. 1–5. doi: 10.1109/EEM64765.2025.11050108.

•J. P. R. de Almeida, A. Carrillo-Galvez, **J. P. Morán**, T. A. Soares, and Z. S. Mourão. "Optimizing Quay Crane Operations Considering Energy Consumption." In: *Progress in Artificial Intelligence: EPIA 2025*, Faro, Portugal, Lecture Notes in Computer Science, vol. 16122, Cham: Springer, 2026, pp. 464–476. doi: 10.1007/978-3-032-05179-0_35.